Novel Functionality of Carbodiimide Chemistry as Non-Isocyanate Solution for Addition Polymerization

Dissertation

with the Aim of Achieving the Doctoral Degree

at the Faculty of Mathematics, Informatics and Natural Sciences

Department of Chemistry

University of Hamburg

Submitted by

Linyu Mu

2020 in Hamburg

The experimental work described in this thesis has been carried out between August 2015 and January 2019 at the Institute of Technical and Macromolecular Chemistry, University of Hamburg in the research group of Professor Dr. Gerrit A. Luinstra.

Date of thesis defense: 10. 07. 2020

Approval for printing:

The following referees recommend the acceptance of this doctoral thesis:

1st referee: Prof. Dr. Gerrit. A. Luinstra

2nd referee: Priv. Doz. Dr. Christoph Wutz

There is a crack in everything

That's how the light gets in

Leonard Cohen

List of Abbreviations

A	pre-exponential factor
c	concentration
$CDCl_3$	chloroform-d
CDI	carbodiimide
DCC	dicyclohexylcarbodiimide
DCM	dichloromethane
DEGEE	di(ethylene glycol) ethyl ether
DGME	diethylene glycol monomethyl ether
DIC	diisopropyl carbodiimide
DMA	dynamic mechanical analysis
DMPO	1,3-dimethyl-3-phospholine oxide
DMSO-d6	dimethyl sulfoxide-d6
DMTDN	dimethyltin dineodecanoate
DNA	deoxyribonucleic acid
DSC	differential scanning calorimetry
Ea	activation energy
EDC	1-ethyl-3-(3-dimethylaminopropyl)carbodiimide
ESI	electrospray ionization
f(α)	reaction mechanical function
FT	Fourier transform
FWO	Flynn-Wall-Ozawa (FWO) model
G'	storage modulus
G"	loss modulus
g(α)	integral form of the mechanical function
GPC	gel permeation chromatography
H	heat absorbed or released from reaction
$H_{12}MDI$	4,4′-diisocyanato dicyclohexylmethane
HCFCs	hydrochlorofluorocarbons
HDI	hexamethylene diisocyanate
HFC	hydrofluorocarbons
i	different heating rate denoted in the isoconversional methods
I(E, T)	temperature-integral in the isoconversional methods

I

IPDI	isophorone diisocyanate
IR	infrared
j	ordinal numbers in the Vyazovkin method
J	integration form in the Vyazovkin method
k	rate constant
k_1	rate constant
k_2	rate constant
KAS	Kissinger-Akahira-Sunose model
KPG	sealed-precision-glass stirrer
m	ordinal numbers in the autocatalytic model
M_c	network parameter
MDI	methylene diphenyl diisocyanate
M_{hard}	molecular weight of the hard segment
MPPO	3-methyl-1-phenyl-2-phospholene 1-oxide
M_{soft}	molecular weight of the soft segment
MWD	molecular weight distributions
n	reaction order / the number of moles / the number of the repeating units in the polymer
NDI	1,5-naphthalene diisocyanate
n_{hard}	the number of moles of the hard segment
NIPU	non-isocyanate polyurethane
NMR	nuclear magnetic resonance
n_{soft}	the number of moles of the soft segment
o-DTC	di-o-tolyl carbodiimide
p-DTC	di-p-tolyl carbodiimide
PE	polyethylene
PEG	polyethylene glycol
PIU	polyiso-urea
polyTHF	poly(tetramethylene oxide) diol
PP	polypropylene
PPDI	p-phenylene diisocyanate
PPG	polypropylene glycol
PU	polyurethane
PVC	polyvinyl chloride

R	universal gas constant
RIM	reaction injection molding
RNA	ribonucleic acid
SD	standard deviation
SSRR	sequential self-repetitive reaction
t	time
T	temperature
T_0	initial temperature of reaction
tan δ	loss factor
TBD	1,5,7-triazabicyclo[4.4.0]dec-5-ene
TDA	toluene diamine
TDI	toluene diisocyanate
T_g	glass transition temperature
$T_{g, DSC}$	glass transition temperature determined by DSC
$T_{g,G''}$	glass transition temperature determined by the maximum value of the loss modulus in DMA
TGA	thermogravimetric analysis
T_{gel}	gel point
THF	tetrahydrofuran
TOF	time-of-flight mass spectrometry
TPU	thermoplastic polyurethane
TTIP	titanium isopropoxide
USD	United States dollar
UV	ultraviolet
V_g	volume of the gel fraction
V_m	molar volume
$V_{m,s}$	molar volume of the solvent
V_s	volume of the absorbed solvent
α	conversion
β	heating rate
$δ_{hard}$	solubility parameter of the hard segment
$ΔH_{total}$	sum of the reaction heat
$δ_p$	solubility parameter of the polymer
$δ_s$	solubility parameter of the solvent

δ_{soft}	solubility parameter of the soft segment
v_c	crosslink density
v_p	volume fraction of the polymer
ρ_{hard}	density of the hard segment
ρ_{soft}	density of the soft segment
$\Phi(E_\alpha)$	integration form in the Vyazovkin method
χ	Flory-Huggins interaction parameter

Table of Contents

Abstract

In this thesis, the reactions of carbodiimide with alcohols are reported next to their application in polymer chemistry. The thesis was divided into three parts. In part one, the reaction kinetics of a model system with mono-functional compounds was investigated. A side reaction between carbodiimide and *iso*-urea to give a series of guanidine-type compounds was observed at low temperatures. In the second part, the guanidine-entities were utilized in a linear polyiso-urea system as a temperature-sensitive crosslinking option. In the last part, the guanidine groups were used in the context of a "blocked carbodiimide strategy" in polyiso-urea resins prepared from oligomeric carbodiimide and polyol.

The first part of the work is based on the idea that polycarbodiimide can be used as non-isocyanate building blocks to react with polyols and form novel materials. In order to increase the understanding of the reaction behavior between carbodiimide and alcohol, the reaction kinetics of mono-functional carbodiimide with mono-ol catalyzed by metal-based homogeneous catalysts was studied. It was found that the reaction rate reveals an order of ca. 0.5 with respect to titanium isopropoxide (TTIP) and dimethyltin dineodecanoate (DMTDN) concentration in the early stage of the reaction between di-*p*-tolyl carbodiimide (*p*-DTC) and diethylene glycol monomethyl ether (DGME). A side reaction between carbodiimide and *iso*-urea product can take place that results in the formation of polyguanidines after multiple additions of carbodiimides. The side reaction is only favored at lower temperature and the formed polyguanidines react back to carbodiimide and *iso*-urea at elevated temperatures.

In the second part of the work, the thermal reversibility of the polyguanidine was utilized in a linear polyiso-urea system as temperature-sensitive crosslinker. The linear polyiso-urea was prepared from biscarbodiimide and poly(tetramethylene oxide) diol by polyaddition. The guanidine groups are formed by adding biscarbodiimide in excess. The guanidine groups can appear as pendant groups or side chains but can also react to form crosslinks in the material. At higher temperature, the guanidine-entities decompose and the material turns into a fluid, which gives the potential to be utilized as a reprocessable material.

In the last part, guanidine groups were also introduced into polyiso-urea resins produced from oligomeric carbodiimide and polyol for using as an inherent source of carbodiimide. At lower temperature, the carbodiimide functionality is blocked by reaction with the *iso*-urea groups in the polymer, thus decreasing the reactivity and toxicity of the raw materials. At higher temperature, the carbodiimide groups can be regenerated and it is able to react with nucleophilic

agents in a curing reaction. Also, the guanidine groups can act as temperature-sensitive crosslinks in polyiso-urea, giving the material better mechanical properties.

Zusammenfassung

In dieser Arbeit wird die Reaktion zwischen einem Carbodiimid und einem Alkohol mit dem Augenmerk auf neuen Anwendungen in der Additionspolymerisation vorgestellt. Die Arbeit gliedert sich thematisch in drei Abschnitte. Im Ersten wurde die Reaktionskinetik eines Modellsystems auf der Basis monofunktioneller Verbindungen aufgeführt. Bei niedrigerer Temperatur wurde eine Nebenreaktion zwischen Carbodiimid und Isoharnstoff unter Bildung von Guanidine beobachtet. Im nächsten Abschnitt wird berichtet, wie die Guanidinverbindungen in einem linearen Polyisoharnstoff als temperaturempfindliches Vernetzungssystem verwendet werden können. Im letzten Teil wird beschrieben, wie die auf Guanidin basierenden Einheiten auch als blockierte Carbodiimid in aus Carbodiimid-Oligomer und Polyol hergestellten Polyisoharnstoff-Harzen reagieren.

Der erste Teil der Arbeit basiert auf der Idee, dass Polycarbodiimide als isocyanatfreie Bausteine in einer Polyaddition verwendet werden können, die zusammen mit Polyolen zu neuen Materialien führen könnten. Um das Reaktionsverhalten zwischen Carbodiimiden und Alkoholen zu verstehen, wurde die Kinetik der Reaktionen zwischen monofunktionellem Carbodiimid und Mono-ole untersucht. Die Reaktion wurde durch homogene Metallkomplexe katalysiert. Es konnte beobachtet werden, dass die Reaktionsgeschwindigkeit am Anfang der Reaktion zwischen Di-*p*-tolylcarbodiimid (*p*-DTC) und Diethylenglycolmonomethylether (DGME) eine Ordnung von ca. 0,5 bezogen auf die Konzentration des Tetraisopropylorthotitanats (TTIP) und Dimethylzinndineodecanoat (DMTDN) zeigt. Es wurde auch festgestellt, dass eine Nebenreaktion zwischen Carbodiimid und Isoharnstoff stattfinden kann, wobei Polyguanidine entstehen. Dies führte zu einem Unterschied in dem Umsatz beider Reaktionspartner. Die Nebenreaktion fand nur bei niedrigeren Temperaturen statt und die gebildeten Polyguanidine bauten sich bei höherer Temperatur unter Freisetzung des Carbodiimids und des Isoharnstoffs ab.

Im zweiten Teil der Arbeit wird über die thermische Reversibilität der Guanidinbildung in einem linearen Polyisoharnstoff-System als temperaturempfindliche Vernetzungsoption berichtet. Der lineare Polyisoharnstoff wurde aus Biscarbodiimid und Polytetramethylenoxiddiol durch Polyaddition in Masse hergestellt. Die Guanidineinheiten wurden durch Zugabe von Biscarbodiimid im Überschuss gebildet. Die Guanidineinheiten lagen als Seitenketten vor und konnten miteinander reagieren, wodurch das Material vernetzt wurde. Bei höherer Temperatur spalteten sich die Guanidingruppen, und das Material wurde flüssig. Es entsteht so die Möglichkeit, das Harz als wiederverarbeitbares Material zu nutzen.

Im letzten Teil der Dissertation wird ausgeführt wie die thermische Reversibilität der Guanidinbildung in den aus Carbodiimid-Oligomer und Polyol hergestellten Polyisoharnstoff-Harzen genutzt wird, um nachträgliche Netzwerke durch Reaktionen mit vorhandenen Nukleophilen zu erzeugen (blockierte Carbodiimid-Strategie). Bei niedriger Temperatur wurden die Carbodiimid-Gruppen durch Reaktion mit Isoharnstoff-Gruppen im Polymer blockiert, um so die Reaktivität und auch die Toxizität des Carbodiimids zu verringern. Bei höherer Temperatur wurden die Carbodiimid-Gruppen regeneriert und konnte mit weiteren anwesenden nukleophilen Agenzien an einer Härtungsreaktion teilnehmen. Des Weiteren können die Guanidingruppen als temperatur-responsive Nachvernetzer in den auf Polyisoharnstoff basierenden Polymeren wirken, sodass das Material bessere mechanische Eigenschaften erhält.

1 Introduction

1.1 Polyurethane Chemistry

1.1.1 Background on the Polyurethane Chemistry

Discovered by Prof. Otto Bayer in 1937, polyurethane (PU) is still of increasing interest in the materials map worldwide, on account of the easy variation of the chemical structure and the resulting broad field of applications.[1–4] The global PU consumption was estimated at 60.5 billion USD in 2017 and was predicted to achieve 79 billion USD by 2021.[5] The substantial growth of increasing demand comes from the fact that a large variety of products can be prepared and manufactured from isocyanates, and then utilized in various end-use industries, in form of foams, elastomers, adhesives/sealants and coatings.
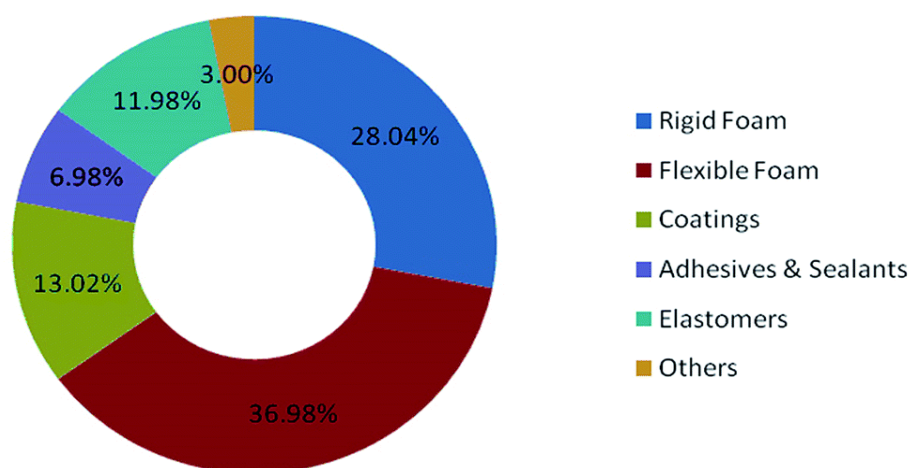
Figure 1. Overview of the polyurethane end-use market in 2010.[6]

Over 65% polyurethane raw materials are utilized in foam applications.[1] Their low density and thermal conductivity, as well as their versatile mechanical properties make PU foam leading the competition in the market of plastic foams. The formation of PU foams is based on the gelling reaction of multifunctional isocyanates with polyols, which leads to urethane linkages, and the blowing reaction between isocyanate and water. The blowing reaction comprises two consecutive reactions: isocyanate first reacts with water to form an unstable carbamic acid, which spontaneously decomposes to carbon dioxide and amine. Latter can further react with

additional isocyanate, giving the urea linkage in the polymer. The carbon dioxide produced during the reaction serves as a blowing agent (**Scheme 1**).

**Scheme 1.** Gelling reaction and blowing reaction during the production of polyurethane foams.
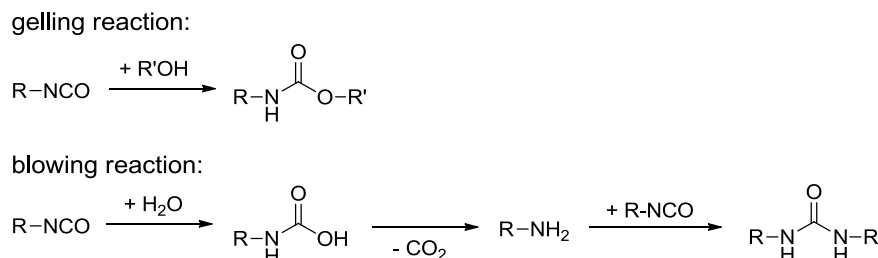
Although PU foams are based on similar chemistry, materials with very different properties can be obtained by choosing different isocyanates, polyols, catalysts, blowing agents and additives. In general, PU foams are classified as rigid or flexible foam. The major of rigid foams are used in the construction industry for thermal insulation, on account of their low thermal conductivity, good adhesion to commonly used materials (e.g. steel, PE, PP and PVC) and excellent mechanical properties at low density.[1] Rigid foams are mainly produced from polymeric MDI, the mixture of monomeric 4,4´-MDI, its isomer and the oligomeric MDIs with the functionality of 3-6. A wide variety of polyols can be used including petroleum oil based and biomass-based polyether and polyester polyol. Next to water as a chemical blowing agent, a physical blowing agent may be required, such as pentane or hydrofluorocarbons (HFCs), added together with further additives, such as catalysts, surfactant and fire retardants. The high functionality of reactants and physical blowing agents give rigid foams a glassy network structure with closed cells, which leads to good heat stability, high compression strength at low density and good barrier properties.[7]

Flexible foams are often found in furniture, bedding and in automotive industries as mattresses, pillows and seating. Flexible foams are mainly produced from TDI or MDI-based prepolymers. The polyether polyols, with a functionality of 3-6 and molecular weight of 3000 to 12000 g/mol are usually used, to create the polyurethane structure. Flexible foams can be produced by the one-shot process, where the gelling and blowing reaction take place simultaneously or in a two-step process.

Elastomers are another important class of PU material, which can be applied in shoe soles, integral foams and vibration damping. According to the production process, PU elastomers can be divided into the cellular elastomer, cast elastomer, thermoplastic elastomer (TPU), RIM

elastomer, spray elastomer etc. PU elastomers are generally produced from a diisocyanate, polyether or polyester polyols and a low molecular weight diol or diamine as the chain extender. As diisocyanate, MDI, TDI and NDI are more often used, however, aliphatic diisocyanates, such as HDI, IPDI, H_{12}MDI have also been increasingly used on account of their excellent UV-stability. Structurally, elastomers consist of polymer chains with alternating soft and hard segments (**Scheme 2**). The soft segments refer to the polyol-based segments, which have a glass transition temperature well-below ambient temperature, while the hard segments are formed by reaction of the diisocyanate with the chain extender. The resulting hard domain has a melting point or glass transition temperature generally above 100 °C. A chemical crosslinking may be introduced by adding polyfunctional alcohol or excess of diisocyanate to form allophanate or biuret linkages.

**Scheme 2.** Schematic representation of segmented polyurethane.
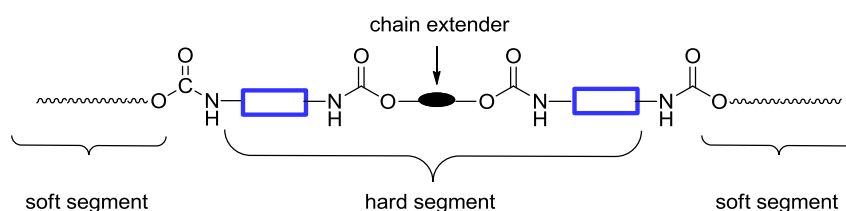
In recent years, the market for PU resins in coatings, adhesives and sealants expands rapidly, based on the versatile derivatizations and crosslinking reactions between isocyanates and their derivatives. In the automotive industry as an example, isocyanates and PU resins can be found in all four layers of a typical metallic finish.[1] The PU resins are mainly produced from polyisocyanates or isocyanate-terminated prepolymers with a polyol by polyaddition, and may consist of urethane, urea, biuret or allophanate functionalities. Depending on the formulation, PU resins can be supplied as one-component (1K) or two component (2K) mixture, in solvent-based, water-based, solvent-free solution or even as powder.

1.1.2   Isocyanate Chemistry

According to the latest research report, the global isocyanates market is expected to grow by 6.56% per year during 2016-2022. [8] The rapid growth of the isocyanates market is stimulated primarily by the polyurethane consumption expansion. The most frequently used isocyanates in the polyurethane production are toluene diphenyl diisocyanate (TDI), comprising the isomers of 2,4- and 2,6-TDI, and methylene diphenyl diisocyanate (MDI), comprising 4,4'- and 2,4'-MDI and polymeric MDI. Both occupy approximately 80% of the total isocyanates production. In addition, other aromatic as well as aliphatic diisocyanates used in the polyurethane

production include 1,5-naphthalene diisocyanate (NDI), *p*-phenylene diisocyanate (PPDI), 1,6-hexamethylene diisocyanate (HDI) and isophorone diisocyanate (IPDI), and also polyisocyanates.

**Scheme 3.** Common isocyanates in the polyurethane production.
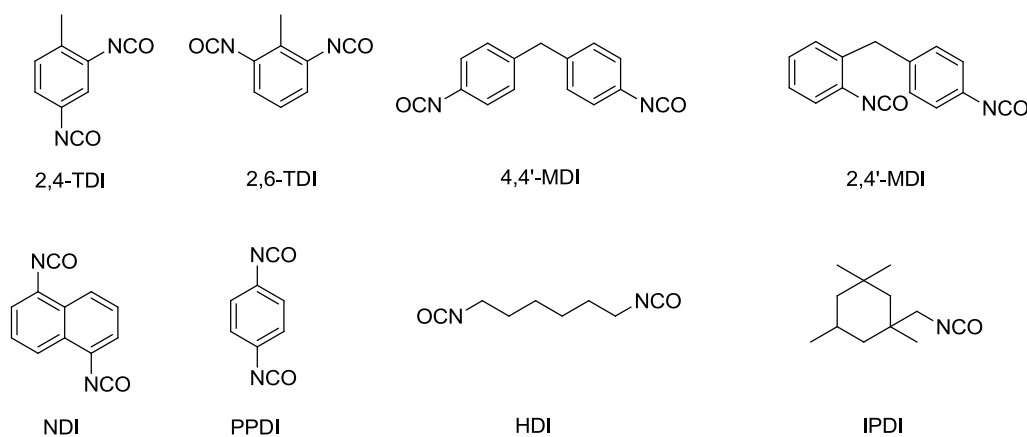
Conventionally, isocyanates are produced from the corresponding amines. The production process of TDI is mentioned here as an example (**Scheme 4**). Toluene is thus first nitrated in a mixture of nitric acid and sulfuric acid to yield dinitrotoluene. An isomer mixture of 2,4- and 2,6-dinitrotoluene in the ratio of 77:19 is obtained. The rest ca. 4% byproducts are 2,3- and 3,4-dinitrotoluene, known in the industry as *ortho*-isomers. The mixture is then catalytically hydrogenated to toluene diamine (TDA). The 2,3- and 3,4-TDA are removed by fractional distillation, and the 2,4- and 2,6-isomers are phosgenated to the corresponding diisocyanates.

The isocyanate chemistry is mainly based on the reactivity of the cumulated N=C=O double bonds. On account of the high electronegativity of nitrogen and oxygen atoms, the carbon atom is strongly electrophilic and can easily react with many nucleophilic reagents, such as an alcohol to give urethane (also called as carbamate) or an amine to give urea. The reaction of isocyanate with water or carboxylic acid can generate unstable carbamic acid or acid anhydride, which then decompose under decarboxylation to generate amine or amide, respectively. Among these reactions, the reactions with water and alcohol are extensively used in the industry to produce polyurea- and polyurethane-based polymers.

Urethane and urea can further react with isocyanate by nucleophilic attack of the nitrogen linked to the hydrogen, giving allophanate and biuret respectively. However, the reactivity of urethane and urea N-H entity is much lower than alcohols or amines, on account of the lower electron density caused by the presence of the carbonyl group. Former reactions occur mostly only when

the isocyanate is in excess and at temperatures above 110 °C or in the presence of a catalyst (**Scheme 5**).

Scheme 4. Industrial production of toluene diphenyl diisocyanate.
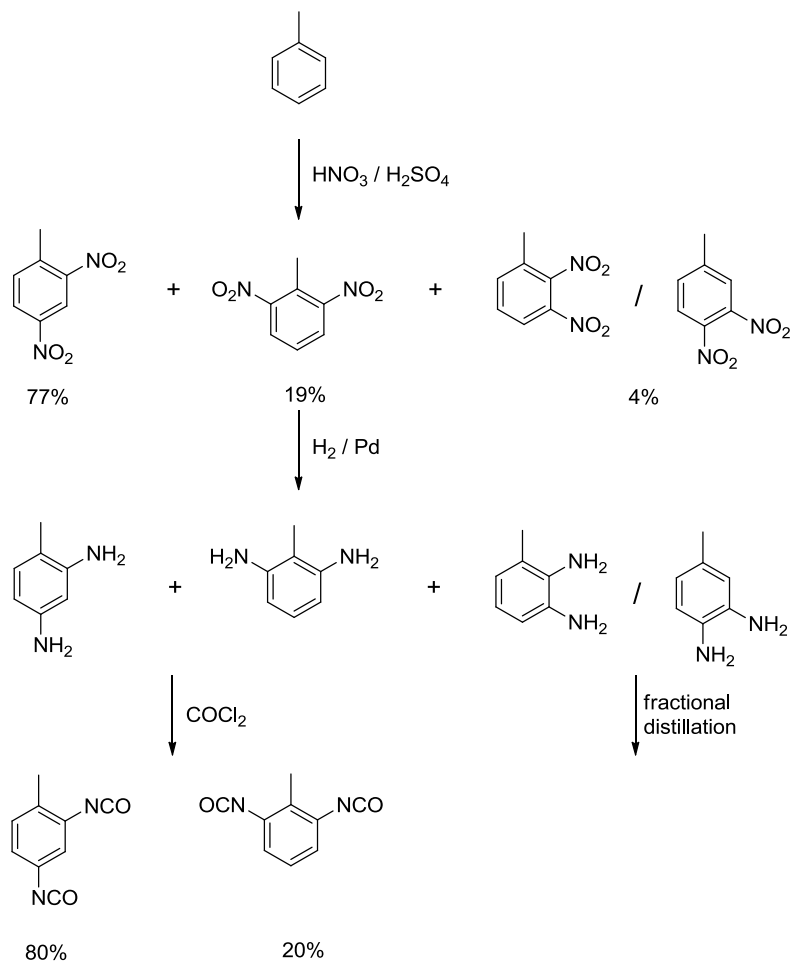
Scheme 5. The reactivity of isocyanates against nucleophiles.
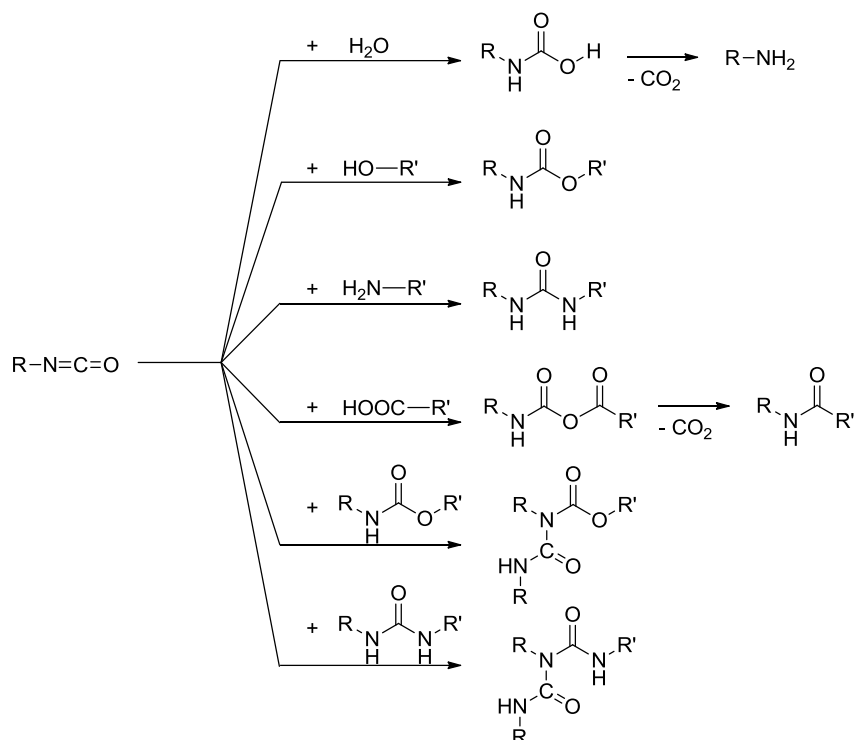
Scheme 6. Cyclization and homopolymerization of isocyanates.
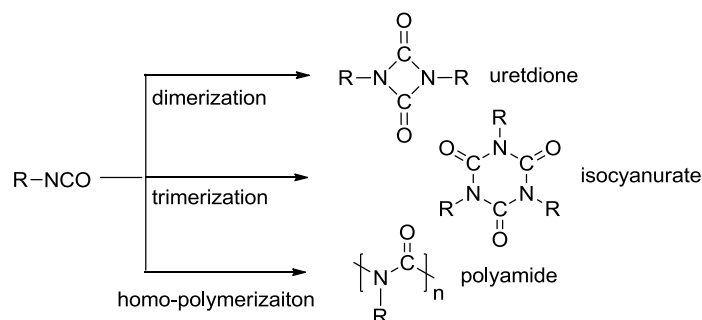
In addition to the above mentioned nucleophilic additions, isocyanates also undergo dimerization, trimerization and homo-polymerization, giving uretdione, isocyanurate and polyamide respectively (**Scheme 6**). The dimerization of isocyanates is an equilibrium reaction. The formation of the uretdione is favored by heating and in presence of a nucleophilic catalyst, such as trialkylamine, trialkyl phosphine and substituted pyridines. On account of low reactivity, the dimerization of an aliphatic isocyanate is difficult.

Unlike uretdione, isocyanurate is thermally a much more stable compound. The trimerization of isocyanate mostly takes place at above 250 °C, or at lower temperature in the presence of a catalyst, e.g. alkali metal alkoxide, organotin compounds or tertiary amines. A new study shows

that *N*-heterocyclic carbene can also catalyze the trimerization of phenyl isocyanate with a quantitative conversion.[9]

Homopolymerization of isocyanates can take place well-below 100 °C, however, the obtained polyamide is thermally not stable. The unzipping reaction occurs at above 140 °C or in the presence of basic impurities and isocyanurate will be obtained as the product.

The reaction of isocyanate with an epoxy function leads to oxazolidone. The reaction is mostly accompanied with trimerization of isocyanate and/or homopolymerization of epoxide.[10] With increasing temperature, the reactions take place step by step: the trimerization of isocyanate is favored at relatively low temperatures. If the temperature is higher, isocyanate also reacts with epoxides to yield oxazolidones. At elevated temperature, opened epoxide alkoholate can attack isocyanurate, leading to oxazolidone (**Scheme 7**).

Scheme 7. Reactions of isocyanate with epoxy.
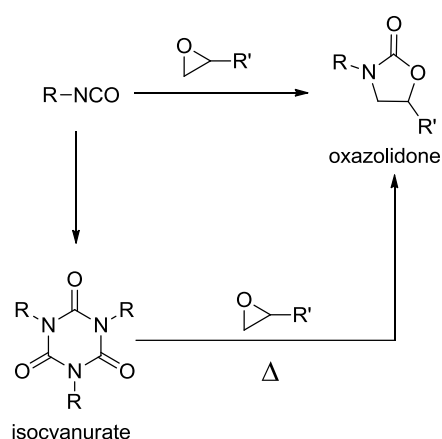
Moreover, isocyanate can also convert to carbodiimide at elevated temperature or in the presence of a catalyst. This will be discussed in detail in **Chapter 1.2.2**.

1.1.3 "Non-Isocyanate" Polyurethanes

Although polyurethanes have gained a unique position in the material map, the inherent toxicity of diisocyanate is a major drawback in their synthesis. To improve on this, a number of alternative pathways to produce polyurethanes without free isocyanates were suggested, leading to the so-called non-isocyanate polyurethanes (NIPUs). Most studies with this focus use the transurethanization reaction between a dicarbamate and a polyol (**Scheme 8**). The bisalkyl carbamate can be prepared from a dialkyl carbonate or a cyclic carbonate and a diamine. As dialkyl carbonate, the most used is dimethyl carbonate, which can be synthesized from carbon

dioxide and methanol. Then, the biscarbamate is obtained by the reaction of the dialkyl carbonate with a diamine, e.g. hexamethylene diamine. The route from cyclic carbonate and amine is similar, a cyclic carbonate compound, e.g. ethylene carbonate and propylene carbonate, reacts with a diamine, giving the bishydroxyalkylcarbamate (**Scheme 9**).

Scheme 8. Transurethanization.
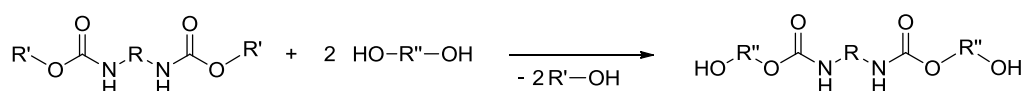
Scheme 9. Synthesis of dicarbamate from dimethyl carbonate or ethylene carbonate with hexamethylene diamine.
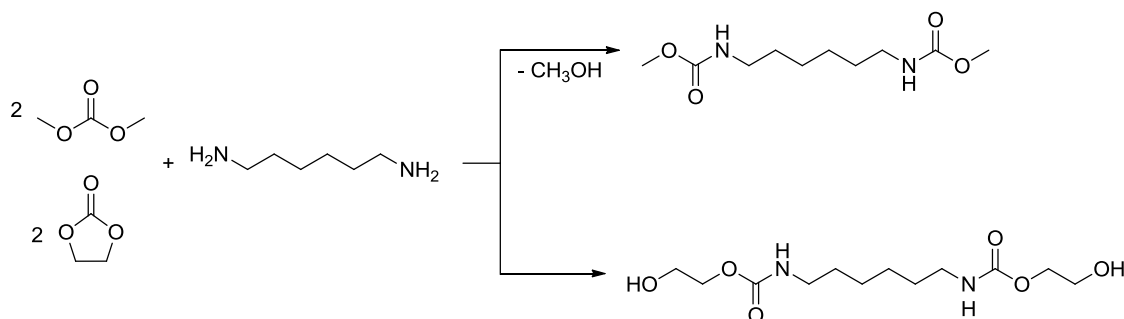
The polycondensation of dialkyl carbamate with a polyol usually requires a catalyst and a high temperature. After a polyurethane oligomer is formed, reduced pressure should be applied, to remove the low molecular weight alcohol and shift the reaction to the polymer product. Several catalysts, such as dibutyl tin oxide, barium oxide and titanium butoxide have been reported for this reaction.[11]

Another non-isocyanate solution, which has already been widely utilized in the industry, deals with "blocked isocyanate". Blocked isocyanates generally refer to an adduct that contains a weak bond formed by the reaction of isocyanate with a nucleophilic compound. Taking advantage of the thermal reversibility, isocyanate can be regenerated from the blocked form at high temperatures, and react with another nucleophile, e.g. alcohol and amine, giving the desired thermal stable polymer. Since the blocked isocyanate is often insensitive to the nucleophile compound at room temperature, it also allows preparing a one-component (1K) system with long pot life and low toxicity. However, the presence of the blocking agent may also consume regenerated isocyanate and affect the properties of the final product.
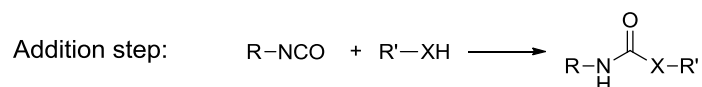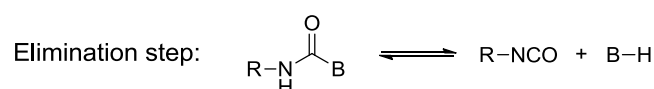
A large variety of blocking agents have been mentioned in previous studies, including phenols, anilines, oximes, amides and imides as well as some cyclic *N*-containing compounds, such as

imidazole, pyrazole, and triazole.[12–16] Even the dimer and trimer of the isocyanate have also been declared a blocked isocyanate source.[17,18] In general, two reaction mechanisms are supposed that may take place during the curing reaction with blocked isocyanates. The first is the elimination-addition mechanism. The mechanism has two steps: in the first step, the so-called elimination step, the isocyanate is released from the blocked form. In the second step, the released isocyanate can react with another nucleophilic agent, preferably giving a more stable bond. Another mechanism is based on the nucleophilic addition directly on the blocked isocyanate to yield a tetrahedral intermediate, which is then followed by the elimination of the blocking agent to give the desired product (**Scheme 10**). While the elimination-addition mechanism was frequently mentioned in the literature, the addition-elimination mechanism was only demonstrated in some systems of which the kinetics were specifically studied.[2]

Scheme 10. The proposed mechanisms of the deblocking and curing reaction.
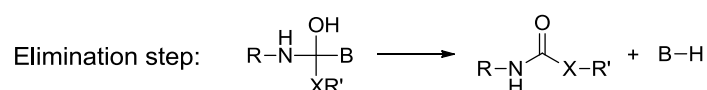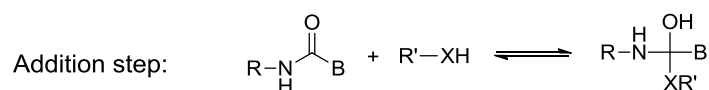
1.2 Carbodiimide Chemistry as a Novel Non-Isocyanate Solution

1.2.1 Carbodiimide Chemistry

Carbodiimide (CDI) is a class of organic compounds with the heterocumulene structure R-N=C=N-R'. They can be considered the diimides derived from carbon dioxide.[19] The two nitrogen attached groups, which can also be identical, may be alkyl, aryl, acyl-, trimethylsilyl-, thioacyl-, imidoyl-, or even halogens. In this thesis, only organic CDIs with aliphatic or

aromatic substituents are discussed. The cumulative double bonds are not linear, the N=C=N bond angles vary from 160 – 170° for aliphatic and aromatic CDIs.[20] Theoretically, CDIs exist as stereoisomers, but only a few of their enantiomeric forms have been isolated.[21] The isomerization of CDIs to form cyanamides has been studied with *N*-phenyl-*N'*-trityl carbodiimide. The mechanism is still unclear, it may occur via a radical or ionic route (**Scheme 11**).[20]

Scheme 11. Isomerization of carbodiimide by a radical or ionic route.
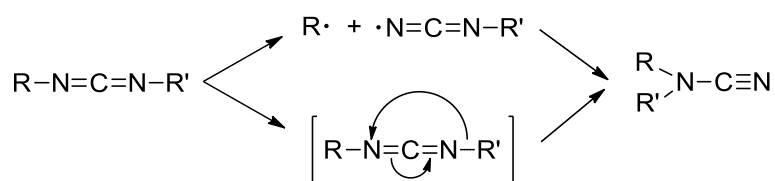
In general, the carbodiimide group has two types of reactive centers, the electrophile central carbon and both nucleophilic nitrogen atoms. In analogy to isocyanates, CDIs can also react with a wide range of nucleophilic agents, such as water, alcohols, amines and carboxylic acids (**Scheme 12**). However, the reactivity of carbodiimide is clearly lower than that of isocyanate. For example, the reaction of CDIs with water only takes place in the presence of acidic or basic catalysts. The reaction may proceed through a cationic or an anionic intermediate.[20] (**Scheme 13**). The substituents were reported to have an influence on the reaction rate. In the case of substituted diphenyl carbodiimide, the reaction rate of an alkaline catalyzed reaction is: *m*-CH$_3$ > *p*-Cl > *m*-CH$_3$CO > *m*-Cl >> H > *p*-CH$_3$ > *p*-(CH$_3$)$_2$N, the acid catalyzed reaction follows the reversed order.[19]

Scheme 12. The reactivity of carbodiimides towards nucleophilic agents.
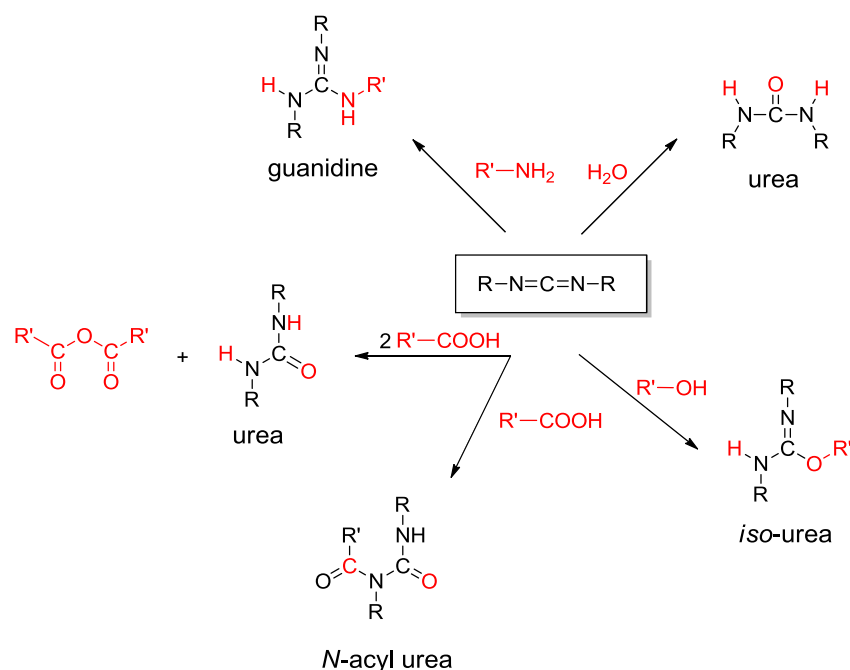
Scheme 13. Reactions of acid/base catalyzed water addition to carbodiimides.
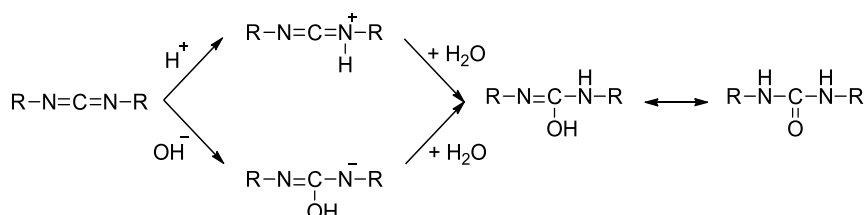
The reaction of CDIs with alcohols gives *O*-alkyl *iso*-urea. The reaction condition will be discussed in more detail in **Chapter 3.1**. In general, *iso*-urea can be considered the isomer of *N*-substituted urea. The close relationship among CDI, urea and *iso*-urea is based on the fact that urea is one of the traditional sources of CDI, and the conversion between substituted urea and *iso*-urea has also been reported.[22]

Surprisingly, aromatic CDIs react with phenol spontaneously at room temperature without any catalyst. The reaction of CDIs with phenols may lead to various products. Weakly acidic phenols reacting with aromatic CDIs affords the corresponding *O*-acyl *iso*-ureas, while strongly acidic phenols lead to the corresponding *N,N,N'*-triaryl ureas after an *O-N* shift (**Scheme 14**).[20] It is suggested that an *O*-chloro-substituent on phenol may prevent the *O-N* shift.[23] Moreover, if CDI reacts with a mixture of alcohol and phenol, high yield of alkylarylether together with the corresponding urea is obtained (**Scheme 15**).[19]

Scheme 14. The reaction of carbodiimide with phenol.
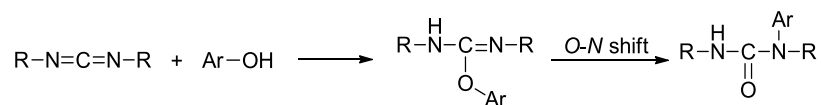
Scheme 15. The reaction of carbodiimide with alcohol and the subsequent reaction with phenol.
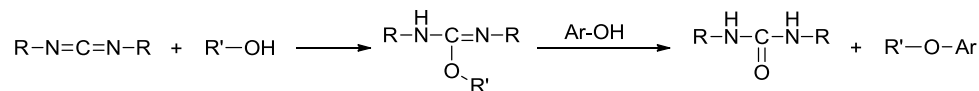
The reaction of CDI with a primary or secondary amine occurs in general spontaneously, giving the corresponding guanidine. Tetrafluoroboric acid[20] and phenalenyl cation[24] catalysis have been reported for the 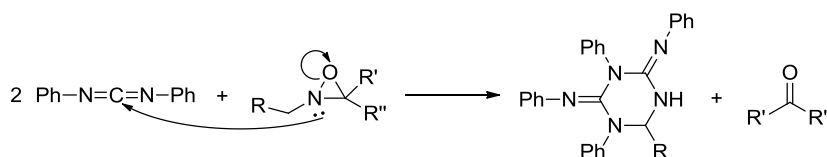transformation. Interestingly, a reaction between diphenyl carbodiimide and *N*-substituted oxaziridine was reported, a reaction that may involve an unusual *tert*-amine nucleophilic reaction (**Scheme 16**).[20]

Scheme 16. Reaction of diphenyl carbodiimide with N-substituted oxaziridine.

Although the reaction of CDI with carboxylic acid has been already applied in industry, the reaction mechanism is not fully clear. Earlier studies show that a mixture of acid anhydrides, *N,N'*-substituted urea and *N*-acyl urea can be obtained.[25] The reaction may first form *O*-acyl *iso*-urea as intermediate and then may undergo a number of different pathways. It seems that the aromatic CDIs favor the reaction to produce *N*-acyl urea, while the aliphatic CDIs lead to anhydride and *N,N'*-substituted urea.[26] Ferrocene carboxylic acid was able to selectively react with aromatic CDIs, giving a high yield of *N*-acyl urea.[27] The reaction between aromatic CDIs and aromatic acids yields generally high selectivity towards *N*-acyl urea.[28] The formed *N*-acyl urea is relatively stable at lower temperature. However, if the *N*-acyl urea is heated at a higher temperature, the decomposition will take place and amide and isocyanate will be generated (**Scheme 17**).[28,29]

Scheme 17. The reaction of aromatic carbodiimide with carboxylic acid to give amide and isocyanate.

$$\text{Ar-N=C=N-Ar} \ + \ \text{R-COOH} \ \xrightarrow{\text{r.t.}} \ \text{Ar-N-C-N-Ar} \ \xrightarrow{\Delta} \ \text{Ar-N-C-Ar} \ + \ \text{R-NCO}$$
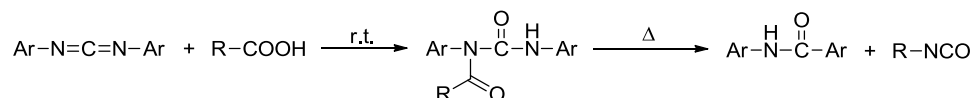
The reaction of CDI with propylene oxide was reported under the mediation of an organotin halide-Lewis base catalyst.[30] It first forms 2-oxazolidinimines, then isomerization may occur, giving 2-imidazolidinone (**Scheme 18**).

Scheme 18. The reaction of carbodiimide with propylene oxide.

$$\text{R-N=C=N-R} \ + \ \text{(epoxide)} \ \longrightarrow \ \text{(oxazolidinimine)} \ \longrightarrow \ \text{(imidazolidinone)}$$
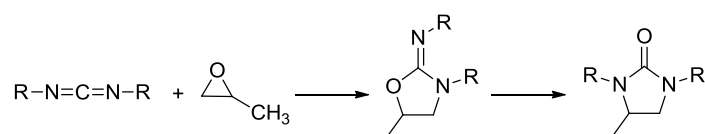
Like isocyanates, CDIs can also undergo dimerization and trimerization, leading to diazetidine and *iso*-melamine respectively. The dimerization of aliphatic CDIs is catalyzed by tetrafluoroboric acid at room temperature, the salt of the dimer is formed as intermediate.[31] Theoretically, diazetidine favors a *Z, Z'*-structure.[19] The dimerization of aromatic CDIs takes place at a higher temperature (> 165°C) and can be catalyzed by tributylphosphine.[32]

Trimerization of aliphatic CDIs is easier than that of aromatic CDIs, the reactive dimethyl carbodiimide undergoes trimerization at room temperature without any catalyst and can further isomerize to 2,4,6-tris-dimethylamino-1,3,5-triazine at above 160 °C (**Scheme 19**).[33] The trimerization of aromatic CDIs usually requires high temperatures. Heating of diphenyl carbodiimide in the presence of *N*-methylhexamethyldisilazane affords the corresponding *iso*-melamine derivative. Crosslinking reactions of oligomeric and polymeric CDIs were observed at 200 - 250 °C, which may be preceded by initial dimerization and trimerization.[34]

Scheme 19. The trimerization of dimethyl carbodiimide and the consecutive reaction.

$$\text{H}_3\text{C-N=C=N-CH}_3 \ \xrightarrow{\text{r.t.}} \ \text{(iso-melamine)} \ \xrightarrow{>160\,°C} \ \text{(triazine)}$$
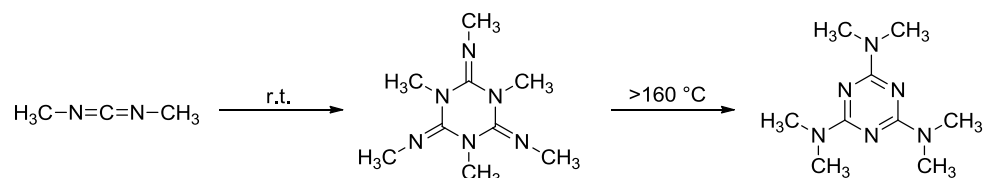
The [2+2] cycloaddition of CDIs with other heterocumulenes, such as isocyanate, isothiocyanate and ketene, is also well-documented. A wide range of CDIs can react with aliphatic or aromatic isocyanates to form 4- or 6-membered-ring (1:2 or 2:1) products (**Scheme**

20). The addition reaction proceeds across the C=N bond of the isocyanate and the 1:2-adduct is majorly obtained as the main product. Interestingly, aliphatic CDIs react faster than aromatic ones, while aromatic isocyanates are more reactive.[19]

Scheme 20. [2+2] cycloaddition of carbodiimide with isocyanate.
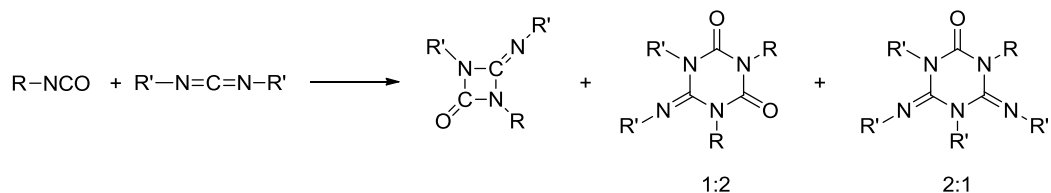
The homopolymerization of aliphatic CDI was reported using *n*-butyl lithium as a catalyst, giving nylon-1 imides. The reaction is thermally reversible, the monomer is regenerated at higher temperature by an unzipping reaction. The living polymerization of aliphatic and aromatic CDIs catalyzed by a series of titanium organic compounds was also reported.[21]

Scheme 21. Homopolymerization of carbodiimide.

1.2.2 Synthesis of Carbodiimides

Although CDI is the formal diimide derivative of carbon dioxide, no direct synthesis route from amine and carbon dioxide is known. The first synthesis of carbodiimide was reported about 1.5 centuries ago.[19] Most CDIs are prepared from isocyanates, *N,N'*-disubstituted ureas and *N,N'*-disubstituted thioureas.
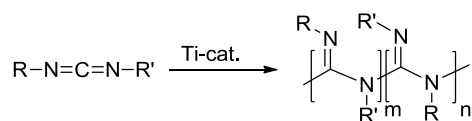
Preparation of CDIs from *N,N'*-disubstituted thioureas by desulfurization is the earliest reported route. The first efficient synthesis route of aromatic CDIs starts from the corresponding thioureas and yellow mercuric oxide (**Scheme 22**).[25] Lead oxide may also be used in the preparation of some CDIs, but are not as efficient as yellow mercuric oxide and in some cases may not work, all depending on the substituents. Since water is also formed during the reaction, a dehydration agent, such as $CaCl_2$, $NaSO_4$, $MgSO_4$ and $MgCO_3$, is also required to prevent the hydrolysis of CDI to urea. Several CDIs can be prepared using this method, including dialkyl-, alkyl aryl-, diaryl- and heterocyclic CDIs. A dehydrating agent for the preparation of aliphatic CDIs is not necessary.

Scheme 22. Synthesis of diphenyl carbodiimide by yellow mercuric oxide.
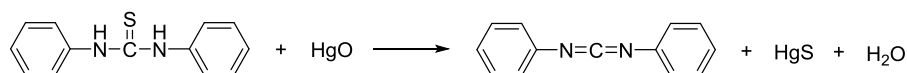
Over time, many chemical compounds were reported as desulfurization agent for this reaction. As an example, a series of sulfur chlorides and their derivatives, such as SCl_2, S_2Cl_2, $SOCl_2$, SO_2Cl_2, $MeSO_2Cl$ and $PhSO_2Cl$ were used.[35–37] Phosgene, thiophosgene and triphosgene were also reported as an efficient desulfurization agent to prepare varies CDIs in good yield.[19,38] An excess of phosgene derivatives may lead to side reactions.

Scheme 23. Synthesis of carbodiimide from phosgene and the accompanied side reaction.
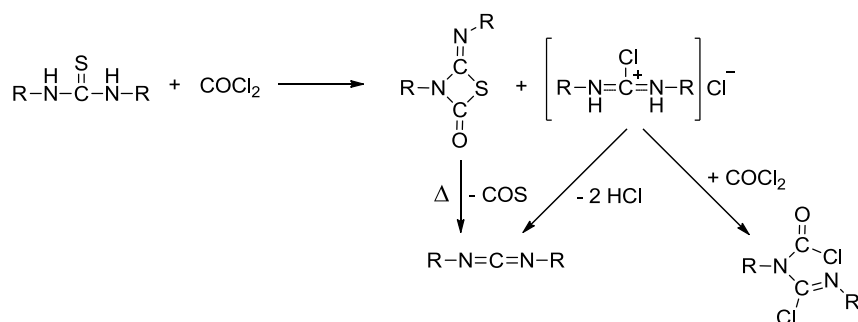
Aliphatic CDIs can also be efficiently produced by oxidation of thiourea by alkaline hypochlorite. Alkali chlorite in the presence of cuprous salt can also be used for this reaction.[39] This method was then also used to prepare aliphatic biscarbodiimide.[40] The desulfurization reaction may also take place in the presence of a CDI. The reaction is an equilibrium reaction and used to prepare heterocyclic compounds.

Scheme 24. Synthesis of aliphatic carbodiimide from sodium hypochlorite.
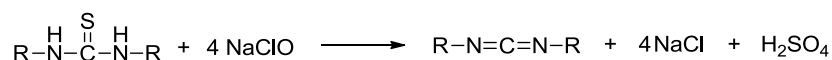
The routes to prepare CDIs from *N,N'*-disubstituted urea mostly also work for the corresponding thioureas using phosphor-containing compounds as reagents, such as phosphorous pentoxide and phenyl dichlorophosphoridate.[19,41] One of the most commonly used methods to prepare CDIs from urea is to use triphenylphosphine or its derivative, triphenylphosphine dibromide in the presence of triethylamine (**Scheme 25**).[42,43]

Scheme 25. Synthesis of carbodiimide from triphenylphosphine, triethylamine and carbon tetrachloride.
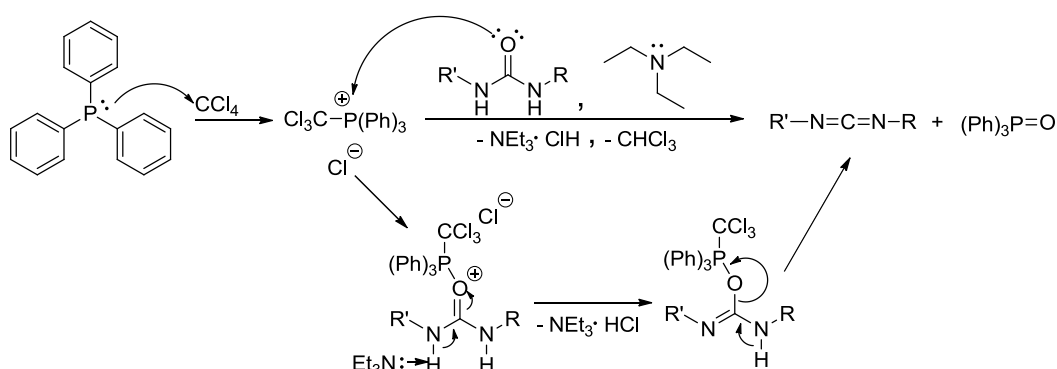
Symmetrical CDIs can also be prepared from the corresponding isocyanates. The reaction often takes place at above 180 °C, but very slowly. The unsymmetrical isocyanate dimer is supposed to be formed as an intermediate (**Scheme 26**).[44]

Scheme 26. Formation of carbodiimide from isocyanate without any catalyst.
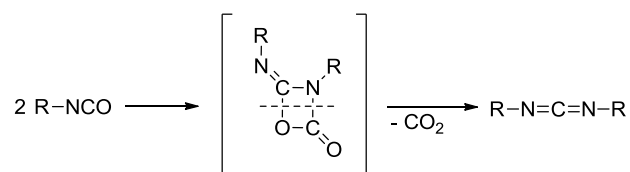
Today, the symmetrical CDIs are produced in the industry mainly using catalytic amounts of phospholine oxides, a procedure based on the discovery of Campbell and Monagle in 1962.[45] The reaction can be performed in bulk or in an organic solvent. The most efficient catalyst in this catalytic family is 1,3-dimethylphospholine oxide. However, 1-ethyl-3-methylphospholine oxide and 1-phenyl-3-methyl phospholine oxide (MPPO) are more commonly used on account of an easier production route. The mechanism of the catalysis comprises a [2+2]-cycloaddition of the isocyanate and the phospholine oxide to form a phosphine imine (iminophosphorane) intermediate.

Scheme 27. Reaction pathway of 1-phenyl-3-methyl phospholine oxide catalyzed carbodiimide formation.
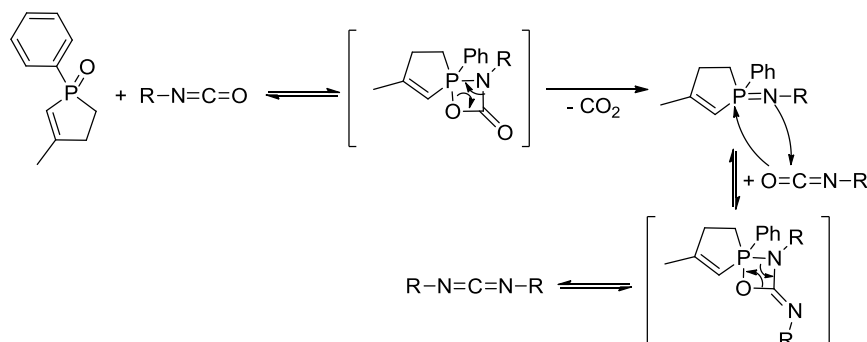
Later, many phospholines and phospholanes, as well as their oxides and sulfides, were also identified as catalyst in the CDI preparation.[46] The catalytic activity of the catalysts is found as follows: phosphine oxide > phosphinate > phosphonate > phosphate.[19,47] Corresponding catalytic activity for triphenylarsine oxide and triphenylantimony oxide have also been reported.[48] Moreover, a solid phase catalyst in form of a phospholene oxide modified divinylbenzene/styrene copolymer was also developed, specifically for the industrial production of the so-called "liquid MDI" (CDI-modified 4,4'-MDI).[19]

Polymeric CDIs are also easily produced from corresponding aliphatic or aromatic diisocyanates using phospholine oxide as a catalyst. However, a linear polycarbodiimide with high molecular weight cannot be obtained, because of a [2+2]-cycloaddition between isocyanate and CDI that takes place and results in crosslinking during the production. Although a linear polycarbodiimide with high molecular weight cannot be produced, an oligomeric CDI containing isocyanate end groups (also called oligomeric α,ω-diisocyanatocarbodiimides) can be produced from sterically hindered diisocyanates using a strong base as catalyst.[46]

Scheme 28. Synthesis of α,ω-diisocyanatocarbodiimides from sterically hindered diisocyanates.
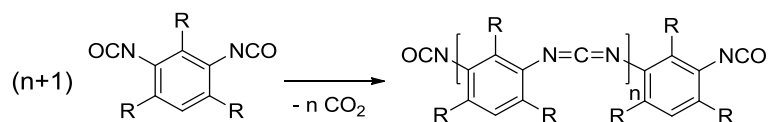
1.2.3 Applications of Carbodiimides

Aliphatic CDIs are useful compounds in the organic and bioorganic synthesis. For example, CDIs are often used as coupling agents, which promote the reaction of carboxylic acids with compounds consisting of amino group, hydroxyl group or carboxyl group in the total synthesis

of valuable compounds, including polypeptide, nucleotide and β-lactam antibiotics. The CDIs with primary alkyl substituents appear thermally less stable.[19] The most widely used aliphatic CDIs are dicyclohexylcarbodiimide (DCC) and diisopropyl carbodiimide (DIC). Some water-soluble CDIs, e.g. 1-ethyl-3-(3-dimethylaminopropyl)carbodiimide (EDC) are also used in some special applications, such as in combination with *N*-hydroxysuccinimide for the immobilization of acidic biomolecules.[49] Such water-soluble CDIs often have a tertiary amino group and can be converted to quaternary ammonium salt in the presence of an alkylation agent, like methyl iodide.

Scheme 29. The reaction of a carboxylic acid with an aliphatic carbodiimide and consecutive reactions with common nucleophilic entities.
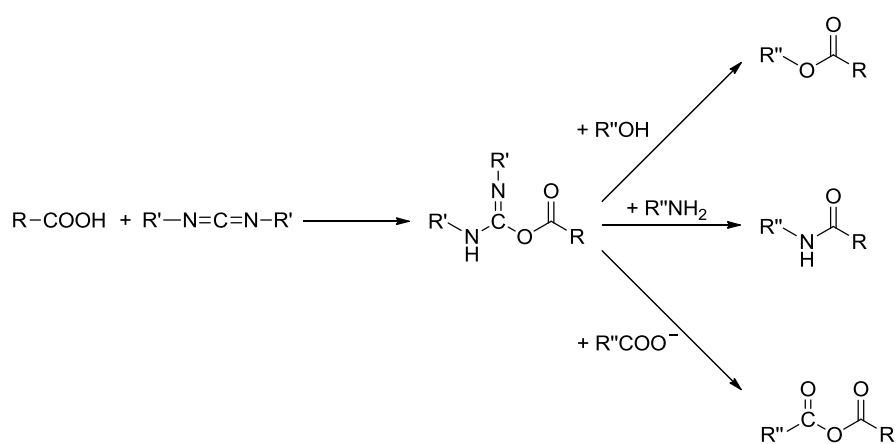
DCC is used as dehydration agent in inter- and intramolecular esterification reactions. The reactions should be carried out under Steglich conditions. After the coupling reaction, a dicyclohexyl urea is formed, which is insoluble in most organic solvents and thus can be easily removed from the reaction system. It is noted that traces of dicyclohexylurea remaining in the reaction system may disrupt the subsequent chromatographic purification. In this case, DIC and EDC may preferably be used. DIC is better suitable for solid phase synthesis on account of its better solubility in solvents like dichloromethane. EDC and its corresponding urea are easier removed completely, making use of their good water-solubility.[50]

Merrifield used DCC for the amide bond formation in his Nobel-price work of automated stepwise synthesis of polypeptides on the solid phase.[51] The synthesis generally involves two steps: a peptide chain is first attached to a polymer bead, then the following peptides react with the deprotected amino group using DCC as a coupling agent. Separation and purification of the polypeptide chain can be simply accomplished by filtering and washing the beads with appropriate solvents. A similar reaction of CDI is also used in DNA-synthesis.[52]

Scheme 30. Merrifield synthesis for the preparation of polypeptides using dicyclohexylcarbodiimide (DCC) as a coupling agent.
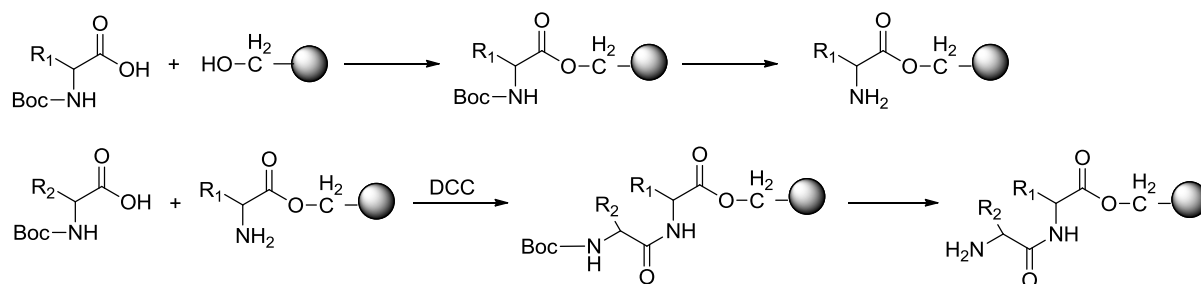
Aliphatic CDIs are widely used in the total synthesis of β-lactam antibiotics. Sheehan used DCC in his Nobel-price work of the total synthesis of phenoxymethylpenicillin by the ring closure of natural penicilloic acid. DCC was used to form the amide bond from carboxylic acid and a secondary amino group.[53] Later, DIC was used in the production of trityl penicillin.[54]

Another application of DCC is in the formation of organic carbonates from alcohols and carbon dioxide. The reaction takes place under mild conditions with high selectivity and acceptable rate. During the reaction, DCC first reacts with alcohol to form *O*-alkyl *iso*-urea which then interacts with a second alcohol molecule via hydrogen bonding and CO_2, giving a cyclic intermediate (**Scheme 31**).[55]

Scheme 31. Synthesis of carbonates from alcohol and carbon dioxide promoted by dicyclohexylcarbodiimide.
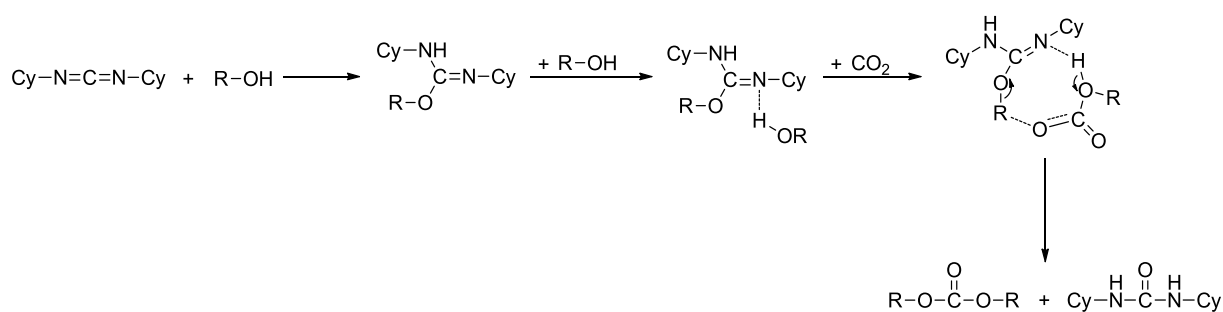
Furthermore, CDIs are also often used in the synthesis of proteins, DNA and RNA. CDIs are members of "zero-length" protein crosslinking reagents. The name "zero-length" is based on the fact that CDI is one of the lowest molecular weight reagents to induce the formation of amide linkages between carboxylates and amines.[56] Thus, CDI is widely used in forming conjugates between two protein molecules, a protein and a peptide or an oligonucleotide and a protein. In the synthesis of nucleotides, EDC is used together with cyanogen bromide as a coupling agent for the template-directed assembly of DNA duplexes and DNA-RNA hybrids.[57]

Compared to aliphatic CDIs, aromatic CDIs and polymeric CDIs are more often used commercially, on account of their higher reactivity and more economical production. However, aliphatic CDIs are more often used as cross-linker in industrial coating and adhesive applications, where aqueous carboxyl acrylates act as main binders, on account of their higher inreactivity against water, low toxicity and higher photo-stability. [58]

The sterically hindered monomeric and oligomeric CDIs are being utilized as stabilizers in ester-based polymers, such as polyester, polyester-based polyurethane, and polycarbonate. The carboxylic acid formed in the hydrolysis reaction could autocatalyze the hydrolysis of the polyesters. CDI is used to scavenge the carboxylic group rapidly and improve the polymer's general resistance towards hydrolysis. [46,59–61]

The reactivity of aromatic CDI against carboxylic acid was also utilized to prepare polyamides. A novel sequential self-repetitive reaction (SSRR) was reported to prepare the polyamide with narrow molecular weight distributions (MWD) from diisocyanate and diacid.[62] A sterically hindered CDI, *N,N'*-bis(2,6-diisopropylphenyl) carbodiimide was added as the reaction initiator. The reaction involves *in situ* generation of CDI groups with a different reactivity from diisocyanate in the presence of a CDI catalyst, giving control over the MWD. Segmented thermoplastic poly(ether amides) and poly(ester amides) can so be obtained.

Scheme 32. "SSRR" polyamide synthesis from diisocyanate and diacid using sterically hindered carbodiimide as initiator and 1,3-dimethyl-3-phospholine oxide (DMPO) as a catalyst.
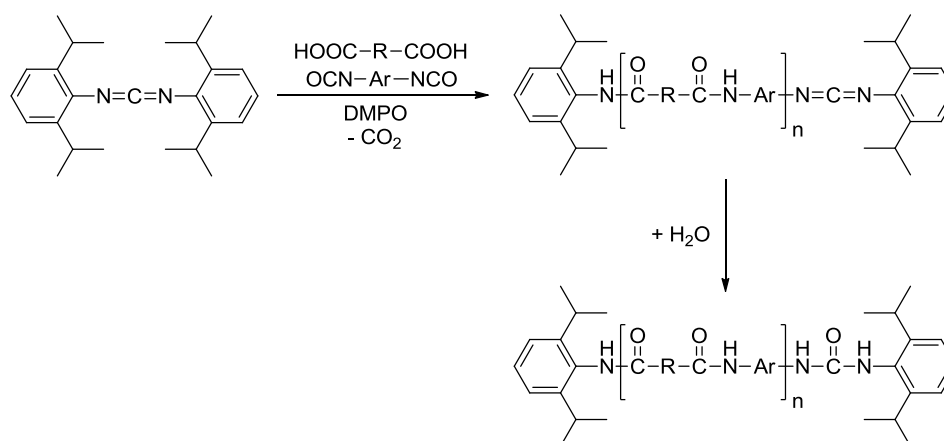
CDIs have also been found in numerous applications in the polyurethane industry. Based on the reaction between CDI and isocyanate to form uretdione, a CDI catalyst is often added into the 4,4'-MDI to form small amount of CDI groups, in order to disrupt the crystal structure of the MDI and to produce a liquid product.[63] Low-density rigid foams with open cells can be

produced from polymeric MDI in the presence of a CDI catalyst, such as phospholene oxide.[64] Carbon dioxide is generated during the reaction, which is also used as a blowing agent. Hydrogen-containing fluorocarbons (HFC) can also be added as physical blowing agents. Polycarbodiimide foams have very different properties to those of polyurethane and polyisocyanurate foams. Their heat stability and flammability properties were reported to be improved.[19] Modification of polycarbodiimide foams with urethane and isocyanurate segments have also been reported.[65] However, introduction of urethane linkages will lead to a decrease of the thermal stability.

1.3 Model-fitting and Model-free Kinetic Studies

Physical and chemical changes during polymerization have been studied by differential scanning calorimetry (DSC) and thermogravimetry (TGA).[66] Although the thermally stimulated processes proceed through multiple stages, some kinetic models have been developed to simulate the progress as one single reaction, such as n^{th} order model and the Kamal-Sourour model.[2,67] With these kinetic models, overall thermal parameters such as the apparent activation energy of the whole process can be determined.

The simplest model is n^{th} order model. It can be expressed as:

$$\frac{d\alpha}{dt} = k(1 - \alpha)^n \tag{1}$$

Where α is the conversion degree, $d\alpha/dt$ is the conversion rate, n is the order of the reaction. The parameter k is the rate constant, which is assumed to have a temperature dependence according to the Arrhenius equation:

$$k = A \cdot e^{-(E\alpha/RT)} \tag{2}$$

Here, A is the pre-exponential factor, E_a is the apparent activation energy, R is the gas constant (R = 8.314 J/mol·K) and T is the absolute temperature. According to **Equation 1**, a rate maximum is achieved at the beginning of the reaction for an isothermal process. However, a different kinetic behavior is often observed in thermal curing. Physical transitions such as phase separation, gelation and vitrification that occur at a later stage during the thermally stimulated processes can make the kinetics more complicated.

The nth order model was appropriately modified to account for such effects by adding more terms, which makes it more applicable to auto-accelerated processes, such as in the curing process of the epoxy-based resins and the polyurethanes (**Equation 3**).[68–70]

$$\frac{d\alpha}{dt} = (k_1 + k_2\alpha^m)(1 - \alpha)^n \tag{3}$$

Where *m* is also a reaction order, which describes the contribution of the autocatalytic effect on the kinetics. k_1 and k_2 are the rate constants that are dependent on the temperature.

Presuming a kinetic model, no matter whether a mechanistic or an empirical model, will always have limitations.[2] Thus, isoconversional kinetic studies are relatively reliable since the kinetic data is obtained without assuming any kinetic model. Furthermore, the isoconversional kinetic studies are more applicable for processes with complex mechanism, since the activation energy obtained is often a function of the conversion.

The isoconversional methods are based on the hypothesis that the mechanism of the process is independent of the temperature change. Under this assumption, the conversion rate can be expressed as follows:

$$\frac{d\alpha}{dt} = k \cdot f(\alpha) = A \cdot e^{-(E_\alpha/RT)} \cdot f(\alpha) \tag{4}$$

Here, *f(α)* is a function that only depends on the reaction mechanism and is independent on the temperature change.

Since several conversion rates at a constant extent of conversion are needed for the isoconversional methods, multiple temperature programs are usually performed, including dynamic measurement with different heating rates and isothermal measurement at different temperatures. It is worth noting that each kinetic equation is applicable to a certain conversion extent and to the temperature region that is related to this conversion extent. Thus variations of activation energy with the conversion may be found, which would indicate a complex process consisting of multiple steps.[66]

1.3.1   Friedman Model

The Friedman model is also called the differential method. For isothermal measurements, the activation energy can be easily determined by transforming **Equation 4** into the logarithm form and plotting *ln(dα/dt)* as a function of *-1/RT*, the slope of the plotting is the activation energy E_α.[71]

$$\ln(\frac{d\alpha}{dt})_{\alpha,i} = \ln[A \cdot f(\alpha)] - \frac{E_\alpha}{RT_{\alpha,i}} \tag{5}$$

The subscript *i* in **Equation 5** denotes a different heating rate. For the dynamic measurement, the temperature is increased with a constant rate. Thus *dα/dt* can be expressed as:

$$\frac{d\alpha}{dt} = \left(\frac{dT}{dt}\right)\frac{d\alpha}{dT} = \beta\frac{d\alpha}{dT} \tag{6}$$

Where β is the heating rate. In this case, **Equation 5** can be transformed as:

$$\ln\beta\left(\frac{d\alpha}{dT}\right) = \ln[A \cdot f(\alpha)] - \frac{E_\alpha}{RT} \tag{7}$$

Because the *f(α)* is independent on the temperature and heating rate, *ln[A·f(α)]* is constant. For a certain conversion, the activation energy can be determined by plotting *ln[β(dα/dT)]* as a function of *-1/RT*.

1.3.2 Integral Methods

Since the application of the Friedman model requires numerical differentiation of the conversion α versus *T*, it often leads to systematic error in the determination of the activation energy.[2,66,72] Thus, a series of integral isoconversional methods were developed. For the isothermal measurement, **Equation 4** can be transformed as:

$$g(\alpha) \equiv \int_0^\alpha \frac{d\alpha}{f(\alpha)} = A \cdot \exp\left(-\frac{E_\alpha}{RT}\right) \cdot t \tag{8}$$

Where *g(α)* is the integral form of the conversion. **Equation 8** can also be transformed as:

$$-\ln t_{\alpha,i} = \ln\left[\frac{A_\alpha}{g(\alpha)}\right] - \frac{E_\alpha}{RT} \tag{9}$$

By plotting *-ln t* as a function of *-1/RT*, the activation energy can be obtained. For the dynamic measurement, **Equation 8** can also be transformed as:

$$g(\alpha) \equiv \frac{A}{\beta}\int_0^{T_\alpha} \exp\left(-\frac{E_\alpha}{RT}\right) \cdot dT = \frac{A}{\beta}I(E,T) \tag{10}$$

Where *I(E, T)* is the temperature integral which cannot be exactly calculated. Fortunately, several approximations were suggested to solve it. The most popular method is the Flynn-Wall-Ozawa (FWO) model based on the Doyle approximation.[73–75] For $20 < E_\alpha/RT < 60$, **Equation 9** can be transformed as:

$$\ln\beta_i \approx \text{Const.} - \frac{1.05 \cdot E_\alpha}{RT_{\alpha,i}} \tag{11}$$

Another approximation method was supposed by Kissinger, Akahira and Sunose (KAS) using the more accurate approximation proposed by Coats and Redfern.[76] For $20 < E_\alpha/RT < 50$, **Equation 9** can be transformed as:

$$\ln\frac{\beta_i}{T_{\alpha,i}{}^2} \approx \text{Const.} - \frac{E_\alpha}{RT_{\alpha,i}} \tag{12}$$

The KAS model can be traced back to the Kissinger model.[77] The equation form is actually very similar to **Equation 12**, but for the Kissinger model, only the maximum of the conversion peak is used to calculate the average activation energy for the whole process.

$$\ln\frac{\beta_i}{T_{p,i}{}^2} \approx \text{Const.} - \frac{E_\alpha}{RT_{p,i}} \tag{13}$$

Here $T_{p,i}$ refers to the temperature where the rate maximum is located. The location of the peak maximum is dependent on the heating rate and doesn't occur at the same conversion.

Later, Vyazovkin suggested an advanced integral method based on calculating the minimum of the function $\Phi(E_\alpha)$.[66,78]

$$\Phi(E_\alpha) = \sum_{i=1}^{n}\sum_{j\neq 1}^{n}\frac{J[E_\alpha, T_i(t_\alpha)]}{J[E_\alpha, T_j(t_\alpha)]} \tag{14}$$
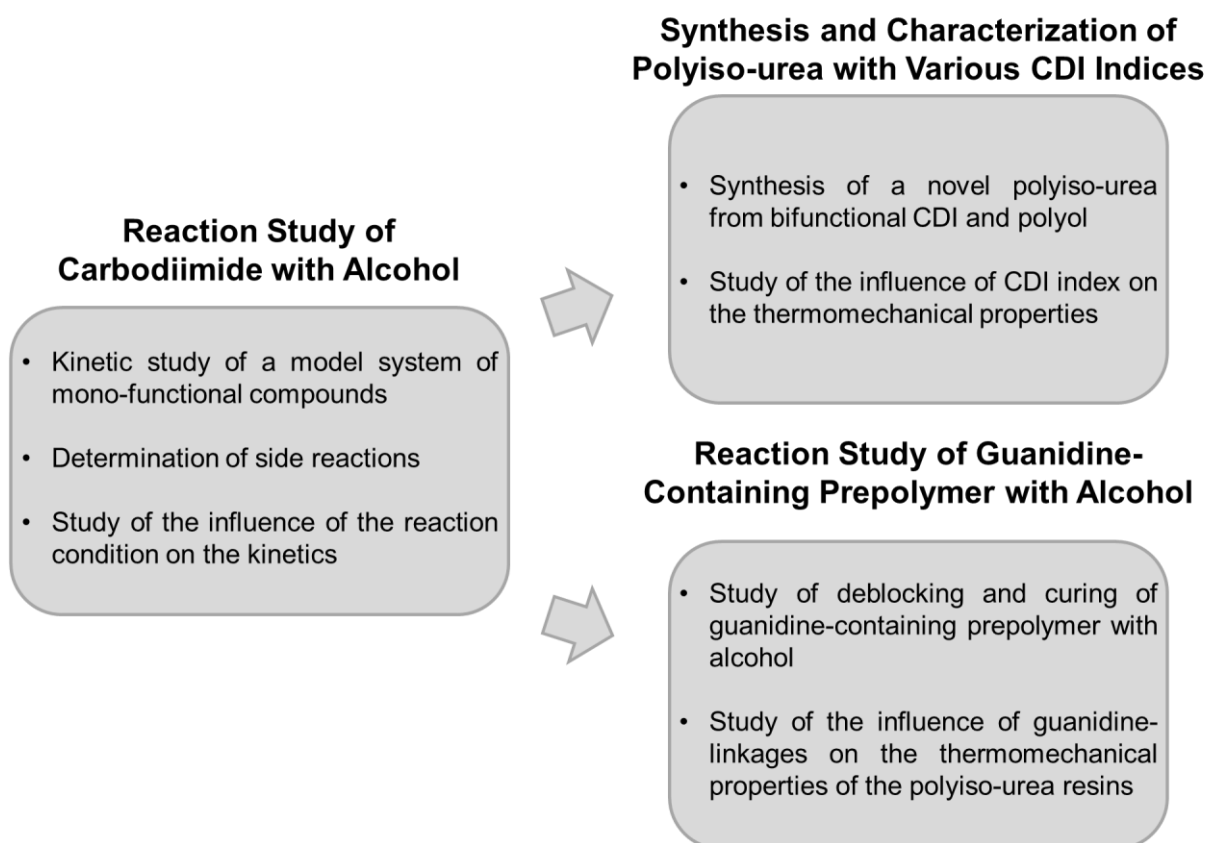
Where i and j are the ordinal numbers of two experiments with different heating rates. The integration form J can be calculated as follows:

$$J[E_\alpha, T_i(t_\alpha)] \equiv \int_{t_{\alpha-\Delta\alpha}}^{t_\alpha} \exp\left[\frac{-E_\alpha}{RT_i(t)}\right] dt \tag{15}$$

2   Motivation

Conventional polyurethanes are produced from polyisocyanate and polyol. The inherent toxicity of polyisocyanate is a major issue in their production.[2] A number of alternative pathways were suggested to produce the so-called non-isocyanate polyurethanes.[82–85] However, on account of the inherent reversibility of the carbamate bond, the release of isocyanate e.g. after a thermal treatment shows that carbamates remain potential toxic.[2] In order to develop polyurethanes comparable versatile products, novel polymers based on CDI were suggested as a new solution. This thesis aims at gaining insights into the mechanistic process of the reaction between CDI and the hydroxyl entity by studying the reaction kinetics of model systems in form of mono-functional compounds. The insights should be used to progress the polymer chemistry involving CDIs.

Synthesis and Characterization of Polyiso-urea with Various CDI Indices

- Synthesis of a novel polyiso-urea from bifunctional CDI and polyol

- Study of the influence of CDI index on the thermomechanical properties

Reaction Study of Carbodiimide with Alcohol

- Kinetic study of a model system of mono-functional compounds

- Determination of side reactions

- Study of the influence of the reaction condition on the kinetics

Reaction Study of Guanidine-Containing Prepolymer with Alcohol

- Study of deblocking and curing of guanidine-containing prepolymer with alcohol

- Study of the influence of guanidine-linkages on the thermomechanical properties of the polyiso-urea resins

3   Results and Discussion

3.1 Reaction Study of Carbodiimide with Alcohol

The intermolecular addition of alcohols to CDIs gives *iso*-urea. The reaction is very slow at room temperature and may request a catalyst, such as HBF$_4$,[86] copper salts,[26] alkoxides[22] and transition metal complexes.[87,88] Recently, it was reported that 1,5,7-triazabicyclo[4.4.0]dec-5-ene (TBD) and its alkali metal salts can also catalyze this reaction.[89] Generally speaking, catalysts either act as Lewis acid towards CDI or as a base to increase the nucleophilicity of the O-H bond of alcohol.
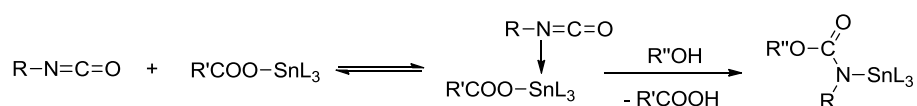
In this work, the reaction of aromatic CDIs with alcohols is catalyzed by titanium isopropoxide (TTIP) and dimethyltin dineodecanoate (DMTDN). Titanium alkoxides are well-known as effective catalysts for esterification and transesterification reactions.[90] The reactions of CDIs catalyzed by titanium alkoxides have also been extensively studied. The catalytic metathesis induced by insertion of CDI into TTIP is an example.[91]   Another report is on the homopolymerization of CDI catalyzed by titanium alkoxides.[21] Both studies show that titanium alkoxides can activate the cumulative N=C=N bond by coordination of the nitrogen atoms to the titanium metal center (**Scheme 33**).

Scheme 33. Insertion of CDI into titanium alkoxide.[21]
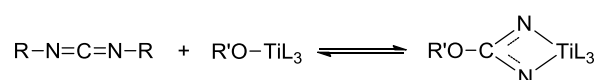
Organotin carboxylates are important catalysts in polyurethane production. On account of the societal importance of polyurethane, many efforts have been taken to study the mechanism of the organotin catalyzed carbamate formation from isocyanate and alcohol. Recent studies tend to support the intermediacy of a N $\rightarrow$ Sn coordination of the isocyanate [2,92].

Scheme 34. The initial step of organotin carboxylate catalyzed isocyanate/alcohol reaction proposed by Bloodworth.[2]

In this chapter, the reaction of aromatic CDIs with alcohols catalyzed by TTIP and DMTDN was carried out in bulk, which is of relevance to the industrial practice. A model was selected
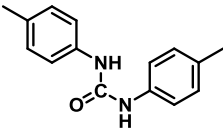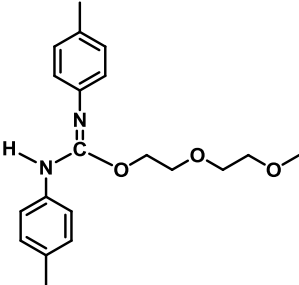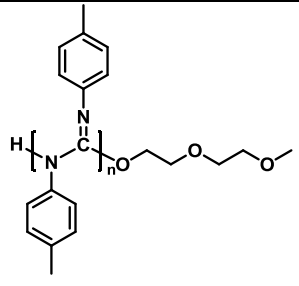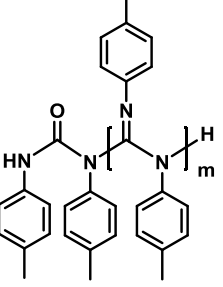
in form of the reaction of di-*p*-tolyl carbodiimide (*p*-DTC) with a primary alcohol. Performing initial reactions gave evidence for an obvious difference in conversion between both reactants, which could be attributed to a side reaction between CDI and the initial product *iso*-urea. The side reaction was studied with different reactants at varying temperatures. A sterically more hindered CDI, di-*o*-tolyl carbodiimide (*o*-DTC) was also used to study the influence of the steric effect on the side reaction. A primary alcohol and a secondary alcohol were chosen in form of diethylene glycol monomethyl ether (DGME) and 1-methoxy-2-propanol. These both have ethylene glycol or propylene glycol based units in the structure and may be considered derivatives of polyethylene glycol (PEG) and polypropylene glycol (PPG), soft segment components of PU systems.

3.1.1 Kinetic Study of the Model Reaction

The model reaction between *p*-DTC and DGME (molar ratio: 1:1) catalyzed by TTIP was studied at 60 °C in bulk for 1 hour to generate the corresponding *iso*-urea (**1-1** in **Table 1**). It was found that while the conversion of *p*-DTC reached ca. 90%, the conversion of DGME was only ca. 60%. Apparently, a side reaction occurs that leads to the unbalanced conversions of the *p*-DTC and DGME. In order to identify the byproducts, the product mixture of the reaction between *p*-DTC and DGME was analyzed by ESI−TOF mass spectrometry (**Figure 2**). Three species were identified in the spectrum and their structures are shown in **Table 1**. The major compound was identified as the expected addition product of *p*-DTC and DGME, the *iso*-urea **1-1** (343 Da). There were also some polydisperse guanidine products (**1-2,** n = 2 − 4 in **Table 1**), originating from DGME and 2 − 4 *p*-DTC repeating units. These were formed by the reaction of the *iso*-urea **1-1** with several mols of *p*-DTC. Thus, the formation of the guanidine-type products acted as a side reaction that was in competition with the formation of *iso*-urea and this leads to the unequal conversion of both reactants.

A further group of species (**1-3** in **Table 1**) is di-*p*-tolyl urea (**0-1**) and its addition products with several mols of *p*-DTC. IR spectroscopy on the reaction mixture gives no evidence of urea formation during the reaction. Therefore, it is supposed that the urea related compounds were formed in the mass spectrometrical analysis procedure.

Table 1. Structural assignments for the masses observed in the ESI−TOF mass spectrum of the product mixture of the reaction of *p*-DTC with DGME.

Fragment Species	Structure	$(M + H)^+$ (Da)
0-1		241.089
1-1		343.138
1-2		565.214 (**n = 2**)
		787.290 (**n = 3**)
		1009.363 (**n = 4**)
1-3		463.168 (**m = 1**)
		685.236 (**m = 2**)

Scheme 35. Pathways of the reaction between CDI and alcohol at low temperatures in bulk.
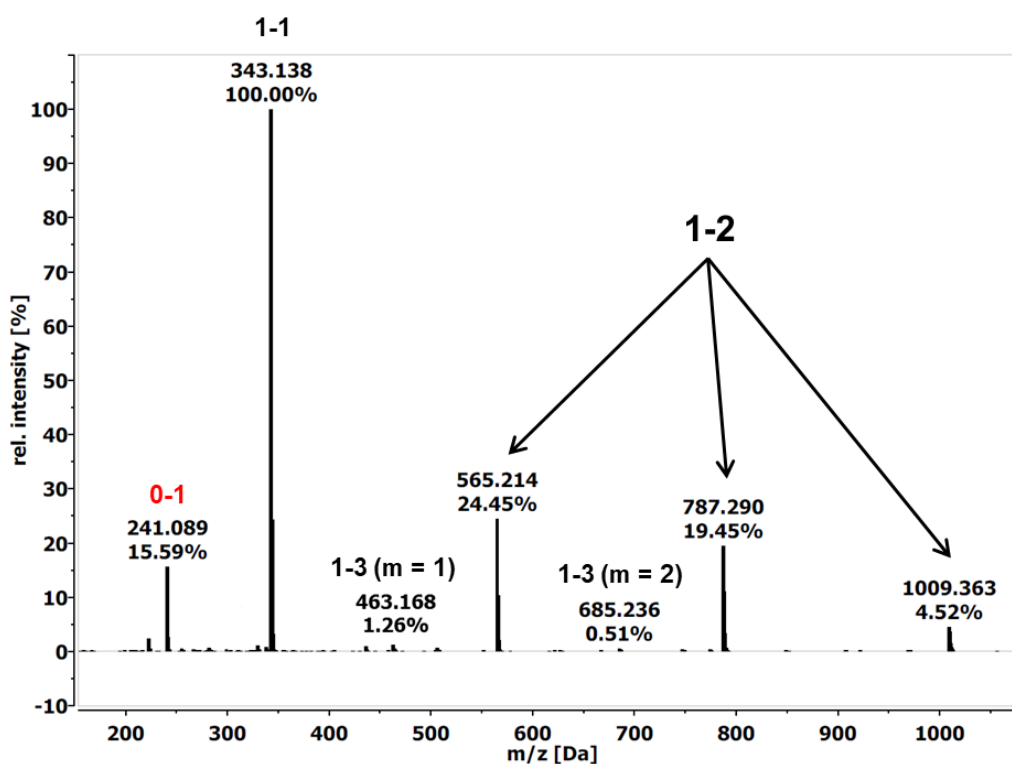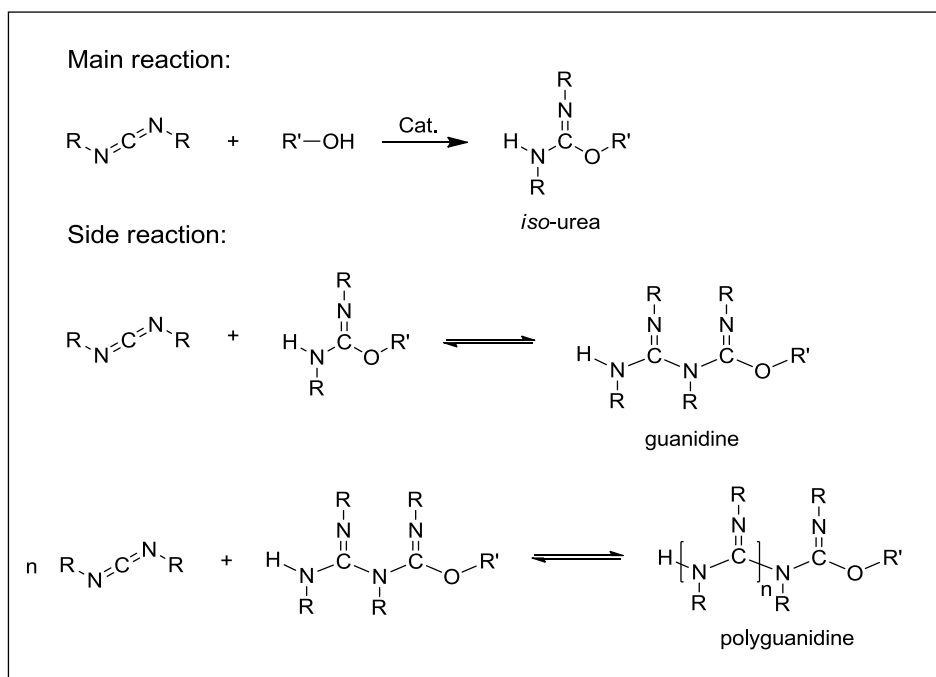
Figure 2. ESI−TOF mass spectrum of the product mixture of the reaction between *p*-DTC and the primary alcohol at 60 °C using 0.03 mol% TTIP as the catalyst.

A further series of reactions between *p*-DTC and the *iso*-urea **1-1** (molar ratio: 1:1) were carried out at temperatures of 60 °C, 100 °C and 130 °C. The *iso*-urea **1-1** was prepared at 100 °C from *p*-DTC and DGME using 0.03 mol% TTIP as the catalyst (about quantitative after 1 h, catalyst was not removed). The conversion of *p*-DTC in reaction with the *iso*-urea **1-1** after 1 h was found to be 74.2% at 60 °C and 38.5 % at 100 °C. At 130 °C, the conversion of *p*-DTC could not be detected, which indicates that the reaction of the *iso*-urea **1-1** and *p*-DTC was not proceeding at temperatures above 130 °C. Furthermore, when the reaction product that was prepared at 60 °C was heated to 130 °C for 60 min, the concentration of *p*-DTC was increased again and over 95% *p*-DTC was regenerated. This indicates that the reaction between CDI and *iso*-urea is reversible and is sensitive to temperature. The reaction of *p*-DTC and the *iso*-urea **1-1** was monitored by FT-IR spectroscopy and evaluated by integration of the CDI absorbances at 2106 and 2130 cm^{-1} (**Figure 3**).
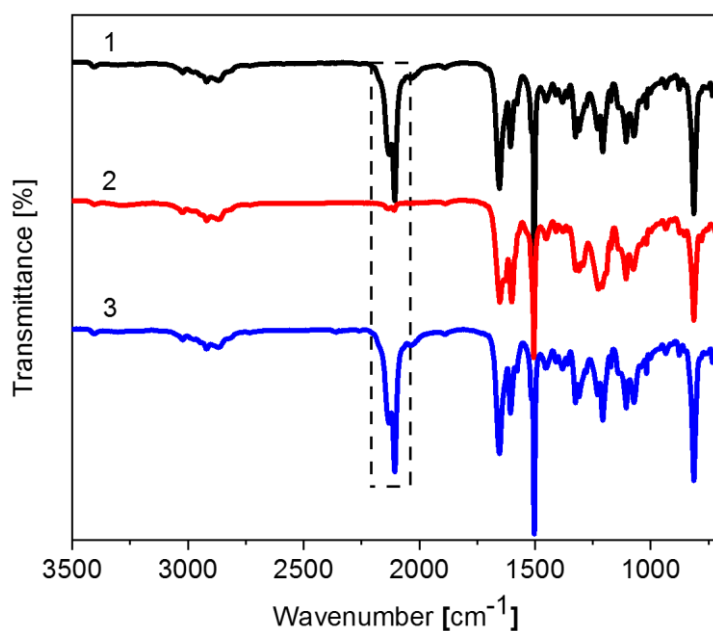
Figure 3. Infrared spectra of the reaction product between *p*-DTC and the *iso*-urea **1-1**. The spectra correspond to the initial reaction mixture (1, black trace), after 60 min at 60 °C (2, red trace), and after consecutive heating for 60 min at 130 °C (3, blue trace).

3.1.2   Influence of Reactants and Catalysts on the Reaction Kinetics

With the establishment of the reversibility of the reaction of CDI and *iso*-urea to the guanidine-type products, several reaction parameters that may influence the reaction kinetics, such as

catalyst and temperature, were studied. It is worth noting that the reaction between CDI and *iso*-urea doesn't request the presence of a catalyst. The guanidine-type byproducts were also found in the reaction between *p*-DTC and DGME in bulk in the absence of a catalyst at 100 °C. Once the *iso*-urea is formed, the imine nitrogen can nucleophilically attack CDI, giving the guanidine-type products. The reaction of CDIs with alcohols was investigated at 60 °C in bulk at various concentrations of TTIP. In order to study the influence of the catalyst on the reaction pathway, the reaction was also carried out in the presence of an organotin catalyst, DMTDN. Furthermore, a sterically hindered CDI, di-*o*-tolyl carbodiimide (*o*-DTC) was used to study the influence of steric hindrance on the side reaction. A primary alcohol, DGME and a secondary alcohol, 1-methoxy-2-propanol were chosen as substrates.

In the reaction between *p*-DTC and DGME (*prim.* ROH in **Table 2**), it was found that the ultimate conversion of the primary alcohol was only 60% to 75% while the conversion of *p*-DTC was basically quantitative (**Table 2**, entries 1 and 2). Taking the highest conversion of the alcohol as a measure of the selectivity of the reaction to *iso*-urea, then DMTDN gives a higher selectivity than TTIP in the reaction of *p*-DTC and primary alcohol. The conversion of the primary alcohol was plotted as a function of the conversion of *p*-DTC (**Figure 4**). Different concentrations of catalyst do not affect the selectivity of the reaction significantly. The reaction rate reveals an order of 0.4 and 0.5 with respect to TTIP and DMTDN concentration respectively in the early stage of the reaction (at t $\rightarrow$ 0, **Figure 37**) between *p*-DTC and the primary alcohol (c.f. **Chapter 5.3.4**). The side reaction between *p*-DTC and the formed *iso*-urea is a consecutive reaction, its importance at the beginning of the reaction is neglected; the obtained reaction orders describe the catalytic action of both catalysts in the main reaction between *p*-DTC and the primary alcohol.

3. Results and Discussion

Table 2. Conversion of carbodiimides and alcohol after 60 min of reaction.

Entry	Catalyst	CDI	ROH	Cat. concentration (mmol/L)	Highest conv. of CDI (%)	Highest conv. of ROH (%)
1	TTIP		*prim.*	3	93	61
2	DMTDN		*prim.*	7	96	73
3	TTIP	*p*-DTC	*sec.*	11	> 99	94
4	DMTDN		*sec.*	13	> 99	83
5	TTIP		*prim.*	13	> 99	94
6	DMTDN		*prim.*	74	88	84
7	TTIP	*o*-DTC	*sec.*	43	88	84
8	DMTDN		*sec.*	214	90	87

[a]Reaction condition: 0.0125 mol of both reactants in bulk, 60°C. [b]Determined by ^{1}H-NMR spectroscopy.
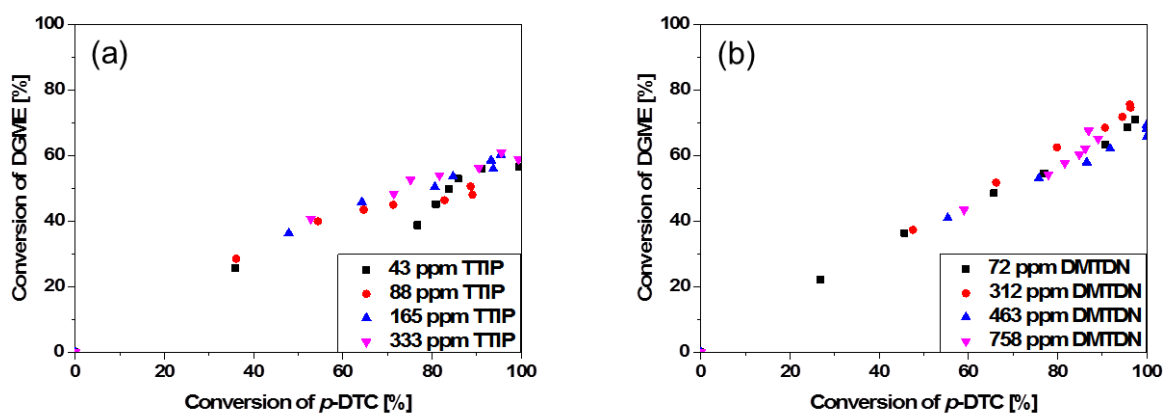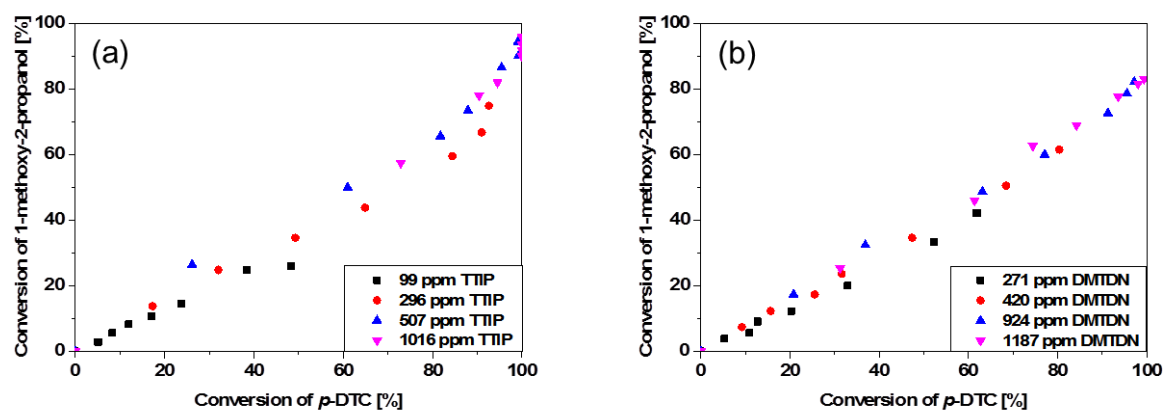

Figure 4. The conversion of DGME as a function of the conversion of *p*-DTC with different concentration of TTIP (a) and DMTDN (b).

In the reaction between *p*-DTC and 1-methoxy-2-propanol (*sec.* ROH in **Table 2**), the conversion of latter is substantially higher than of the primary alcohol (**Table 2**, entries 3 and 4). Higher conversion of alcohol indicates a higher selectivity towards the formation of *iso*-urea. It also shows that there is no significant influence of the catalyst concentration on the selectivity of the reaction (**Figure 5**). The secondary alcohol is less reactive in the reaction with *p*-DTC

compared to the primary alcohol for both catalysts. With the same molar amount of *p*-DTC and catalyst, the reaction rate decreases by a factor of 3 – 5 (**Table 3**).

Figure 5. The conversion of secondary alcohol as a function of the conversion of carbodiimide with different concentration of TTIP (a) and DMTDN (b).

Table 3. The relative rate constants for the reaction between *p*-DTC and both alcohols in presence of 3 mmol/L catalyst at 60 °C in bulk.

ROH	*prim.*		*sec.*	
Catalyst	TTIP	DMTDN	TTIP	DMTDN
Relative Rate Constants	13	5	4	1

The conversions of *o*-DTC and both alcohols are almost 1:1 after 60 minutes of reaction (**Table 2**, entries 5 – 8), indicating a much higher selectivity to *iso*-urea. It is apparent that the consecutive addition over the N-H bond of *iso*-urea is not favorable for *o*-DTC. On account of the steric bulk at the reactive center, *o*-DTC is much less reactive. With the same alcohol and catalyst, the rates of *p*-DTC and *o*-DTC have an approximate ratio 25:1.

Although the conversion of both reactants were almost 1:1, the addition products from *o*-DTC with the corresponding *iso*-urea could still be detected by ESI−TOF mass spectrometry. It is apparent that this side reaction can still take place to a certain extent at low temperature. Evidence for this was also found from the observation that the signal assigned to unreacted *o*-

DTC in the IR spectra had disappeared after the samples were stored overnight at room temperature.

The molecular structure of the guanidine-type product produced from *o*-DTC and DGME was determined by X-ray crystallography (**Figure 6a**). The guanidine-type product contains a repeating amidine structure. The bond length of N2-C13 bond (**Figure 6b**) formed during the reaction between CDI and *iso*-urea was measured to be 1.40 Å, shows no significant difference with N2-C10 bond (1.42 Å) of the *iso*-urea unit and N4-C13 bond (1.41 Å) of the CDI unit. It has been supposed that polyguanidine reveals a helical structure and the dihedral angle of the CDI repeating units is approximately 60°, depending on the imine and amine nitrogen substituents.[21] In this study, the torsion angle of the N-C backbone (such as C19-N2-C13-N3 in **Figure 6c**) was measured to be around 140 °, except the first (-39.9°, N1-C10-N2-C19 in **Figure 6c**) and the last N-C bond torsion (-24.4°, N5-C18-N6-C38 in **Figure 6c**) on account of the unsymmetrical substituent on the terminal carbon or nitrogen atom. The bond lengths, bond angles and torsion angles of the selected bonds are summarized in **Table 4**.
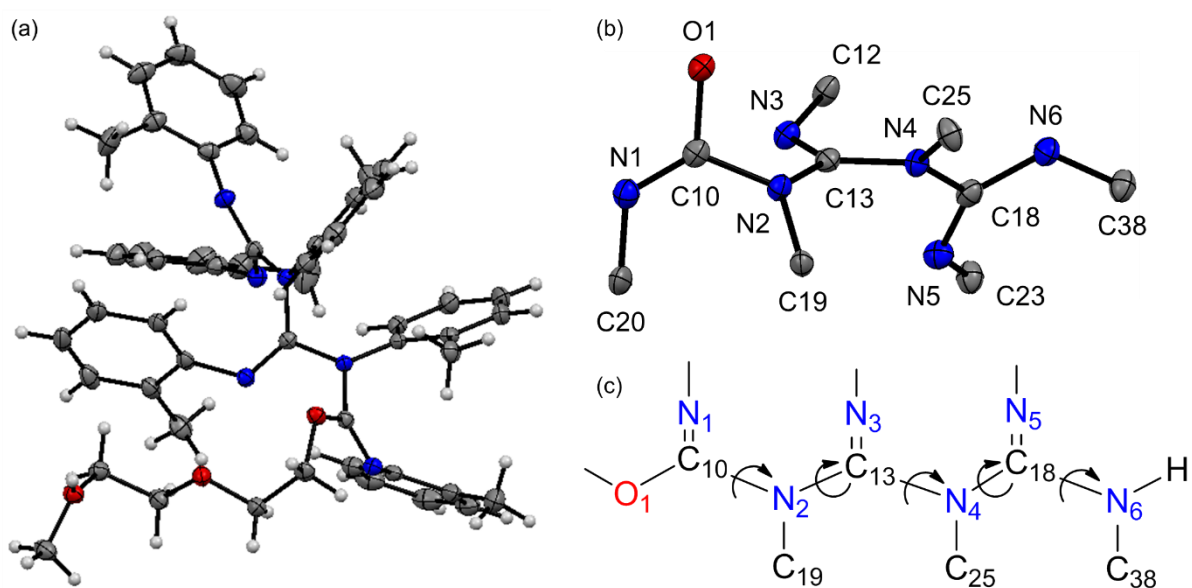
Figure 6. Molecular structure of the guanidine-type compound from crystallographic studies.

Table 4. Selected bond length, angles and torsion angles for the guanidine-type product.

Bonds	Bond length [Å]	Bonds	Bond angles [°]	Bonds	Torsion [°]
O1-C10	1.35	O1-C10-N1	122.8	N1-C10-N2-C19	-39.9
N1-C10	1.26	N1-C10-N2	127.7	C19-N2-C13-N3	135.9
N2-C10	1.42	C10-N2-C19	118.9	N3-C13-N4-C25	137.2
N2-C13	1.40	C13-N2-C19	121.6	C25-N4-C18-N5	143.6
N2-C19	1.43	N2-C13-N3	117.8	N5-C18-N6-C38	-24.4
N3-C13	1.27	N3-C13-N4	128.3		
N4-C13	1.41	C13-N4-C25	117.9		
N4-C18	1.42	C18-N4-C25	123.8		
N4-C25	1.43	N4-C18-N5	116.11		
N5-C18	1.28	N5-C18-N6	130.3		
N6-C18	1.37	C18-N6-C38	125.43		
N6-C38	1.42				

3.1.3 Influence of the Reaction Temperature on the Reaction Kinetics

In order to study the temperature dependence of the guanidine formation, the reaction of *p*-DTC with DGME in a molar ratio of 1:1 was also carried out using 0.03 mol% TTIP as catalyst (**Table 5**). The conversion of DGME increased from 61% at 60 °C to 94% at 100 °C. Concomitantly, the yield of the *iso*-urea **1-1** was increased at higher temperature, indicating fewer guanidine generation. The product mixture of the reaction at 100 °C was therefor also analyzed by ESI−TOF mass spectrometry. Majorly the di-*p*-tolyl urea **0-1**, the *iso*-urea **1-1** and only trace amounts of the guanidine-type product **1-2 (n = 2)** were detected in the spectrum (**Figure 7**). It is apparent that the side reaction between *p*-DTC and the *iso*-urea **1-1** is only kinetically favored at low temperatures on account of the bulk reaction condition, the high concentration of reactants results in the fast formation of guanidine-type products.

Table 5. Conversion scope of carbodiimides and alcohol after 60 min of reaction at different temperatures.

Entry	Catalyst	CDI	ROH	Temp. (°C)	Highest conv. of CDI (%)	Highest conv. of ROH (%)
1				60	96	61
2	TTIP	*p*-DTC	*prim.*	70	97	75
3				80	>99	83
4				100	>99	94

[a])Reaction condition: 0.0125 mol of both reactants in bulk, 0.03 mol% TTIP. [b])Determined by ^{1}H-NMR spectroscopy.
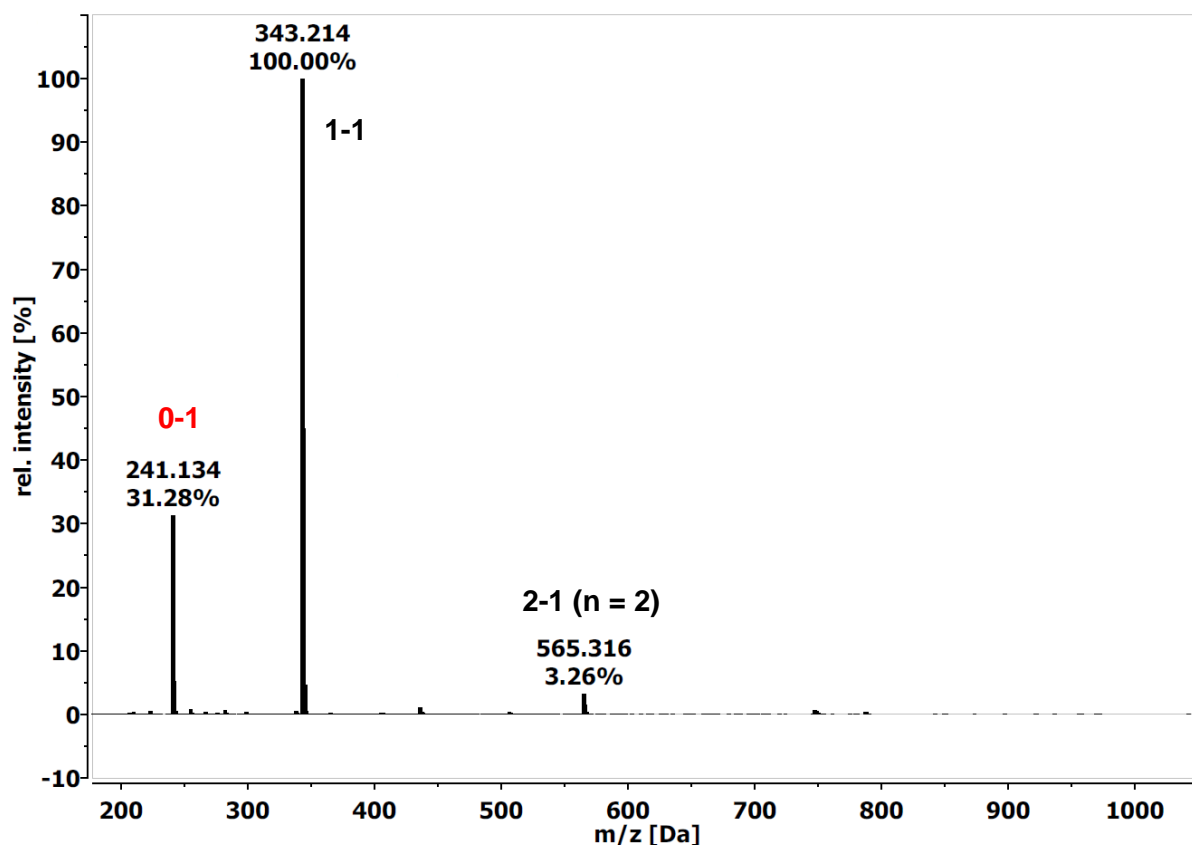
Figure 7. ESI−TOF mass spectrum of the product mixture of the reaction between *p*-DTC and DGME at 100 °C using 0.03 mol% TTIP as the catalyst.

In summary, a side reaction between CDI with the corresponding *iso*-urea was observed during the reaction between equivalent amounts of CDI and alcohol under the bulk reaction condition.

The side reaction only took place at low temperatures, resulting in unbalanced conversion of both reactants. The formed byproduct, polyguanidines are instable at high temperatures, and decompose to CDI and *iso*-urea at above 130 °C.

## 3.2 Synthesis and Characterization of a Novel Polyiso-urea

On account of their similarity in the chemical properties to isocyanates, polymeric CDIs have found applications in polymer chemistry. The polyaddition of polymeric CDIs with polyols gives polyiso-urea (PIU). However, the successful use of bi-functional CDIs (also called biscarbodiimide or dicarbodiimide) as a monomer in polyaddition has not been reported. This may be due to its instability and strong tendency to homo-polymerization.[93,94] Synthesis methods for biscarbodiimide can be traced back to a half century ago. Only some aliphatic biscarbodiimides were successfully synthesized and isolated.[40,94] In this work, an aromatic biscarbodiimide of high-purity was synthesized by dehydration of the corresponding bisureum compound (**Chapter 5.2.3**). The isolated biscarbodiimide was found to be stable at low temperatures and could be used in polyaddition studies.

The initial experiment was performed with the polyaddition of equivalent amounts of biscarbodiimide and poly(tetramethylene oxide) diol (also known as polyTHF, with average molecular weight $M_n = 1000$ g/mol) in order to prepare linear polyiso-urea (**Scheme 36**). The reaction requires thermal activation or a catalyst. TTIP and DMTDN were found to be efficient catalysts for the reaction between CDI and alcohol (**Chapter 3.1**). On account of its high moisture resistance, DMTDN was chosen as a catalyst in this study. However, the formation of linear polymer with high molecular weight could not be achieved. Instead, oligomeric polyiso-urea with a molecular weight of ca. 8500 g/mol was obtained.

Although the preparation of a high molecular linear polyiso-urea was not easy to achieve, it was found that if the biscarbodiimide was added in excess, the biscarbodiimide reacted further with the *iso*-urea groups in the chain, giving guanidine-type linkages in the final polymer. The guanidine linkages will probably exist as side chains and also act as crosslinks between the polyiso-urea oligomers, giving the material a polymer network structure. From the kinetic study of the model system (**Chapter 3.1**), it is expected that the formation of guanidine linkages are only favored at lower temperature. At higher temperature, the guanidine linkages would tend to unzip and the biscarbodiimide would be regenerated, which gives the material a potential

application as a thermally reprocessible resin. Thus, the polyiso-urea products with varying CDI indices (CDI equivalents/polyol equivalents $\times$ 100) were prepared and studied.

Scheme 36. Synthesis of linear polyiso-urea from biscarbodiimide and poly(tetramethylene oxide) diol.
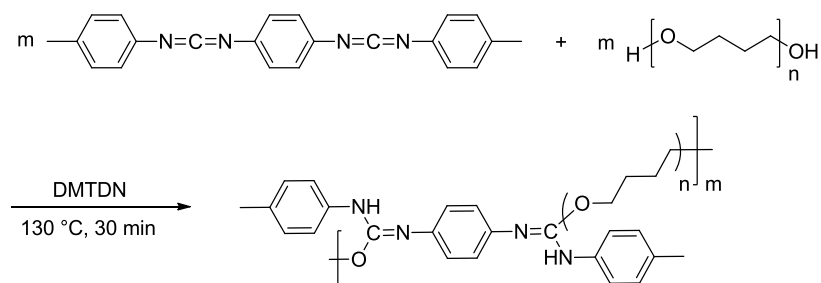
3.2.1 Synthesis of Linear Polyiso-urea and Possible Side Reactions

The experimental study started with the polyaddition of equivalent biscarbodiimide and poly(tetramethylene oxide) diol (polyTHF, $M_n = 1000$ g/mol), in order to create a linear polyiso-urea. The molecular weight of the polyiso-urea samples with different ratios of both building blocks was measured by gel permeation chromatography (GPC). Although the calculated molecular weights are referenced to polystyrene standards, the real molecular weight should not deviate more than an order of magnitude. The polyiso-urea polymers with a higher CDI index than 110 were not soluble anymore in common organic solvents. The sample of index 110 was found to have the highest molecular weight, which may indicate that some of the biscarbodiimide was already undergoing the typical side reactions (**Table 6**).

Table 6. Molecular weight and polydispersity of polyiso-urea with various CDI indices measured by GPC.

| Index	M_n [g/mol]	M_w [g/mol]	PDI
80	3655	11534	3.2
90	4855	19430	4.0
100	6401	33295	5.2
110	8459	86204	10.2

In order to find support for side reactions, the biscarbodiimide was heated at 130 °C under vacuum for 1 hour. There were 3 types of byproducts detected by ESI−TOF mass spectrometry, a mono-functional CDI compound, the dimerization and the trimerization products of the

different CDIs. The dimerization and trimerization are typical side reactions for the heterocumulenes; the mono-functional compounds might be formed by a disproportionation reaction (**Scheme 38**). The presence of a mono-functional compound can terminate the chain growth during the polyaddition, while the formation of dimer and trimer may compete with the polyaddition reaction and cause an inequality in the stoichiometric ratio of both building blocks. Thus, the instability of the aromatic biscarbodiimide may have caused the low molecular weight of the linear polyiso-urea.

Scheme 37. Possible reaction routes of biscarbodiimide at 130 °C.
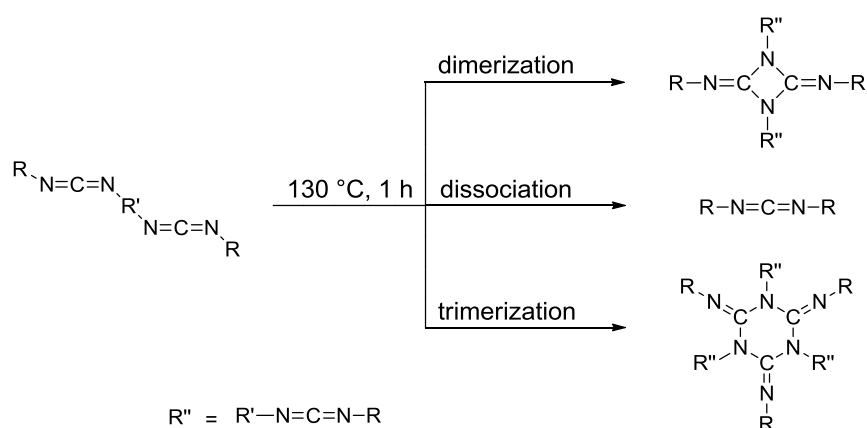
Scheme 38. Disproportionation of biscarbodiimide to form the mono-functional CDI compound.
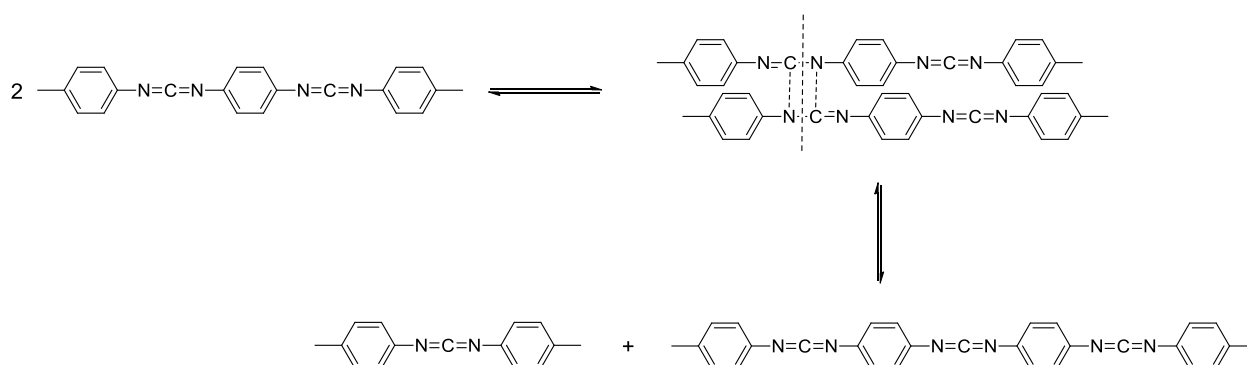

Polyiso-urea samples with varying CDI indices from 150 to 200 were prepared by bulk reactions of biscarbodiimide with poly(tetramethylene oxide) diol using DMTDN as a catalyst at 130 °C (**Chapter 5.4**). Biscarbodiimide was added deliberately in excess, in order to afford the formation of guanidine linkages at a lower temperature. Structurally, the products would consist of the primary chain of polyiso-urea linked oligomers and the guanidine-type pendant side groups or pendant side chains and crosslinks that give the material a three-dimensional

polymer network structure (**Scheme 39**). The presence of a polymer network structure governs the physico-mechanical properties of the material.

Scheme 39. General representation of possible linkages in the polyiso-urea products with a higher CDI index than 150.
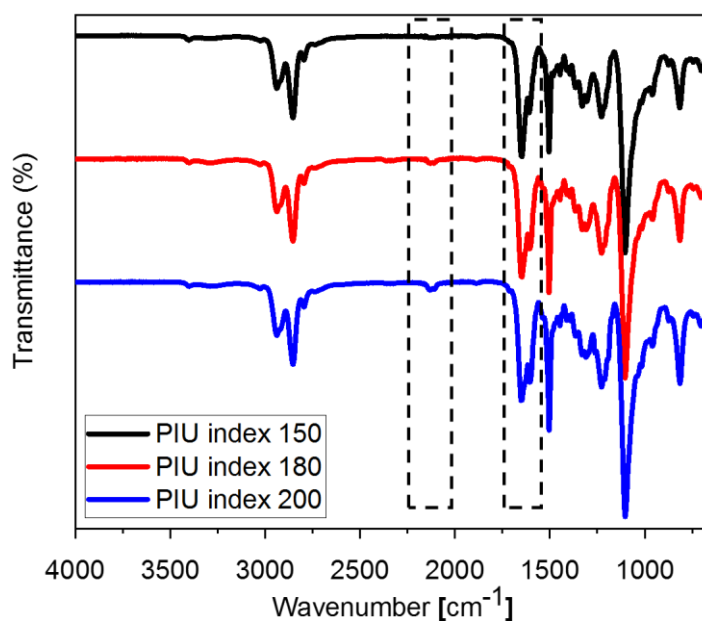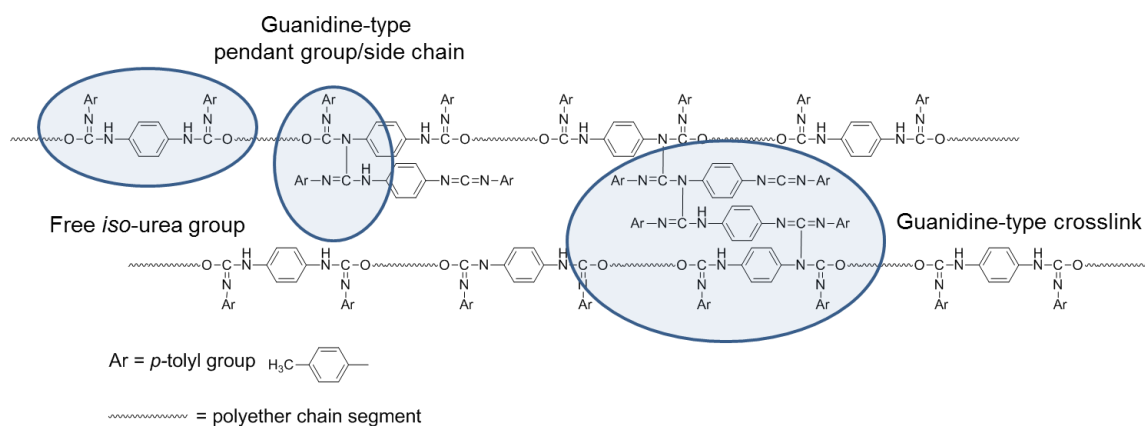
Figure 8. FT-IR spectra of polyiso-urea (PIU) products with various indices from 150 to 200.

In the IR spectra (**Figure 8**) of typical products, two regions are especially relevant for this study: the N=C=N stretch (from biscarbodiimide) located at 2108 and 2134 cm^{-1} and the N=C stretch (from polyiso-urea) located at 1605 and 1645 cm^{-1}. As the index increases, the intensity

of the N=C=N stretch also increases slightly, indicating a higher content of unreacted carbodiimide groups in the material. The peak at 1645 cm^{-1}, which corresponds to the N=C stretch of the *iso*-urea backbone, doesn't show a significant change, but the intensity of the peak at 1605 cm^{-1}, which corresponds to the N=C stretch of the guanidine linkages, increases with increasing index. It is indicative for an increasing content of guanidine linkages in the polyiso-urea polymer with increasing CDI index.

3.2.2   Temperature-dependent Properties

From the kinetic study of the reaction between mono-functional CDI and alcohol, it is known that the guanidine-type byproducts are only formed at a lower temperature. At elevated temperatures, the guanidine-type byproducts tend to decompose and CDI will be regenerated. The conversion between CDI and guanidine-type products was found essentially reversible. The thermal reversibility of the guanidine linkages formation in the polyiso-urea polymers was analyzed by differential scanning calorimetry (DSC) experiments (**Figure 9**). In the DSC thermogram, the glass transitions ($T_{g,\,DSC}$) was observed at -37 to -39 °C, which was mainly attributed to the α-relaxation of the polyether chains. The differences in CDI index don't cause changes of the glass transition temperature. A similar result was obtained by dynamic mechanical analysis (DMA) measurements taking the peak maximum of the loss modulus G'' as a measure of the glass transition (**Table 7**).

The endothermic peaks in the temperature range of 60 °C – 160 °C are attributed to the reaction heat that is absorbed during the release of the guanidine linkages. With increasing index, the intensity of the endothermic peaks thus increases. The thermal behavior was also studied in several consecutive heating/cooling cycles by DSC (**Figure 10**, index 200 as an example). It was found that the intensity of the guanidine-isourea transition decreases after subsequent heating/cooling cycles, indicating a loss in reversibility of the guanidine formation within the time frame of observation.
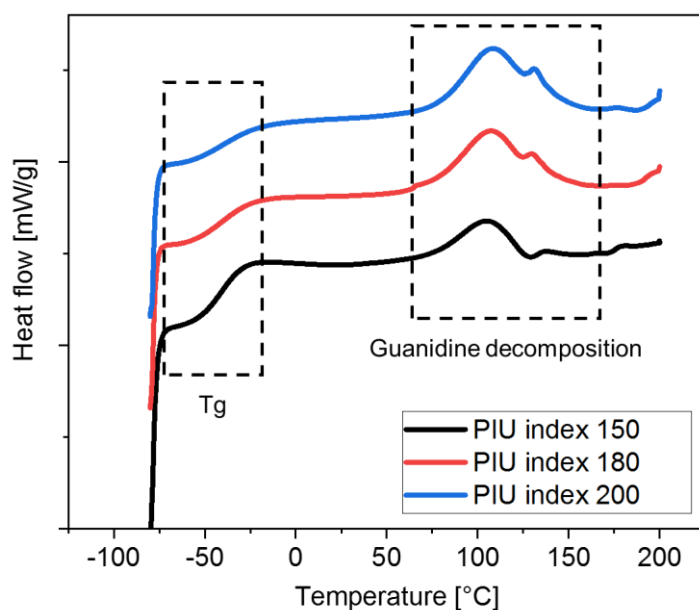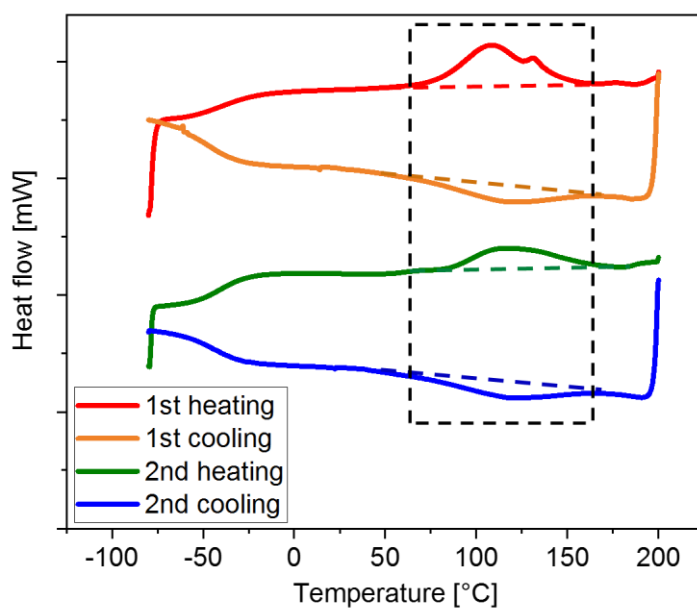
Figure 9. DSC thermogram of the polyiso-urea products with index 150, 180 and 200

Table 7. The glass transition temperature and gel point of the polyiso-urea with various indices.

Index	$T_{g, DSC}$ [°C]	$T_{g, G''}$ [°C]	T_{gel} [°C]
150	-39	-40	124
180	-38	-40	123
200	-37	-35	130

The glass transition temperatures T_g were measured by means of DSC and DMA (the peak maximum of G''), the gel point was determined from an oscillatory temperature ramp using a rheometer.

As mentioned above, it was shown that dimerization and trimerization of biscarbodiimide may take place at elevated temperature as side reactions. These CDI related reactions may also take place if the biscarbodiimide is released at a higher temperature. The dimerization and trimerization of biscarbodiimide may result in thermally stable linkages in the polymer, resulting in the loss in reversibility of the guanidine formation.

Figure 10. DSC thermogram of the polyiso-urea products with index 200 in two consecutive heating/cooling cycles from -80 to 200 °C.

The dynamic mechanical properties of the polyiso-urea samples with varying indices was investigated by DMA (**Figure 11**). The storage modulus (G') decreases as usual with temperature measured, the drop is associated with the glass transition temperature. The G' values exceed 1000 MPa below the glass transition, which is also typical for glassy polymers and is independent of the CDI index. The G' declines over two orders of magnitude during the glass transition. The onset of the α-transition (T_g) starts at about -60 °C and it reaches till 0 °C. The relaxation in this range is mainly attributed to the coordinated movement of the flexible chain segments of the polyether part. Above 0 °C, there is a typical rubbery plateau. The G' value in the rubbery plateau is related to the mobility of the polymer chain and the molecular weight between entanglements or crosslinks. A higher CDI index gives a product with a higher G' in the rubbery plateau. This is indicative of a higher crosslink density. At above 80 °C, the storage modulus G' of all three samples declines further, possibly due to the release of guanidine linkages.
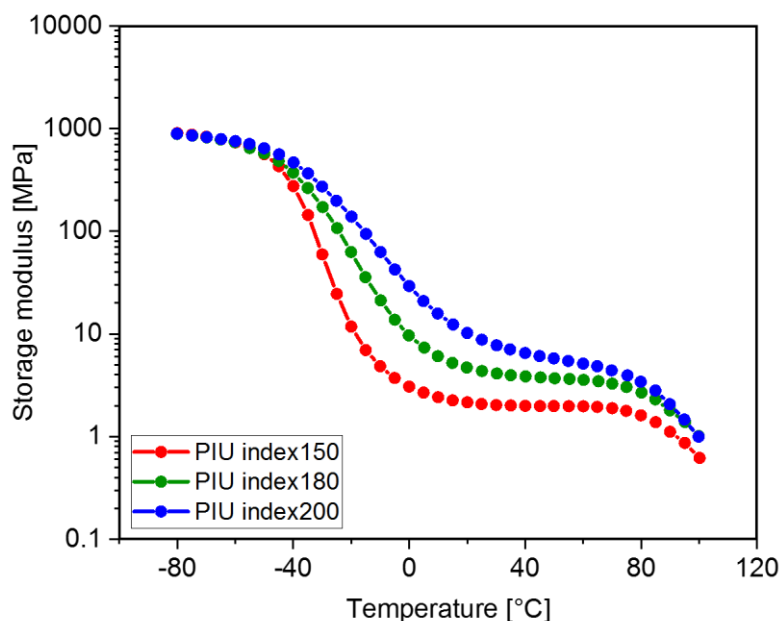
Figure 11. Storage Modulus G' of the polyiso-urea products with index 150, 180 and 200 as a function of temperature.

The release of crosslinks (denominated as "anti-gelation process") in the polyiso-urea products with various CDI indices was studied by oscillatory temperature ramp rheometry. The storage modulus G', loss modulus G'' and loss factor tan δ were represented as a function of temperature from 30 °C to 240 °C (**Figure 12**). The moduli were measured in the linear viscoelastic regime at a fixed frequency of 1 Hz and a fixed strain of 0.05%. The gel point represents generally the transition of a polymer between fluid-like to solid-like states. It has been proposed that the moduli exhibit a power law dependence on the applied frequency at the gel point.[96] In the present temperature ramp study, the gel point of the polyiso-urea samples was determined as the temperature where G' crosses G'' (at about 125 °C in **Figure 12**, where the loss factor tan δ = 1). For the anti-gelation process, it gives the critical temperature, at which the polymer chains are mobile to rearrange due to disconnection of physical and chemical junctions between chains.[97] The G' and G'' were found to increase and cross again at about 145 °C. It is apparent that a new gelation process takes place, which may be attributed to the formation of a new type of thermal-stable linkages. These new type linkages are probably the dimer and trimer of the biscarbodiimide. At above 190 °C, G' and G'' decrease again, which is probably attributed to a decomposition of the *iso*-urea groups in the primary chain.
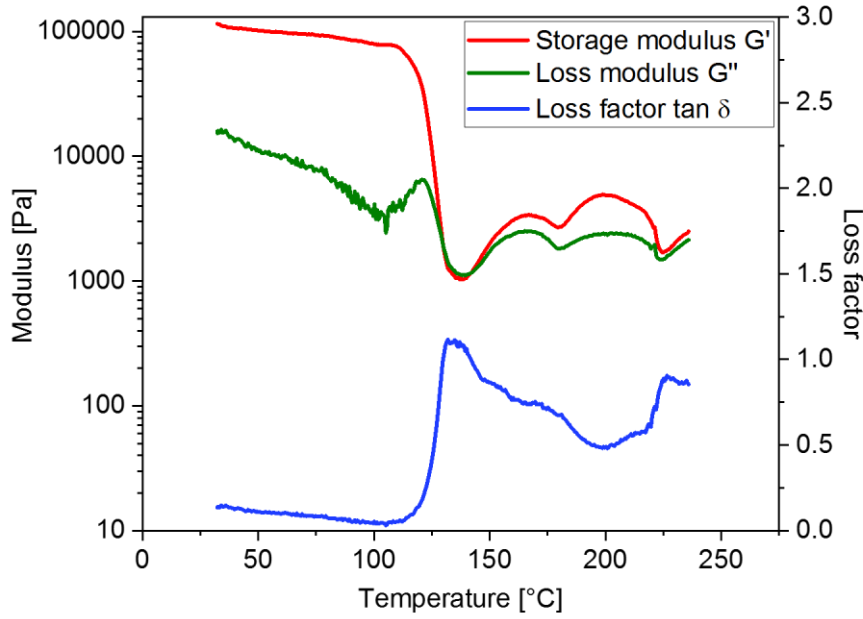
Figure 12. The temperature sweep of the polyiso-urea product with index 150 at 1 Hz.

3.2.3 Determination of the Crosslink Density

The crosslink density of the polyiso-urea products with various CDI indices was determined by swelling measurements. The swelling parameters were obtained by employing the equilibrium swelling method. The swelling equilibrium was obtained by submersing the samples in tetrahydrofuran (THF). The crosslink density was calculated from the Flory and Rehner equation (**Equation 16**).

$$Ln\big(1 - v_p\big) + v_p + \chi v_p{}^2 = -\frac{\rho_p V_m}{M_c}\,(v_p{}^{\frac{1}{3}} - \frac{v_p}{2}) \qquad (16)$$

Where v_p is the equilibrium volume fraction, V_m is the molar volume of the solvent and χ is the polymer-solvent interaction parameter. The polymer volume fraction (v_p) is defined as the ratio of the volume of the gel fraction (V_g) to the volume of the absorbed solvent (V_s). The interaction parameter χ can be calculated using the semi-empirical equation from Bristow and Watson.

$$\chi = 0.34 + \frac{V_{m.s}}{RT}(\delta_s - \delta_p)^2 \qquad (17)$$

The solubility parameter δ_s of the THF was previously determined by Hansen at $\delta_s = 19.5$ MPa$^{0.5}$.[98,99] The solubility parameter of the polyiso-urea δ_p was calculated using the method of

Schneier for amorphous copolymers.[100] The solubility parameter and the density of the hard segment that makes up *iso*-urea and the guanidine linkages are estimated to be approximately equal to the value of the polyurea prepared from MDI and ethylene diamine ($\delta_{hard} = 21.0\,\text{MPa}^{0.5}$); the solubility parameter of the soft segment, the polyether part, was reported in the polymer handbook as $\delta_{soft} = 17.5\,\text{MPa}^{0.5}$.[101]

$$\delta_p = \frac{\left(\frac{n_{hard}M_{hard}^2}{\rho_{hard}}\right)\delta_{hard} + \left(\frac{n_{soft}M_{soft}^2}{\rho_{soft}}\right)\delta_{soft}}{(n_{hard}M_{hard} + n_{soft}M_{soft}) \cdot \left\{\left[\left(\frac{n_{hard}M_{hard}^2}{\rho_{hard}}\right) + \left(\frac{n_{soft}M_{soft}^2}{\rho_{soft}}\right)\right] \cdot \frac{1}{\rho_p}\right\}^{\frac{1}{2}}} \tag{18}$$

Here, the parameters δ, n, M, ρ refer to the solubility parameter, the number of moles, molar mass and density of the corresponding hard and soft segment, respectively. The crosslink density can be obtained from the following relationship:

$$M_c = \frac{\rho_p}{v_c} \tag{19}$$

The calculated solubility parameter of polyiso-urea δ_p, interaction parameter χ, equilibrium volume fraction v_p, network parameter M_c and crosslink density v_c are summarized in **Table 8**. With increasing index, the crosslink density increases as well, which is in agreement with expectation.

Table 8. The swelling parameters and crosslink density of the polyiso-urea with varing indices.

Index	δ_p [MPa$^{0.5}$]	χ	v_p	M_c [g mol^{-1}]	v_c [mol m^{-3}]
150	20.3	0.45	0.33	2016	517
180	20.6	0.48	0.48	723	1466
200	20.7	0.50	0.54	501	2139

The gel content G was also easily calculated from the ratio of the mass of the extracted sample after drying in vacuum to the mass of the sample before the swelling experiment (**Figure 13**). The gel content appears to be associated with the crosslink density, thus the sample with a higher CDI index shows a higher gel content. It was surprising to see that the gel content

decreases, as the days of submersion increase, indicating a loss in crosslink density. The solvent, in which the polyiso-urea sample was submersed, was also analyzed by FT-IR spectroscopy after the swelling measurement was finished. It was shown that biscarbodiimide was liberated (probably from the guanidine network). Thus, the reduction in gel content with time can be related to the liberation of the biscarbodiimide and not from the soft segment, the polyether part.
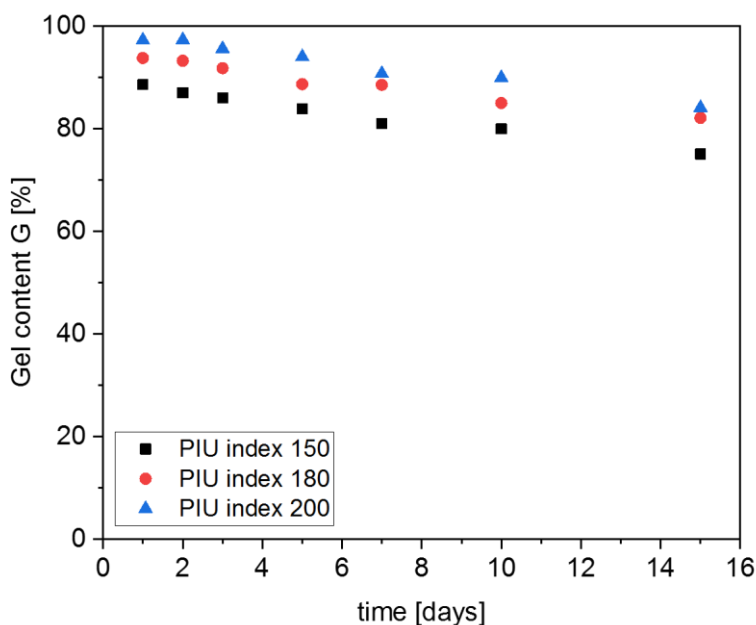
Figure 13. Gel content as a function of time of immersion in THF.

The tensile behavior at room temperature is another measure of the crosslink density of the amorphous polymer material at room temperature. It is well known that the molecular architecture by network formation and branching plays an important role in the mechanical properties of the polymer. Although the effect of the crosslink density of amorphous polymer on the tensile behavior is dependent on the polymer system under consideration, it can be generally said that the crosslink density of the amorphous polymer largely determines the tensile profile.[102] A higher CDI index in the synthesis of the polyiso-urea products leads to a higher content of stiff chain segments and to a higher crosslink density at the same time, thus it also results in a higher tensile strength at break (**Figure 14**). The measured stiff chain segment content is largely responsible for the increase in Young's modulus, but also an increase in crosslink density may contribute to this effect. The elongation at break for all the samples is

about 40%. The measured tensile strength, elongation at break and the calculated Young's modulus as well as the corresponding standard deviation (*SD*) are summarized in **Table 9**.
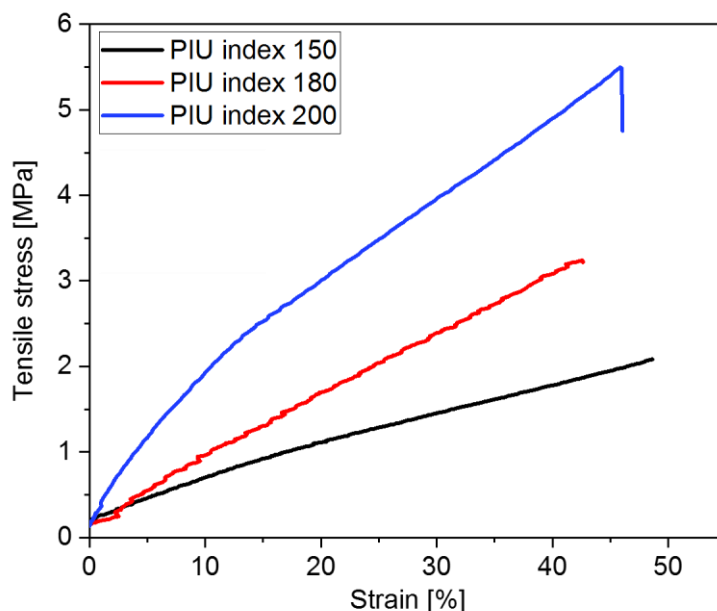
Figure 14. Representative stress-strain curve of the polyiso-urea products.

Table 9. Tensile properties of the polyiso-urea products with various indices.

Index	Tensile strength [MPa]	SD [MPa]	Elongation at break [%]	SD [%]	Young's modulus [MPa]	SD [MPa]
150	2.0	0.2	46	5	5.1	0.7
180	3.4	0.3	39	1	9.4	1.4
200	5.5	0.4	45	5	18.5	3.5

3.3 Reaction Study of Guanidine-Containing Prepolymer with Alcohol

Polycarbodiimides, the condensation products of polyisocyanates, have been extensively studied after the discovery of phospholene oxide as catalyst.[34,45,103,104] Synthesis of a linear polycarbodiimide with high molecular weight is found not possible on account of the formation of branching and crosslinking during the polymerization.[19][105] Thus, a mono-functional

compound in form of an isocyanate or alcohol is often added as a terminating agent in order to obtain an oligomeric product which is liquid. Polycarbodiimide and oligomeric CDI see a growing interest as raw material or as polymer additive in academia and chemical industry, on account of its low toxicity and rich reactivity.[19]

The application of blocked isocyanates in the chemical industry has been a topic for several years and in some cases changed the industrial practice by for example commercializing one-component and water-born polyurethane formulations.[2] Blocked isocyanates are generally defined as the addition product of isocyanate and a weak nucleophile, leading to weak bonds. Under certain conditions, the isocyanate can be regenerated and is able to undergo a curing reaction with a stronger nucleophile, giving a more stable linkage.

Inspired by the concept of blocked isocyanates, a novel guanidine-containing prepolymer was developed as a blocked CDI source. The guanidine linkages were formed by the reaction of oligomeric CDI with polyiso-urea. As mentioned above, the guanidine linkages can only exist at lower temperature. At a higher temperature, the CDI group will be regenerated and is able to undergo a curing reaction with a stronger nucleophile, such as a hydroxyl or amine group (**Scheme 40**). Taking advantage of the thermal reversibility, the presence of the guanidine linkages can further decrease the reactivity and toxicity of the raw material containing CDI at room temperature.

Knowledge of the kinetic parameters of the deblocking and curing reaction is of importance to prepare the present blocked CDI curing system, since it can help to predict the cure pattern over a certain temperature range. Kinetic models and the model-free isoconversional methods have been widely applied to evaluate the kinetic parameters in epoxy- and polyurethane curing systems.[2,68,70,73,106,107] In this chapter, a novel guanidine-containing prepolymer was prepared from oligomeric CDI with a mono-functional alcohol. The deblocking temperature of the guanidine linkages was measured by DSC. The reaction kinetics of the deblocking reaction and the curing reaction with hydroxyl group was investigated by model-fitting and isoconversional methods based on the results obtained from DSC.

Furthermore, it was found that the guanidine-entities may also give a temperature-sensitive crosslinking in the polyisourea-based resins. This kind of crosslinking is only present at lower temperature, brings polyiso-urea a better mechanical property and may allow new applications in the industry. The influence of the guanidine linkages on the dynamic mechanical properties of polyiso-urea was also studied by DMA.

Scheme 40. Pathways of deblocking and curing reactions of blocked CDI.
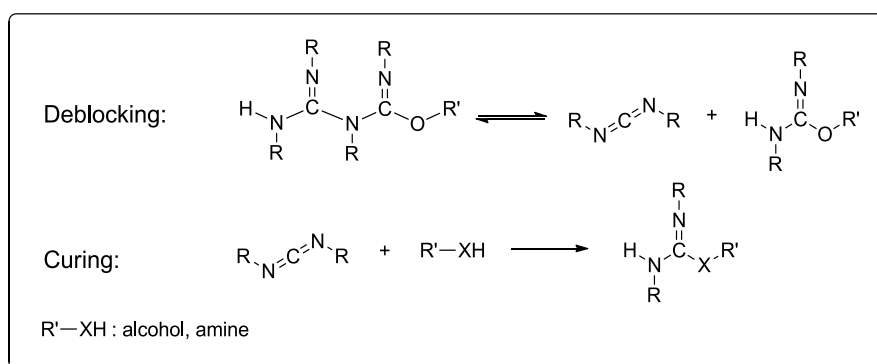
3.3.1 Determination of the Deblocking Temperature

An oligomeric CDI was prepared from TDI using *p*-tolyl isocyanate as a terminating agent and 3-methyl-1-phenyl-2-phospholene 1-oxide (MPPO) as a catalyst (**Chapter 5.2.4**). The obtained oligomeric CDI had an average functionality of 2.3. The guanidine-containing prepolymer used in the DSC experiments was prepared from the oligomeric CDI and di(ethylene glycol) ethyl ether (DEGEE) using DMTDN as a catalyst (the molar ratio of CDI groups to hydroxyl groups: 2:1). The reaction was initially performed at 130 °C for 1 hour under an argon atmosphere. The obtained product mixture was cooled and kept at room temperature for 12 h, allowing the unreacted CDI groups to add to the *iso*-urea groups, giving guanidine moieties. The disappearance of the N=C=N stretch of the oligomeric CDI in the FT-IR spectra (two bands at 2110 cm^{-1} and 2135 cm^{-1} in **Figure 15**) indicates the successful blocking of the CDI.
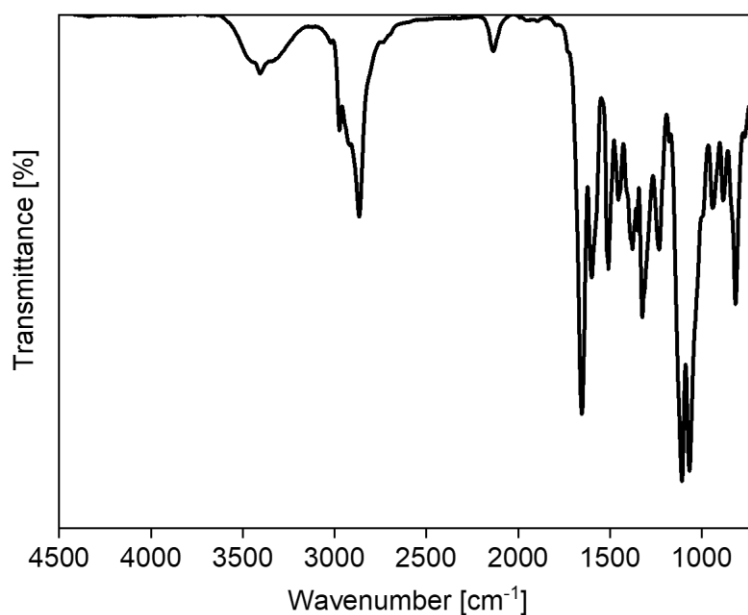
Figure 15. FT-IR spectrum of the guanidine-containing prepolymer.

The deblocking reaction of the guanidine moieties to give CDI and *iso*-urea groups is an equilibrium reaction and the extent of reaction is highly dependent on the reaction temperature. The "deblocking temperature" is thus an important characteristic parameter for the blocked CDI strategy. The deblocking temperature actually doesn't have any physical meaning and is dependent on the experimental set up and the reaction conditions.[2] In this study, the deblocking temperature of the guanidine-containing prepolymer was determined as the initial temperature at which an endothermic feature is indicated in the DSC curve (**Figure 16**). The average deblocking temperature is 63 °C (**Table 10**).

Table 10. Deblocking temperature of the guanidine-containing prepolymer measured by DSC at varying heating rate.

Heating rate β [°C/min]	5	8	10
Deblocking temperature [°C]	63.3	64.3	62.0
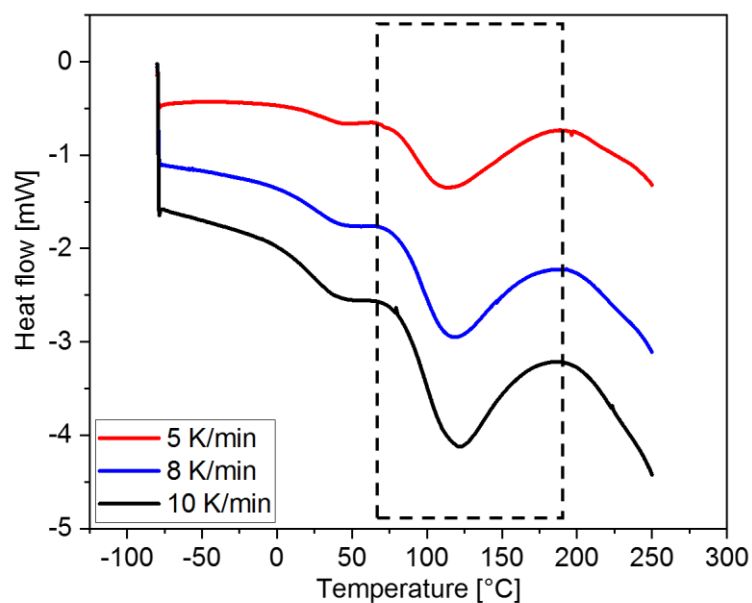
Figure 16. DSC curves of the guanidine-containing prepolymer.

3.3.2 Kinetic Study of the Deblocking Reaction

The reaction kinetics of the deblocking reaction was studied using isoconversional methods based on the dynamic DSC measurements. Experiments were performed with heating rate of 5, 8, and 10 K/min in the range from -80 to 250 °C (**Figure 16**). In the thermograms, the endothermic transition between 63 and 195 °C is related to the deblocking reaction, i.e. decomposition of the guanidine-entities. The peaks shift to higher temperature with increasing heating rate. As mentioned in **Chapter 5.5.2**, the second dynamic run was used to calculate the reaction heat. Under the assumption that the amount of heat is directly proportional to the extent of the reaction, the conversion α can be obtained by using the following relationship:

$$\alpha = \frac{\int_{T_0}^{T} \frac{dH}{dT} \cdot dT}{\Delta H_{total}} \tag{20}$$

Where T_0 is the temperature of the specimen at the onset, which is also defined as the deblocking temperature in this work. ΔH_{total} is the sum of the reaction heat that is required for the deblocking reaction, which is calculated by integration the corresponding area of the feature in the DSC curve in the relevant temperature range.
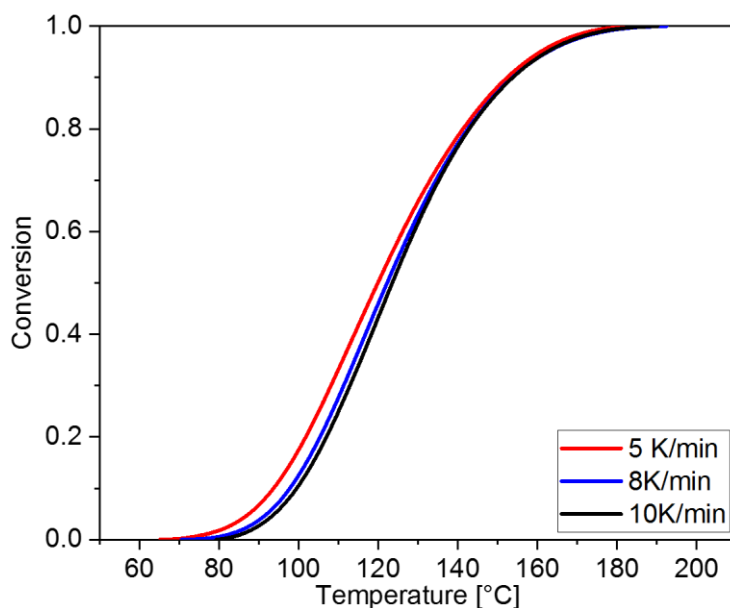
Figure 17. Conversion α as function of the temperature.
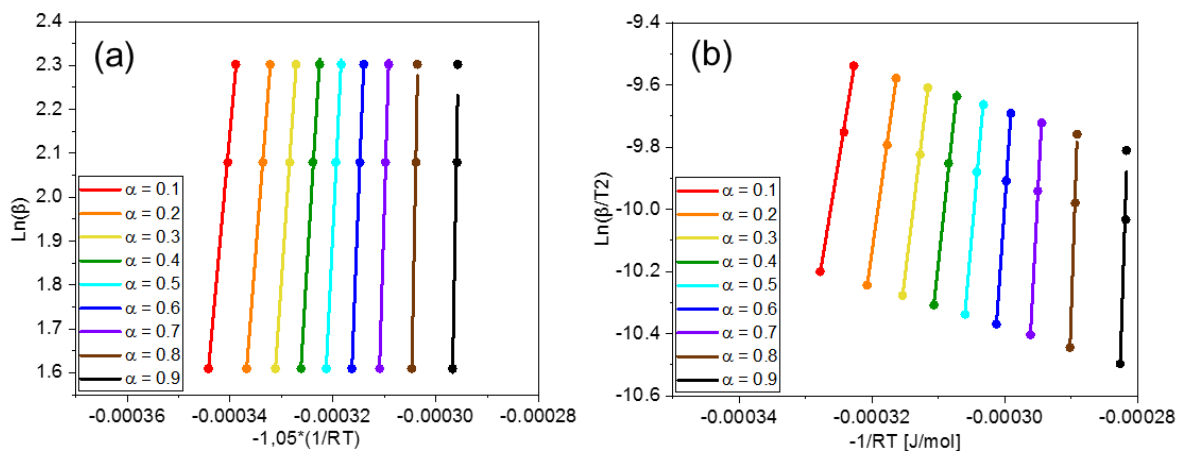
Figure 18. Determination of the activation energy by applying Flynn-Wall-Ozawa (FWO) model (a) and Kissinger-Akahira-Sunose (KAS) model (b).

The conversion of the deblocking reaction follows an S-shaped curve, indicative of a singular reaction type.[66] As mentioned in **Chapter 1.3.2**, the use of the Friedman model often leads to systematic error in the determination of the activation energy. Thus, the conversion-dependent activation energy of the deblocking reaction was determined by applying the integration

methods using Flynn-Wall-Ozawa (FWO) and Kissinger-Akahira-Sunose (KAS) model (**Figure 18**).
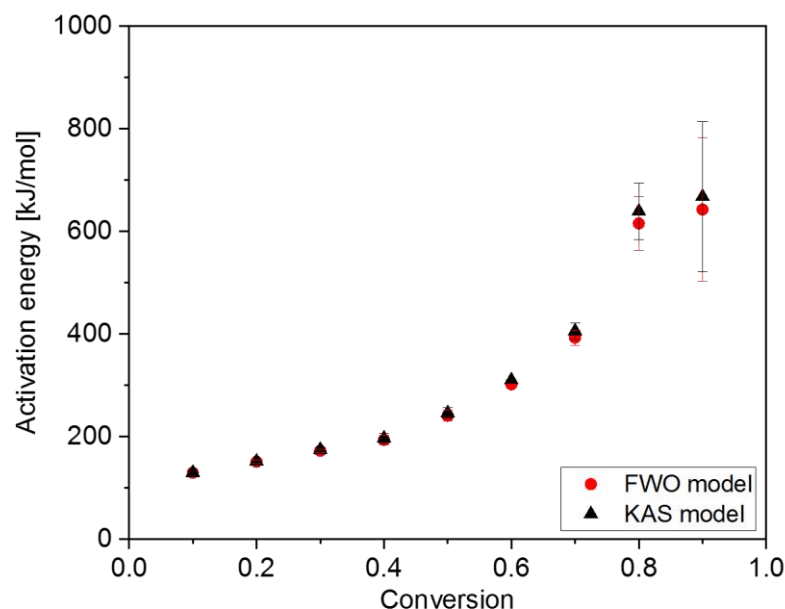
Figure 19. Calculated activation energy as function of extent of deblocking reaction.

The effective activation energy E_a calculated from the both models was plotted as a function of the conversion (**Figure 19**). With the extent of deblocking reaction, the calculated activation energy using the both calculation methods reveals similar trends. The E_a increases from 130 to around 650 kJ/mol. As proposed by Vyazovkin, processes that show an increased E_a with the extent of the conversion often indicate the presence of competing reactions, consecutive reactions or other side reactions.[66] This seems to be the case here too. It was already shown that the released CDI groups may undergo dimerization, trimerization and homo-polymerization at elevated temperatures. These side reactions may act as the consecutive reactions after the deblocking reaction and result in the increase of the effective activation energy at high conversion. The effective activation energy (E_a) and the corresponding standard deviation (SD) are summarized in **Table 11**.

Table 11. Calculated activation energy from DSC experiments.

Reaction conversion α	FWO model		KAS model	
	Ea [kJ/mol]	SD [kJ/mol]	Ea [kJ/mol]	SD [kJ/mol]
0.1	130	4	130	4
0.2	151	3	152	3
0.3	172	3	175	3
0.4	194	10	197	10
0.5	241	10	246	11
0.6	302	1	310	1
0.7	393	15	406	16
0.8	615	53	639	55
0.9	643	139	668	146

3.3.3 Kinetic Study of the Curing Reaction

The kinetics of the curing reaction of the guanidine-containing prepolymer with the hydroxyl substrate was evaluated using the autocatalytic and isoconversional models. Mixture of guanidine-containing prepolymer and DEGEE were reacted and observed either by isothermal measurements at a preset temperature or by dynamic measurement using different heating rates (**Chapter 5.5.3**).

The isothermal DSC measurement was performed at three temperatures in the temperature interval from 110 – 130 °C. Each single measurement took 6 hours (**Figure 20**). After this period, a dynamic scan at 5 K/min was carried out to determine the residual reaction enthalpy. No reaction heat could be detected in all cases. The conversion as function of time was thus taken from the data using **Equation 21.**
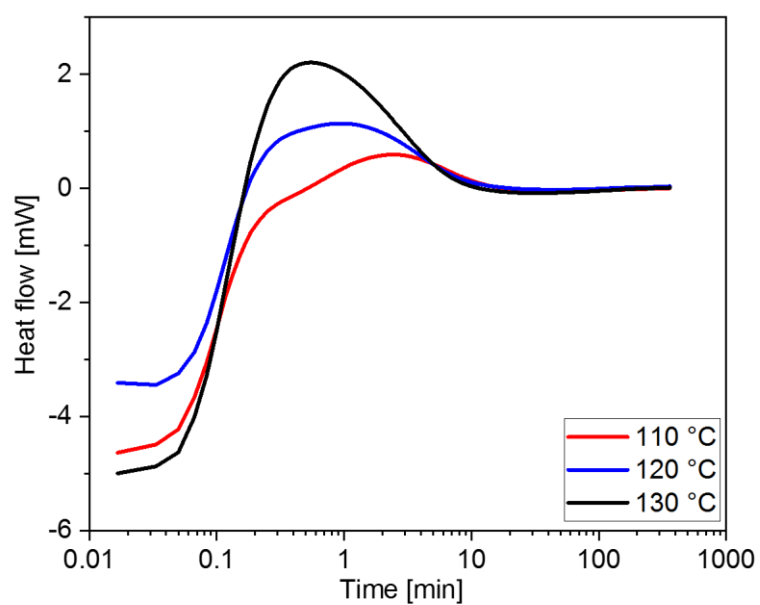
Figure 20. DSC curves for the isothermal measurement of the curing reaction of the guanidine-containing prepolymer with DEGEE.
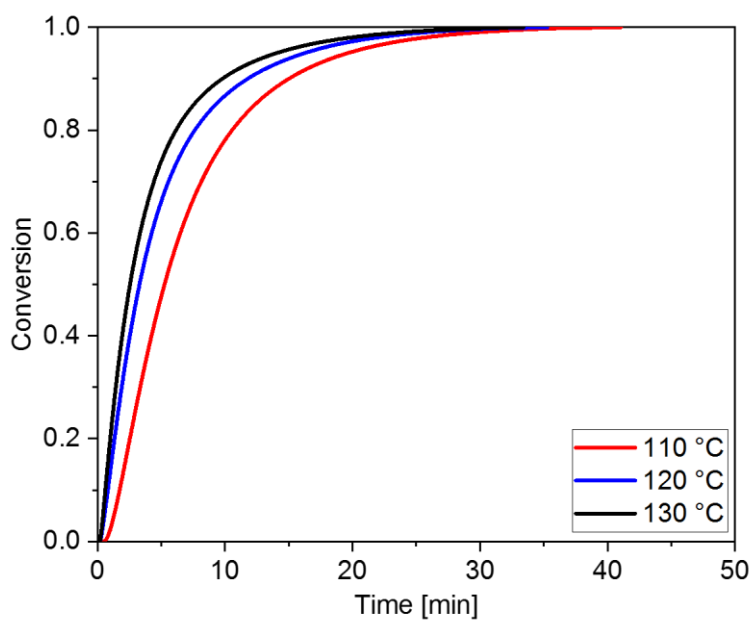
Figure 21. Conversion α as function of time.

The extent of the reaction α is calculated using **Equation 21**.

$$\alpha = \frac{\int_{t_0}^{t} \frac{dH}{dt} \cdot dt}{\Delta H_{total}} \tag{21}$$

Where t_0 is the time at the onset of the curing reaction and ΔH_{total} is the total reaction heat.

For mechanistic studies, various empirical models have been suggested to describe the curing kinetics. Among them, the most commonly used are the nth order model and Kamal-Sourour model (also known as the autocatalytic model). Since the reaction pathways are not known, the more generalized rate expression based on simplified Kamal-Sourour model is used:

$$\frac{d\alpha}{dt} = k\alpha^m (1 - \alpha)^n \tag{22}$$

Where k is the rate constant. m and n are the partial reaction order, the sum $(m + n)$ are the global reaction order. All these reaction parameters can be determined by fitting the experimental data to the logarithmic form of **Equation 22**. According to the Arrhenius equation (**Equation 2** in **Chapter 1.3**), the apparent activation energy was calculated at about 36 kJ/mol by plotting Ln(k) as a function of $-1/RT$ (**Table 12**).

$$\ln\frac{d\alpha}{dt} = \ln(k\alpha^m) + n \cdot \ln(1 - \alpha) \tag{23}$$

Figure 22 represents the fitting of the experimental data to **Equation 23**. The best fitting was obtained for a reaction order of 1.3. It is noticed that the model-fitting only failed in the very later stage of the reaction (α > 0.99).
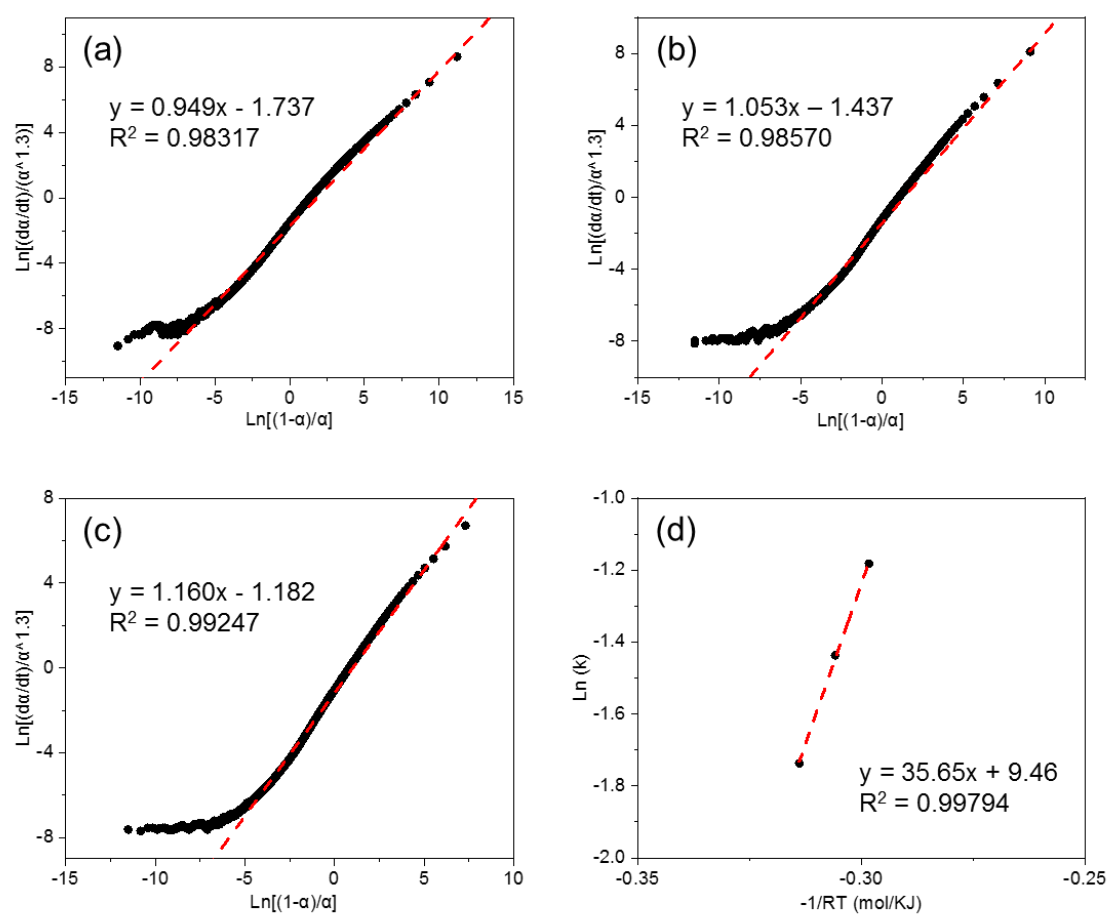
Figure 22. Fitting the experimental data from the DSC isothermal measurement to **Equation 23**.

Table 12. The characteristic kinetic parameters determined using the Kamal-Sourour model.

T [°C]	k [s⁻¹]	m	n	E$_a$ [kJ/mol]
110	0.176	0.35	0.95	
120	0.238	0.25	1.05	35.65
130	0.307	0.14	1.16	

The conversion-dependent activation energy of the curing reaction was determined by applying the integral method. With the extent of the curing, the calculated activation energy decreases from 52 to 8 kJ/mol (**Figure 24**). As supposed by Flynn and Wall, the variation of the effective activation energy might be a sign of the complexity of the curing process.[106] Earlier studies on epoxy- and polyurethane-based curing systems have obtained similar trends, that the E_a

decreases with the extent of the conversion, which were often considered as a characteristic of a diffusion-controlled reaction caused by vitrification in the later stage of the curing (often at $\alpha > 0.6$).[70,107,108] However, because of the mono-functional alcohol that was used in the "curing reaction" of this work, the vitrification would not take place during the whole reaction. The smooth and smaller decrease of the E_a over the whole curing process is consistent with latter view, since the vitrification should be accompanied with a significant decrease of E_a at a certain point of conversion.

It is worth noting that the curing reaction between the released CDI-functionality with alcohol is coupled to the deblocking reaction of the guanidine-containing prepolymer. Latter is an equilibrium reaction. With the extent of curing, the equilibrium between guanidine and CDI groups gives a lower rate to regenerate CDI groups, on account of the high concentration of *iso*-urea entities. As a result, the deblocking reaction may become the rate-determining step in the later stage of the curing process and result in the decrease of the E_a for the whole curing process. Another possible reason for the decrease of the E_a is that the curing reaction between CDI and hydroxyl group may be considered as an autocatalytic process. The reaction may be catalyzed by the formed *iso*-urea functionality.

Furthermore, the apparent activation energy calculated using Kamal-Sourour model is 36 kJ/mol, which represents an overall E_a of the curing process. It coincides well to the results determined by the isoconversional method.
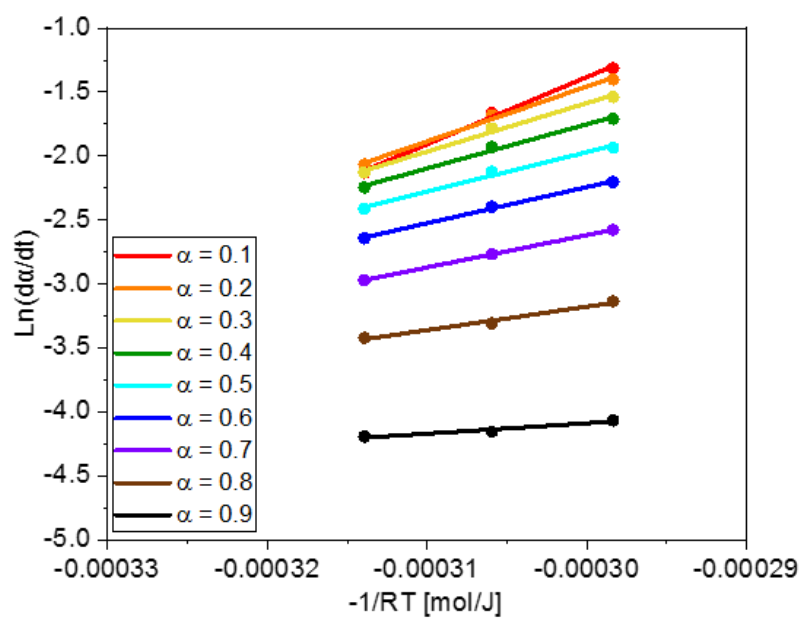
Figure 23. The conversion-dependent activation energy was determined by applying the integral method.
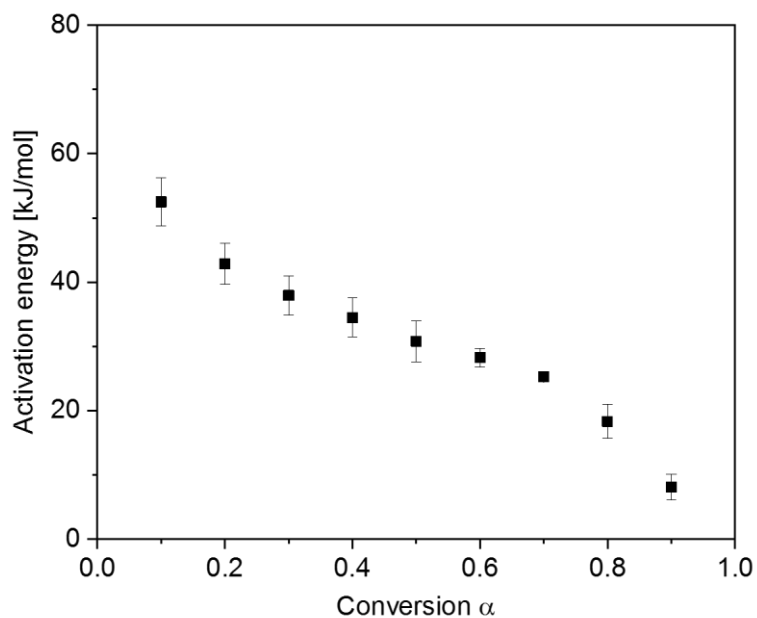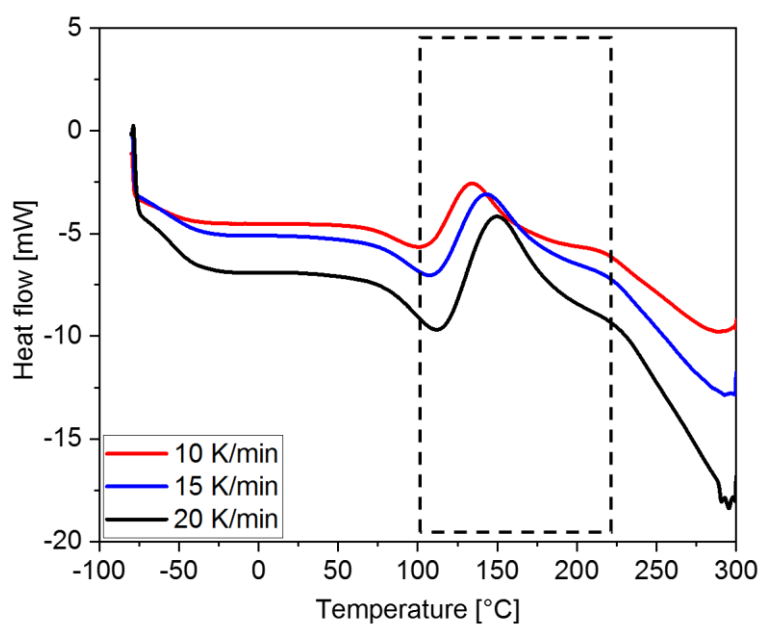

Figure 24. Activation energy as a function of extent of the curing reaction.

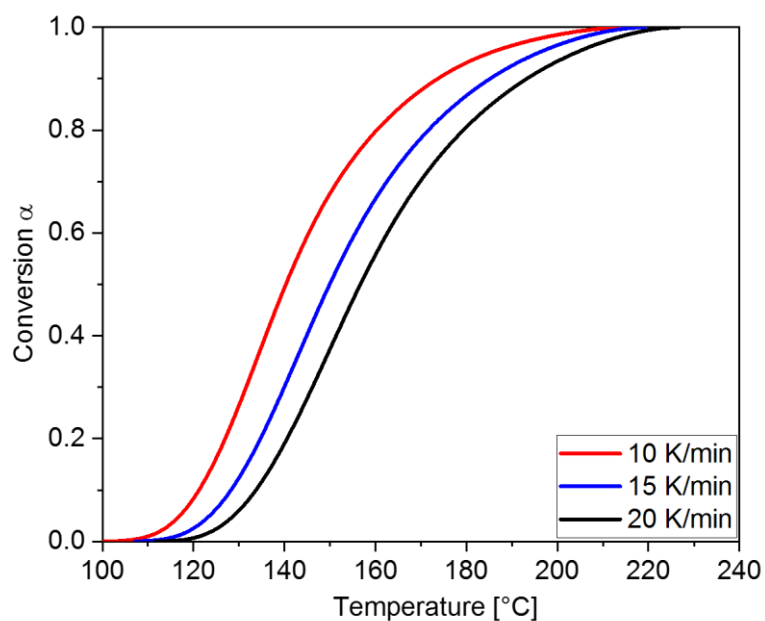**Table 13.** Calculated activation energy measured by isothermal DSC experiments.

α	Ea [kJ/mol]	SD [kJ/mol]
0.1	52.5	3.8
0.2	42.9	3.2
0.3	37.9	3.1
0.4	34.5	3.1
0.5	30.8	3.2
0.6	28.3	1.4
0.7	25.3	0.2
0.8	18.3	2.7
0.9	8.1	2.0

The dynamic DSC measurement was carried out with different heating rates of 10, 15 and 20 K/min in the range between -80 °C to 300 °C (**Figure 25**). In the thermogram, the exothermic transition in the temperature range between 100 and 225 °C is related to the curing reaction of the guanidine-containing prepolymer and DEGEE. The conversion of the reaction was determined by integration of the corresponding peaks and calculated using **Equation 20**. The conversion-dependent activation energy of the curing reaction was determined by applying the Flynn-Wall-Ozawa (FWO) and Kissinger-Akahira-Sunose (KAS) model (**Figure 27**). Both methods provide similar results (**Figure 28; Table 14**).

The initial activation energy is around 70 kJ/mol. As the curing reaction progresses, the activation energy slightly decreased to around 55 kJ/mol. As mentioned above, the variation of the effective activation energy indicates a multistep process. Compared to the results obtained by the isothermal methods, the E_a determined by the dynamic methods is somewhat higher. It is evidently that the blocking reaction (the back reaction of the deblocking reaction) and the curing reaction are in competition and the blocking reaction is kinetically favored at lower temperature. Since the isothermal measurements were performed at a relative high temperature (above 110 °C), the curing reaction between the CDI group and the hydroxyl group is kinetically favored. Thus, the calculated activation energy is also dominated by the curing reaction in the isothermal experiments. Conversely, the dynamic measurements were performed over a wide range of temperature, the higher activation energy might be contributed to the blocking reaction as the competition reaction.
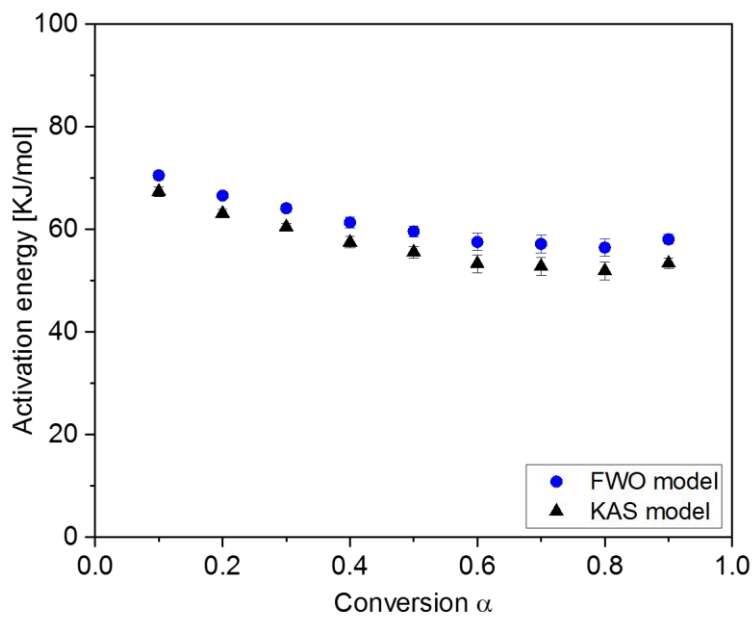
Figure 25. DSC curves of the curing reaction of the guanidine-containing prepolymer with DEGEE within the heating rate of 10, 15 and 20 K/min.

Figure 26. Conversion α as a function of the temperature.
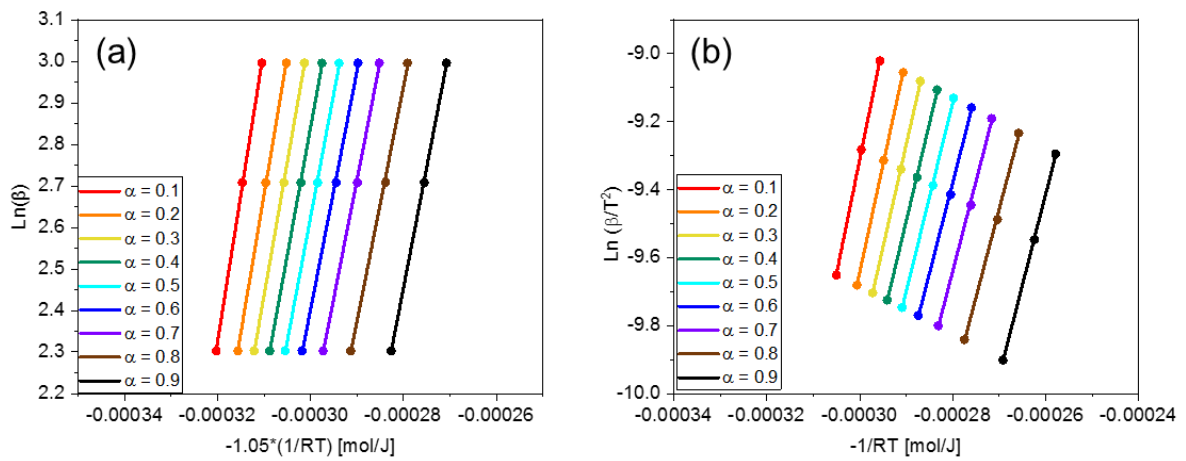
Figure 27. Determination of the activation energy by applying Flynn-Wall-Ozawa (FWO) model (a) and Kissinger-Akahira-Sunose (KAS) model (b).

Figure 28. Calculated activation energy as function of extent of the curing reaction.

Table 14. Calculated activation energy of the curing reaction from dynamic DSC experiments.

Reaction conversion α	FWO model		KAS model	
	Ea [kJ/mol]	SD [kJ/mol]	Ea [kJ/mol]	SD [kJ/mol]
0.1	70.5	0.9	67.4	0.9
0.2	66.6	0.7	63.1	0.8
0.3	64.1	0.7	60.5	0.7
0.4	61.3	1.1	57.5	1.1
0.5	59.6	1.1	55.6	1.1
0.6	57.5	1.7	53.3	1.7
0.7	57.1	1.7	52.8	1.8
0.8	56.4	1.7	51.9	1.7
0.9	58.1	1.0	53.4	1.0

In summary, the activation energy for the curing process between guanidine-containing prepolymer and mono-ol (without considering the vitrification) varies from ca. 50 to 70 kJ/mol and is dependent on the temperature and the extent of the curing. The successful use of Kamal-Sourour model and the decrease of the effective activation energy during the isothermal process may indicate an autocatalytic curing process for the reaction between guanidine-containing prepolymer and mono-ol at elevated temperature. If the mono-ol is replaced by a poly-functional hydroxyl-containing compound in the curing process, the occurrence of the vitrification may also play a role in the kinetics and lead to a diffusion-controlled process.

3.3.4 Influence of Guanidine Groups on Polyiso-urea

In **Chapter 3.2.1**, it has been mentioned that the CDI group can react with the *iso*-urea groups spontaneously at low temperatures, giving the guanidine groups in polyiso-urea. These guanidine groups may act as side chains, or react with a CDI group of another polymer chain, giving a thermally labile crosslink in the material. These kind of observations were also made in the polyiso-urea resins prepared from excess of oligomeric CDI with polyol. In this part, the influence of guanidine groups on the mechanical properties is reported using the polyiso-urea resin prepared from oligomeric CDI and poly(tetramethylene oxide) diol (polyTHF, $M_n = 1000$ g/mol) with a CDI index varying from 100 to 200. The oligomeric CDI was prepared from TDI and had an average functionality of 2.3. The formation of the guanidine-type crosslinks was

inferred from the mechanical behavior detected by DMA measurements (**Figure 29)**. Below the glass transition temperature, the G' is indifferent to the CDI index. The onset of the main α-transition starts at about -60 °C and spans till 0 °C. The relaxation in this range is attributed to the coordinated movement of the flexible segments that belong to the polyether chain segments. Above 0 °C, there is a typical rubbery plateau. The G' value in the rubbery plateau is related to the mobility of the polymer chain and the molecular weight between entanglements or crosslinks. At higher CDI index, the material also reveals a higher G' in the plateau region, indicating a lower chain mobility resulting from an increase in stiff chain segments and a higher crosslink density. At around 80 °C, the G' of the samples with the CDI index of 100 and 120 doesn't show any significant change. However, the G' of the samples with the CDI index of 140 to 200 decreases significantly at this temperature and is caused by the decomposition of the guanidine-entities. Thus, it shows that the guanidine-entities can also act as crosslinks in the polyiso-urea resins.

The influence of higher CDI index on the mechanical properties of polyiso-urea resins was also studied in the tensile tests (**Figure 30**). A typical profile of true elasticity was obtained. As mentioned above, the crosslink density of the amorphous polymer largely determines the tensile profile.[102] The elastic deformation behavior is related to the crosslink density. A higher CDI index leads to a higher content of stiff chain segments and a higher crosslink density. The stiff chain segment content is largely responsible for the increase in Young's modulus. The elongation at break for all the samples is about 60 - 70%, and is related to the extensibility of the polymer network. No obvious effect of increasing CDI index on the maximum elongation of the material is observed (**Table 15**).
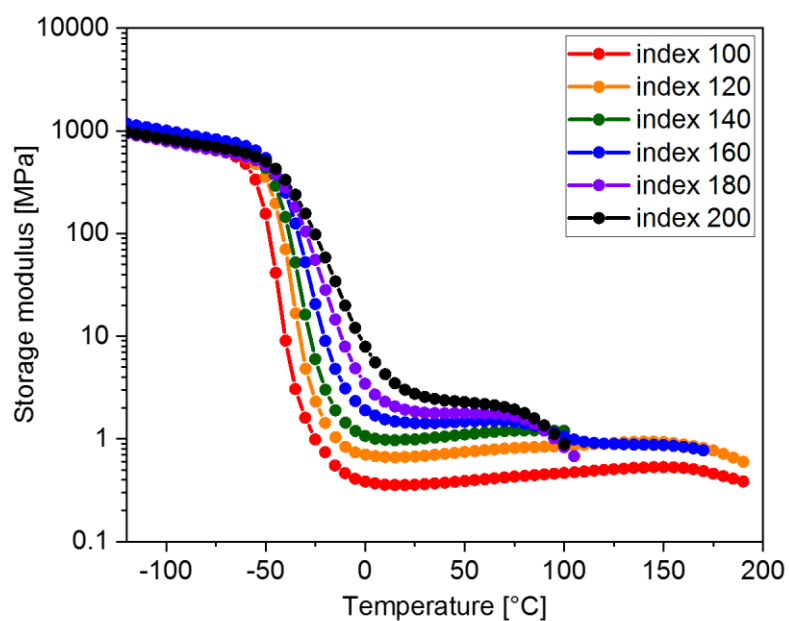
Figure 29. Storage modulus of the polyiso-urea resin with CDI indices from 100 to 200.

Table 15. Tensile properties of polyiso-urea resins with CDI indices from 100 to 200.

Index	Tensile strength [MPa]	SD [MPa]	Elongation at break [%]	SD [%]	Young's modulus [MPa]	SD [MPa]
100	0.44	0.04	65.6	9.5	0.6	0.06
120	0.83	0.13	64.6	11.2	1.4	0.10
140	1.15	0.11	76.7	10.0	1.8	0.09
160	1.21	0.10	61.8	7.4	2.6	0.11
180	2.24	0.26	58.1	5.1	4.4	0.16
200	3.05	0.44	56.1	7.8	6.1	0.31
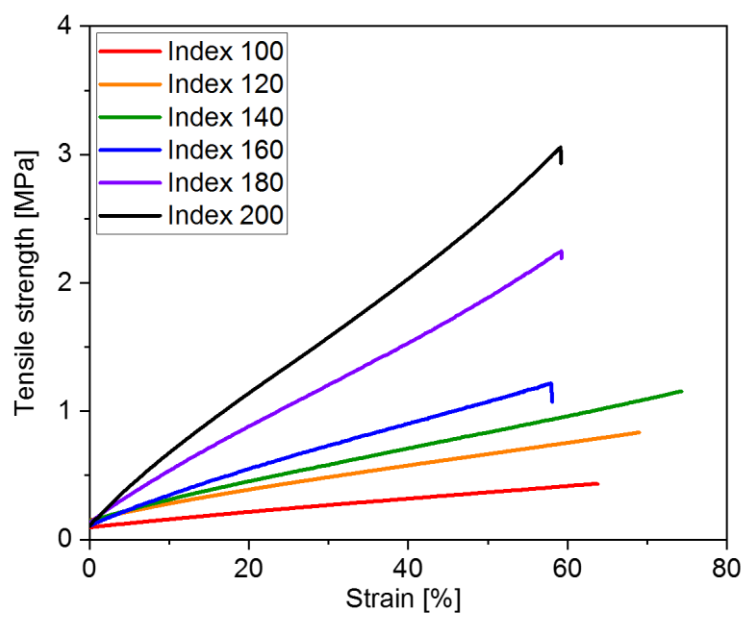
Figure 30. Representative stress-strain curve of the polyiso-urea resin with CDI indices from 100 to 200.

4 Summary

The reaction kinetics of aromatic carbodiimides with alcohols was investigated. The model reaction of di-*p*-tolyl carbodiimide (*p*-DTC) with a primary alcohol was performed in bulk at different temperatures, using titanium isopropoxide (TTIP) and dimethyltin dineodecanoate (DMTDN) as catalyst. Previous studies show that both catalysts have very high catalytic activity for this reaction. The adduct, *iso*-urea was obtained in high yield (> 99 %) at room temperature after short reaction time (shorter than 1 minute) when more than 1 mol% of catalyst was added. With a low concentration of catalyst (< 0.1 mol%), an obvious difference in conversion between both reactants was observed at 60 °C, which was attributed to a side reaction between carbodiimide and the formed *iso*-urea. The formed byproducts, a series of guanidine-type compounds, were identified by ESI-mass spectrometry and X-ray crystallography. The side reaction between carbodiimide and *iso*-urea is sensitive to temperature. The formation of the guanidine-type compounds is kinetically favored at lower temperatures. At higher temperatures (mostly higher than 100 °C), it tends to degrade back to carbodiimide and *iso*-urea. The conversion between the guanidine-type adducts and carbodiimide was also shown to be fully reversible. On the other hand, the reaction selectivity is also dependent on the structure of the reactants. The selectivity is found to be significantly improved when at least one sterically hindered reactant was used, such as di-*o*-tolyl carbodiimide (*o*-DTC) or a secondary alcohol. In the reaction of *o*-DTC with primary and secondary alcohols, the main reaction to *iso*-urea is dominant, an almost 1:1 conversion of both reactants was obtained. It is found that *o*-DTC is less reactive under the comparable reaction condition, the ratio of rates of *p*-DTC and *o*-DTC is approximate 25:1.

Based on the results obtained from kinetic studies, a novel polyiso-urea product was successfully prepared from the reaction of excess of biscarbodiimide and poly(tetramethylene oxide) diol at 130 °C using DMTDN as a catalyst. The biscarbodiimide was prepared from the corresponding bisureum using triphenyl phosphine as dehydration agent. The initial idea was to prepare a linear polyiso-urea from equivalent amounts of both monomers. However, an oligomer was obtained with a molecular weight of ca. 8500 g/mol. Apparently, side reactions prevent the polyaddition to achieve a high-molecular linear polymer. A series of side reactions have been identified that may take place as competition reactions during the polyaddition, including disproportionation and cyclization of the biscarbodiimide.

It was also found that the guanidine groups were formed too, when biscarbodiimide was used in excess. The guanidine-entities may appear as pendant groups, side chains or crosslinks. Latter

can result in a material with a three-dimensional network structure. Thus, a series of polyiso-urea polymers with CDI index from 150 to 200 were prepared. The guanidine-entities were found to be thermally labile at elevated temperatures. The thermal reversibility of the guanidine crosslinks in polyiso-urea was analyzed by DSC. The loss of the reaction heat associated with the guanidine-formation was observed with repetitive heating/cooling cycles, indicating a not fully reversible guanidine-formation in the polymer. As the biscarbodiimide is regenerated from the guanidine-entities at elevated temperatures, the irreversibility of the guanidine-formation might be attributed to the reactivity of the biscarbodiimide. With increasing CDI index, the mechanical properties of the polymer is enhanced with respect to the shear modulus and tensile strength at break, according to the results obtained from DMA and tensile testing. The enhanced crosslink density with increasing CDI index was concluded by swelling experiments. An increasing CDI index gives a higher content of guanidine groups in the polymer. As a result, a higher crosslink density was obtained. A gel point at ca. 125 °C was observed by oscillatory rheology in a temperature sweep. Above the gel point, the gel structure in the polymer was decomposed and the material became a viscous fluid. An increase in modulus was observed at temperatures above gel point (140 – 150 °C), indicating the formation of a new gel structure at elevated temperatures. Cyclization and homo-polymerization of CDI might cause the formation of new thermally stable linkages in the polymer.

Taking advantage of the thermal reversibility, the guanidine-containing prepolymer, prepared from excess of oligomeric carbodiimide and polyol was developed as a blocked carbodiimide precursor for polyiso-urea resins. The deblocking temperature is an important characteristic parameter. In this study, the deblocking temperature was measured as the initial temperature of the endothermic change in dynamic DSC measurements. The isoconversional kinetic study of the deblocking reaction shows an increase in the activation energy with increasing extent of the conversion, which might be attributed to competition reactions.

The autocatalytic model was successfully applied to study the reaction kinetics of the curing reaction between the guanidine-containing prepolymer and alcohol. An order of 1.3 including the autocatalytic contribution was leading to an acceptable description of the isothermal cure process. The curing kinetics was also evaluated by isoconversional methods based on the isothermal and dynamic DSC measurements. The dependence of the effective activation energy with the extent of the conversion shows similar trends. The decrease in the activation energy with increasing extent of the reaction may suggest an autocatalytic process in the later stage of the curing reaction. The higher activation energy obtained in the analysis based on the dynamic

method than that on the isothermal method may be related to the deblocking reaction. The determined activation energy by the autocatalytic model coincides with the results determined by the isoconversional methods.

5   Experimental Part

5.1 Materials and Characterization

5.1.1   Materials

Synthesis of mono-functional CDIs and the corresponding *iso*-urea

p-Tolyl isocyanate (99%), titanium isopropoxide (97%), diethylene glycol monomethyl ether (DGME, 99%) and 1-methoxy-2-propanol (99.5%) were purchased from Aldrich Chemical Company, Inc. *o*-Tolyl isocyanate was purchased from BOC Science. Dimethyltin dineodecanoate (DMTDN, Fomrez UL28) was supplied by Momentive Performance Materials. 3-Methyl-1-phenyl-2-phospholene 1-oxide (MPPO) was provided by BASF Polyurethanes GmbH. DGME and 1-methoxy-2-propanol were refluxed over calcium hydride, distilled, and stored over 4 Å molecular sieves in argon filled Schlenk flasks.

Synthesis of biscarbodiimide and the corresponding polyiso-urea products with various CDI indices

p-Phenylene diisocyanate (PPDI, 98%) was purchased from TCI Deutschland GmbH. *p*-Toluidine (99%) was obtained from Sigma-Aldrich. Triethylamine (99%) was obtained from Gruessing. Tetrachloromethane (99%) was obtained from Alfa Aesar. Dimethyltin dineodecanoate (DMTDN, Fomrez UL-28) was obtained from Momentive Performance Materials. Triphenylphosphine and poly(tetramethylene oxide) diol (polyTHF, M_n = 1000 g/mol) were supplied by BASF SE.

Synthesis of oligomeric carbodiimide and the corresponding polyiso-urea resins

p-Tolyl isocyanate (99%) was purchased from Abcr GmbH. Triphenyl phosphite (97%) and di(ethylene glycol) ethyl ether (DEGEE, 99%) were obtained from Sigma Aldrich. Dimethyltin dineodecanoate (DMTDN, Fomrez UL-28) was obtained from Momentive Performance Materials. Toluene diisocyanate (TDI, 80: 20 mixture of 2,4- and 2,6-isomer), 3-methyl-1-phenyl-2-phospholene-1-oxide (MPPO, 25% in triethyl phosphate) and poly(tetramethylene oxide) diol (polyTHF, M_n = 1000 g/mol) were supplied by BASF SE.

5.1.2 Characterization and Methods

Column chromatography

Silica gel 60 (Merck, 70–230 mesh, 60 Å) was used for separation processes by column chromatography. Thin layer chromatography was carried out on silica gel F254 panels (Merck).

^{1}H-NMR spectroscopy

^{1}H-NMR spectra were recorded on a Bruker Avance I 400 MHz Spectrometer on crude reaction mixtures dissolved in chloroform-d (CDCl$_3$) or dimethyl sulfoxide-d6 (DMSO-d6), chemical shifts for ^{1}H-NMR were reported to relative to tetramethylsilane. The obtained data was analyzed with MestReNova 10.0.1.

IR spectroscopy

Fourier transform infrared (FT-IR) spectra were recorded on a Nicolet ™ iS ™10 spectrometer. The obtained data was analyzed with Omnic 8.3 and Origin 2019.

Size exclusion chromatography (SEC)

The molecular weight distribution and the molecular weight of polyiso-urea were measured using a MZ-Gel Super-FG pre-column (size 50x8.0 mm) and a MZ-Gel Super-FG column (size 300x8.0 mm). A SpectraSERIES P100 isocratic pump and a SpectraSYSTEM AS3000 Autosampler (Thermo Separation Products) were parts of the system. A RI/UV-detector was used. The system was calibrated against polystyrene standards. Tetrahydrofuran was used as solvent with a polymer sample with a concentration of ca. 5 mg/mL at a rate of 0.7 mL/min. Toluene was used as an internal standard.

Differential scanning calorimetry (DSC)

The DSC measurement was performed on a Thermal Analysis System Analyzer from Mettler Toledo. The obtained thermogram was evaluated with STARe Software (V16.10) and Origin 2019.

Dynamic mechanical analysis (DMA)

The DMA experiment was performed using an Ares G2 rheometer with DMA mode from TA Instruments. The modulus was recorded at each 5 °C from -80 °C to 110 °C at a frequency of 1 Hz, under a nitrogen atmosphere.

Oscillatory rheology

The viscoelastic properties were measured using a DHR-2 rheometer from TA Instruments. The modulus was recorded from 30 to 240 °C. The moduli were measured in the linear viscoelastic regime at a fixed frequency of 1 Hz, and a fixed strain of 0.05%.

Tensile stress-strain test

The tensile stress-strain test was performed using a Zwick Roell with an Xforce load cell at room temperature. The crosshead speed is 200 mm/min.

5.2 Synthesis of Carbodiimides

5.2.1 Synthesis of Di-*p*-tolyl Carbodiimide (*p*-DTC)

p-Tolyl isocyanate (100 g, 0.75 mol) was transferred to a Schlenk flask and 3-methyl-1-phenyl-2-phospholene 1-oxide (MPPO) (0.1 g, 0.5 mmol) was added as a catalyst. The mixture was refluxed at 120 °C for 4 hours under an argon protecting atmosphere. After completion of the reaction time, the crude mixture was purified by recrystallization from diethyl ether. (Yield: 88%).

^{1}H NMR (400 MHz, d-chloroform, δ ppm): δ 7.10 (m, 8 H, Ar-H), 2.33 (s, 6 H, CH$_3$).

5.2.2 Synthesis of Di-*o*-tolyl Carbodiimide (*o*-DTC)

o-Tolyl isocyanate (100 g, 0.75 mol) was transferred to a Schlenk flask and 3-methyl-1-phenyl-2-phospholene 1-oxide (MPPO) (0.1 g, 0.5 mmol) was added as a catalyst. The mixture was refluxed at 120 °C for 4 hours under an argon protecting atmosphere. After completion of the reaction time, the crude mixture was distilled at reduced pressure to yield the desired product. (Yield: 91%).

^{1}H NMR (400 MHz, d-chloroform, δ ppm): δ 7.09 (m, 8 H, Ar-H), 2.33 (s, 6 H, CH$_3$).

Scheme 41. Synthesis of *p*-DTC and *o*-DTC.
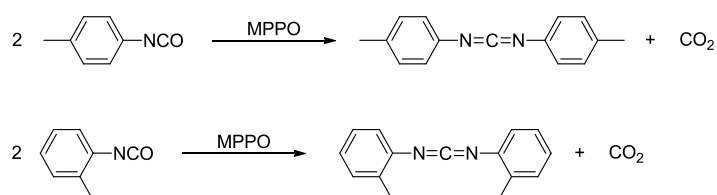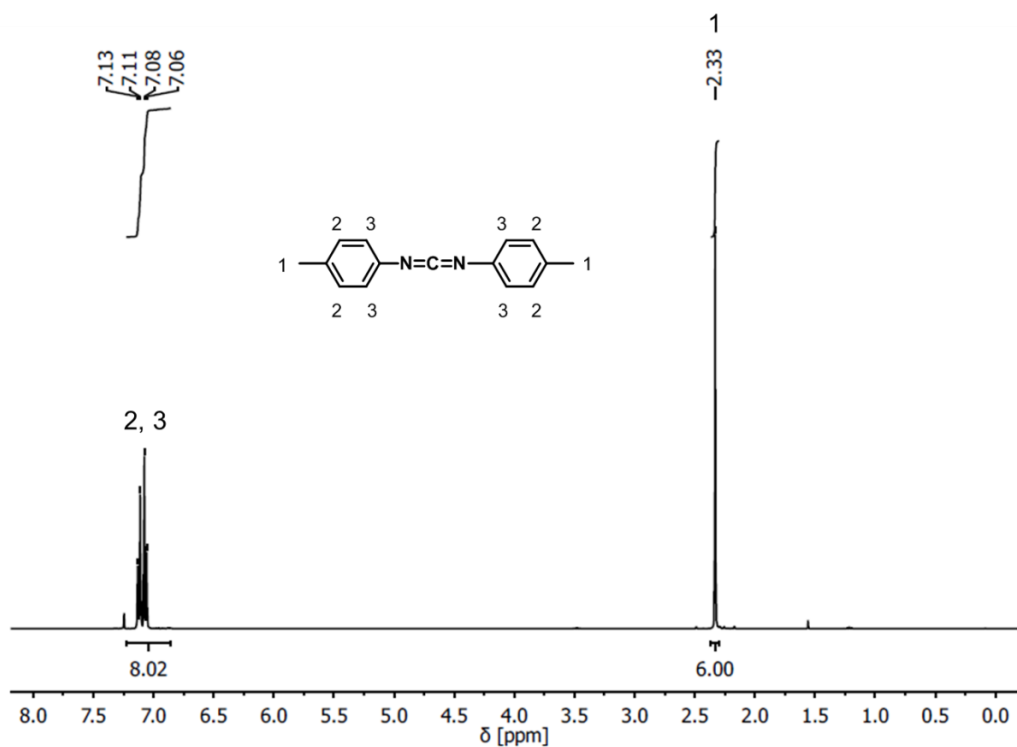
Figure 31. ^{1}H-NMRspectra for di-*p*-tolyl carbodiimide (*p*-DTC).
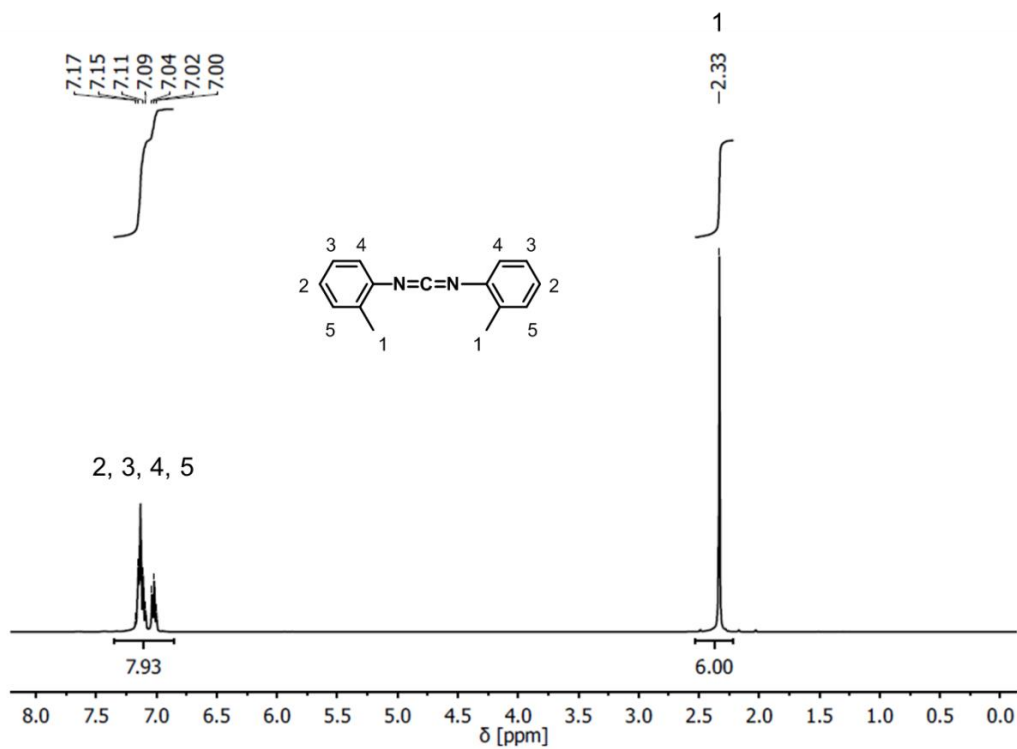
Figure 32. ^{1}H-NMRspectra for di-*o*-tolyl carbodiimide (*o*-DTC).

5.2.3 Synthesis of Biscarbodiimide

Synthesis of 1,1'-(1,4-phenylene)-bis(3-(*p*-tolyl)urea)

p-Toluidine (43.9 g, 0.41 mol) was dissolved in 200 ml THF in an oven-dried 1000 ml round-bottom flask and cooled in an ice bath. Then, *p*-Phenylene diisocyanate (32.0 g, 0.20 mol) dissolved in 200 ml THF was added dropwise over a 2 hours period while stirring. After completion of the addition, the mixture was stirred at room temperature overnight. The product was isolated using filtration, washed three times with THF and dried under vacuum at 50 °C overnight. (Yield: 97%, white solid)

^{1}H-NMR (400 MHz, d-DMSO, δ ppm): 8.12 (s, 4 H, NH), 7.33 (s, 4 H, Ar-H), 7.32-7.06 (m, 8 H, Ar-H), 2.23 (s, 6 H, CH$_3$).

Synthesis of 1,1'-(1,4-phenylene)-bis(3-(p-tolyl)carbodiimide)

In a 500 ml round-bottom flask, the 1,1'-(1,4-phenylene)-bis(3-(p-tolyl)urea) (13.1 g, 0.035 mol), triphenylphosphine (22.0 g, 0.084 mol), triethylamine (8.50 g, 0.084 mol) and carbon tetrachloride (12.9 g, 0.084 mol) were dissolved in 250 ml cold dichloromethane (DCM). The mixture was refluxed at approximately 40 °C for 8 hours. After the mixture was cooled to room temperature, the precipitated solid was filtered and washed with DCM. The product was purified with a silica gel column (eluent: DCM / petroleum ether = 1:1). (Yield: 49%, white or light yellow solid)

^{1}H-NMR (500 MHz, d-chloroform, δ ppm): 7.13-7.05 (m, 12 H, Ar-H), 2.33 (s, 6 H, CH$_3$).

ESI mass (Da): 339.160

Scheme 42. Synthesis of bisureum and its respective biscarbodiimide.
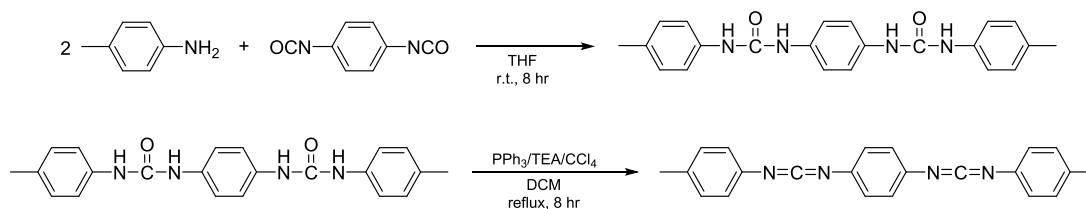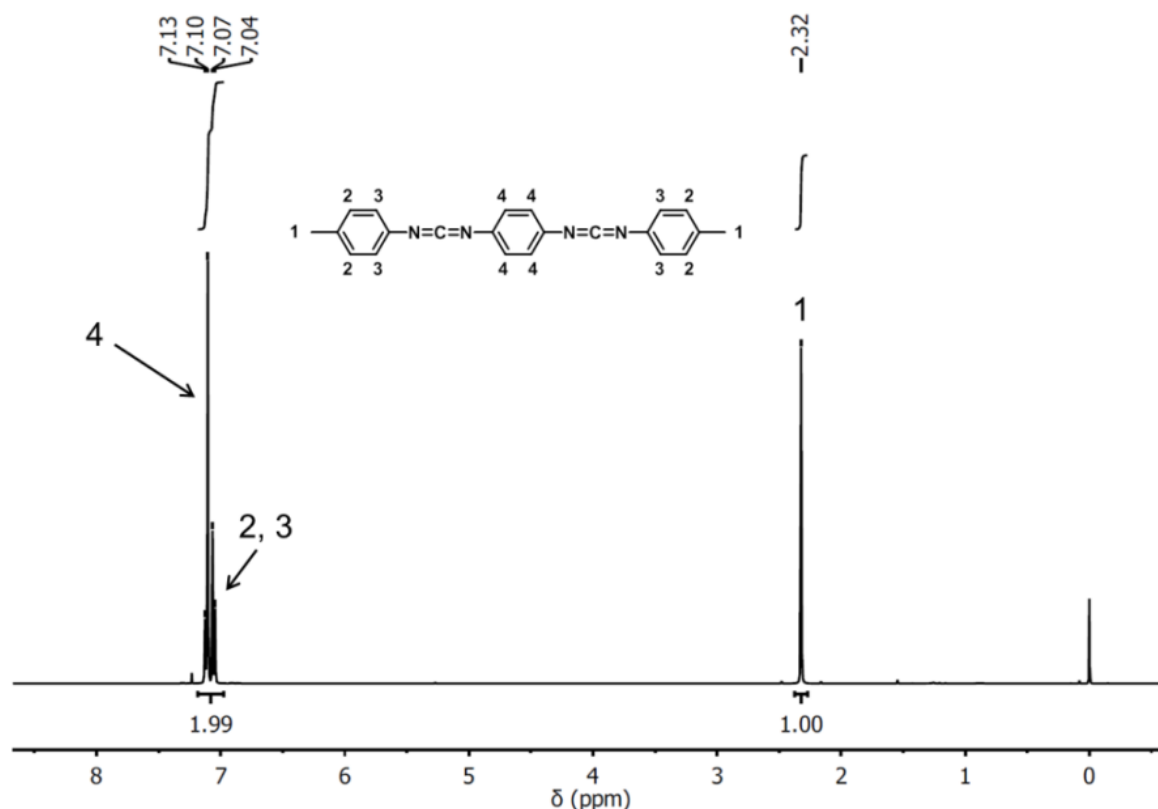
Figure 33. ^{1}H-NMRspectra for 1,1'-(1,4-phenylene)-bis(3-(p-tolyl)carbodiimide).

5.2.4 Synthesis of Oligomeric Carbodiimide

Toluene diisocyanate (23.8 g, 0.137 mol) and triphenyl phosphite (0.0656 g) were placed in a flask with KPG stirrer under argon atmosphere. The mixture was heated to 70 °C. Then *p*-tolyl isocyanate (27.2 g, 0.205 mol) and MPPO (0.05 g) were added. The mixture was further heated at 110 °C for 20 hours. The formation of the CDI functionality was identified by FTIR (2100 cm^{-1}, N=C=N stretch). The trace of isocyanates were also observed in the IR spectra (2260 cm^{-1}, N=C=O stretch).

5.3 Kinetic Study of the Model System

5.3.1 General Procedure for Preparation of *iso*-Urea

In a typical experiment, carbodiimide (2.78 g, 0.013 mol) and equimolar amounts of alcohol (0.013 mol) were transferred in a Schlenk tube. Catalysts were added and the Schlenk tube was subsequently immersed in a constant temperature bath having a temperature variation of 0.3 °C. The reactions were carried out at 60 °C with various concentrations of TTIP or DMTDN for 1 hour and the reaction mixtures were analyzed by ^{1}H-NMR spectroscopy of the sample.

Reactions were performed under an argon atmosphere. The NMR shifts of the *iso*-urea are as follows:
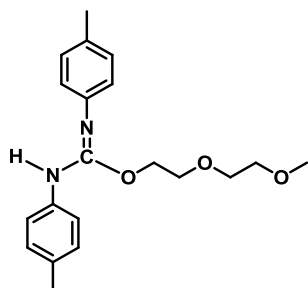
iso-urea **1-1**: The addition product of *p*-DTC and DGME.

^{1}H NMR (400 MHz, d-chloroform, δ ppm): δ 7.15 - 6.84 (m, 8 H, CH), 5.85 (s, 1 H, NH), 4.51 (t, 2 H, CH$_2$), 3.85 (t, 2 H, CH$_2$), 3.68 (t, 2 H, CH$_2$), 3.58 (t, 2 H, CH$_2$), 3.41 (s, 3 H, CH$_3$), 2.33 (s, 3 H, CH$_3$), 2.29 (s, 3 H, CH$_3$).
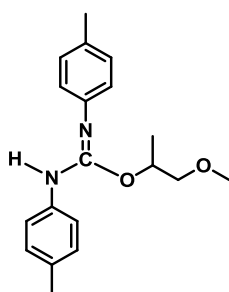
iso-urea **1-2**: The addition product of *p*-DTC and 1-methoxy-2-propanol.

^{1}H NMR (400 MHz, d-chloroform, δ ppm): δ 7.15 - 6.86 (m, 8 H, CH), 5.83 (s, 1 H, NH), 5.39 (m, 1 H, CH), 3.58 (m, 2 H, CH$_2$), 3.43 (s, 3 H, CH$_3$), 2.33 (s, 3 H, CH$_3$), 2.29 (s, 3 H, CH$_3$), 1.40 (d, 3 H, CH$_3$).
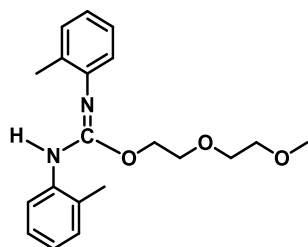
iso-urea **2-1**: The addition product of *o*-DTC and DGME.

^{1}H NMR (400 MHz, d-chloroform, δ ppm): δ 7.39 - 6.90 (m, 8 H, CH), 5.52 (s, 1 H, NH), 4.51 (t, 2 H, CH$_2$), 3.85 (t, 2 H, CH$_2$), 3.68 (t, 2 H, CH$_2$), 3.58 (t, 2 H, CH$_2$), 3.41 (s, 3 H, CH$_3$), 2.24 (s, 3 H, CH$_3$), 2.01 (s, 3 H, CH$_3$).
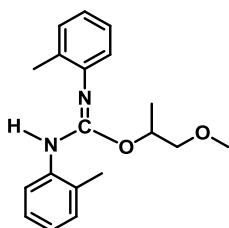
iso-urea **2-2**: The addition product of *o*-DTC and 1-methoxy-2-propanol.

^{1}H NMR (400 MHz, d-chloroform, δ ppm): δ 7.39 - 6.90 (m, 8 H, CH), 5.52 (s, 1 H, NH), 5.40 (m, 1 H, CH), 3.55 (m, 2 H, CH$_2$), 3.37 (s, 3 H, CH$_3$), 2.24 (s, 3 H, CH$_3$), 2.01 (s, 3 H, CH$_3$), 1.39 (d, 3 H, CH$_3$).

5.3.2   Determination of Conversion by ^{1}H-NMR

The conversion of both reactants for the reaction between carbodiimide and alcohol was studied using various concentrations of TTIP and DMTDN while keeping the concentration of both reactants constant. The conversion of both reactants was determined by ^{1}H-NMR spectroscopy. Here, the reaction between *p*-DTC and DGME is shown as a representative example.

The conversion of *p*-DTC was determined by integration of the peaks at 2.08 to 2.33 ppm (**Figure 34**, a), which correspond to the tolyl methyl groups of *p*-DTC, *iso*-urea, and guanidine-type products. The peaks of the tolyl methyl groups of *iso*-urea **1-1** and **1-2** (**Figure 35**, the peaks at 2.27 and 2.31 ppm) are partly overlapped with the peak of *p*-DTC (**Figure 35**, the peak at 2.32 ppm). Thus, the area of the peaks of *iso*-urea **1-1** and **1-2** was determined using the "Line Fitting" function of the program "MestReNova" under the assumption that the signal line-shape is pure Lorenzian, Gaussian, or a mix of both. The guanidine related byproducts are observed at 2.08 to 2.25.
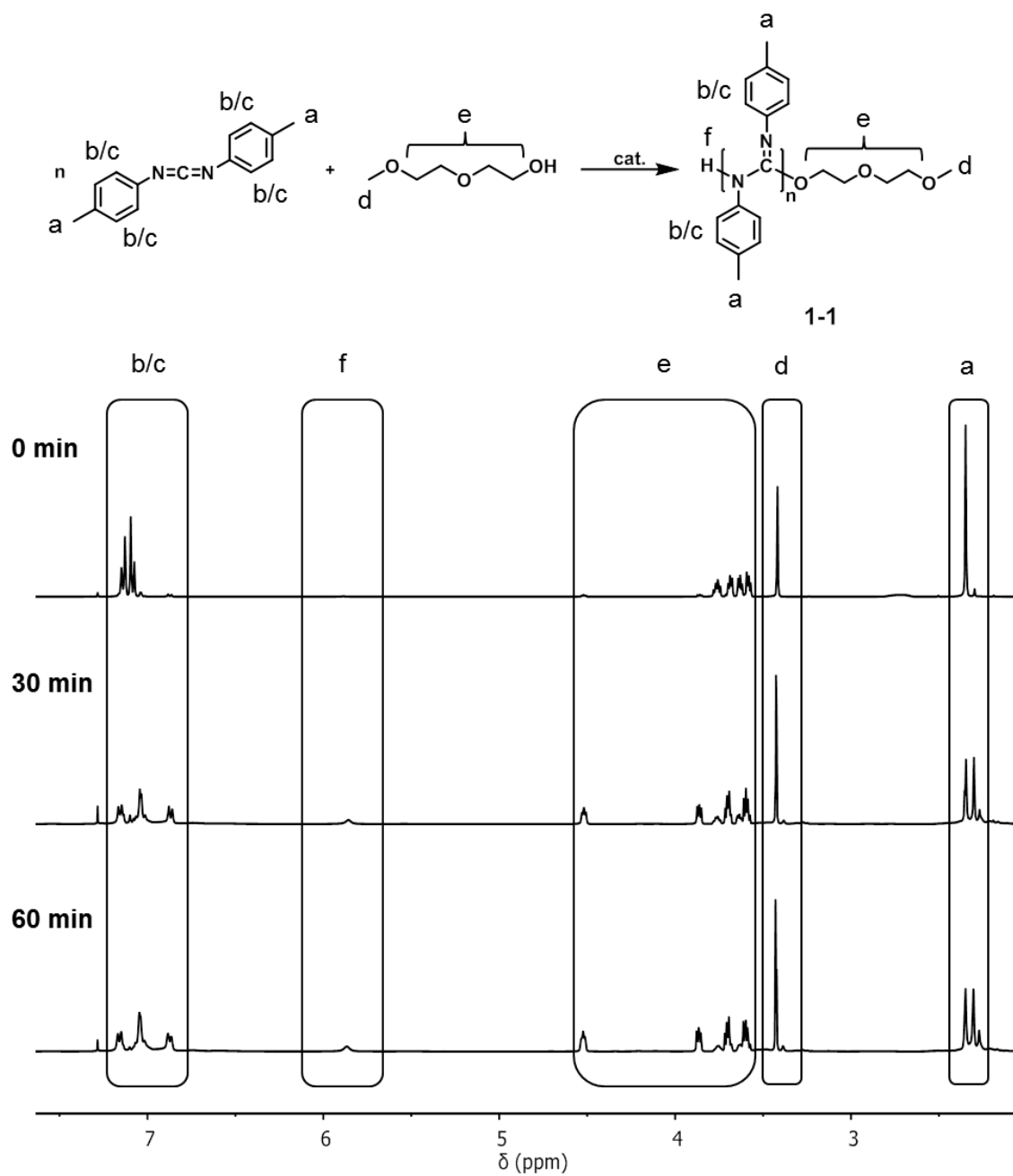
Figure 34. The ^{1}H-NMR spectra of the samples during the reaction between *p*-DTC and DGME catalyzed by TTIP.
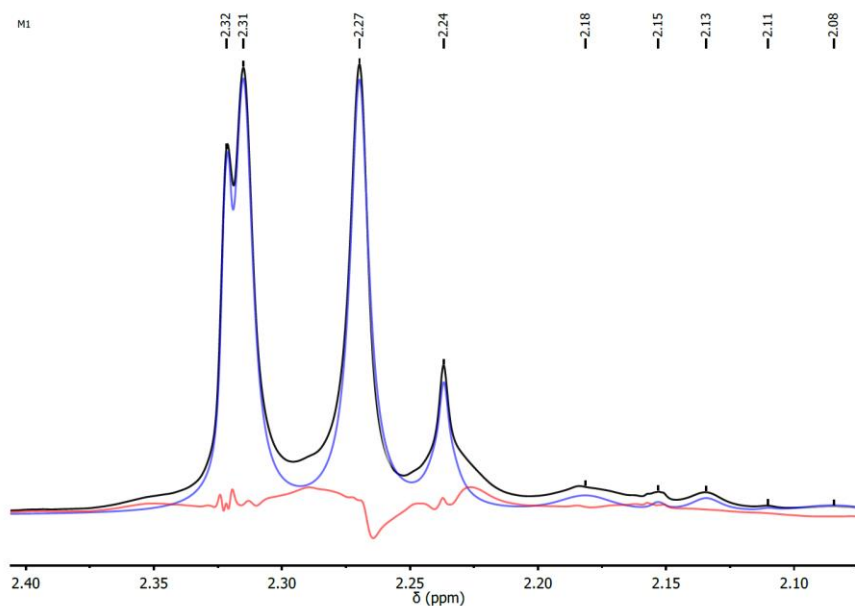
Figure 35. ¹H-NMR spectrum (2.05 – 2.40 ppm) of the sample during the reaction between *p*-DTC and DGME. The peaks are simulated by pure Lorenzian, Gaussian, or a mix of both functions (Blue curve), the rest signal area (red curve) was not counted into the integration.

The conversion of DGME was determined by integration of the peaks at 3.42 and 3.43, which correspond to the methyl group of DGME, *iso*-urea and the guanidine related products (**Figure 34**, d). The peaks of *iso*-urea 1-1 and 1-2 (**Figure 36**, the peaks at 3.43 ppm) are partly overlapped with the peak of DGME (**Figure 36**, the peak at 3.42 ppm). Thus, the area of the peaks of *iso*-urea 1-1 and 1-2 was determined using the "Line Fitting" function of the program "MestReNova" under the assumption that the signal line-shape is pure Lorenzian or Gaussian function, or a mix of both. The peaks corresponding to the guanidine related products are overlapped in the *iso*-urea peak at 3.43 ppm.
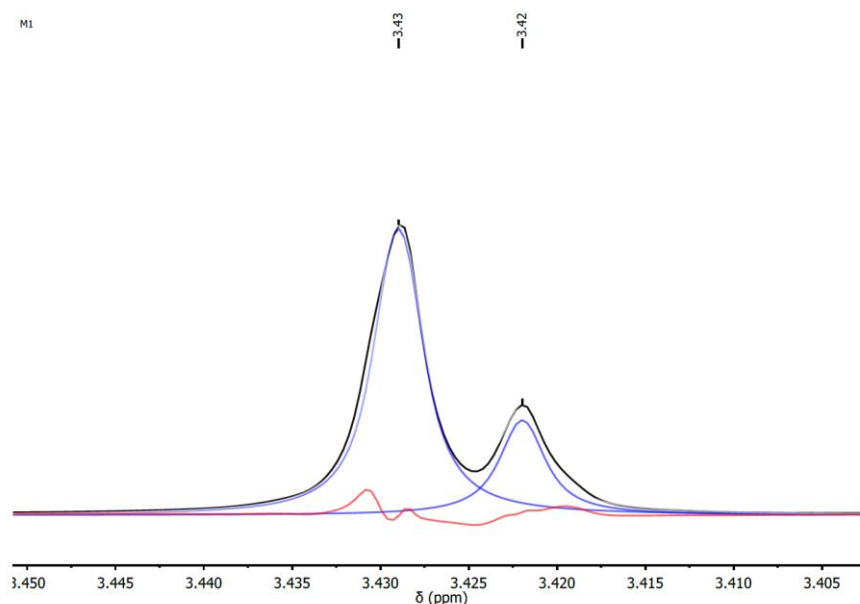
Figure 36. ^{1}H-NMR spectrum (3.40 – 3.45 ppm) of the sample during the reaction between *p*-DTC and DGME. The peaks are simulated by pure Lorenzian, Gaussian, or a mix of both functions (Blue curve), the rest signal area (red curve) was not counted into the integration.

5.3.3 Crystallography

The single crystal X-ray experiment for the guanidine-type compound **2-2** (**n = 3,** in **Chapter 3.1.2**) was performed using omega scans on a SuperNova four-circle diffractometer in Kappa geometry with a 50 W Cu microfocus tube, an Atlas CCD detector (Rigaku Oxford Diffraction), and a Cryostream 700 Plus cooler (100 K, Oxford Cryosystems Ltd). Data collection, cell refinement, data reduction, and absorption correction were done using CrysAlisPro.

The phase problem was solved using the dual-space algorithm implemented with SHELXT.[109] Both space group selection and primary atom site assignments were also done by SHELXT. Full-matrix least-squares refinement was done on F^2 using SHELXL[110] within the OLEX2 software[111] environment. Missing secondary atom sites were located from the difference Fourier map. Non-hydrogen atoms were refined using individual, anisotropic displacement parameters. The fully refined data was reviewed using PLATON.[112] Hydrogen atoms were positioned geometrically and refined riding on their respective parent atoms. Uiso(H) was fixed at 1.5 (CH_3) or 1.2 (all other H atoms) of the respective parent atom's isotropic displacement parameter. Bond lengths were set to 0.95 Å (aromatic C-H), 0.98 Å (C-H of methyl groups), 0.99 Å (C-H of methylene groups), and 0.88 Å (N—H). Hydrogen atoms of methyl groups were fitted to the experimentally observed electron density by allowing free rotation along the C—C

bond (HFIX 137). Positional disorder of the *o*-tolyl functional group attached to N12 gave atom sites C40A > C46A and C40B > C46B with an occupancy of 0.9210(15) for C40A > C46A. The distances N12—C40A and N12—C40B were restrained to be equal (SADI) and displacement parameters of equivalent atoms of the two sites were constrained to be the same (EADP). 1,2- and 1,3-distances within C40B > C46B were idealized using the SAME instruction.

Table 16. The crystal data collection and the refinement information

Crystal data

Cell	$a = 11.81220(10)$ Å $\quad \alpha = 90°$
	$b = 32.27810(10)$ Å $\quad \beta = 115.9700(10)°$
	$c = 12.51230(10)$ Å $\quad \gamma = 90°$
	$V = 4288.91(6)$ Å³
	from 65734 reflns. between $\theta_{min} = 4.1°$ and $\theta_{max} = 76.2°$
Chemical formula	$C_{50}H_{54}N_6O_3$
Z / Z'	4 / 1
M_r	786.99
Crystal system, space group	Monoclinic, $P2_1/c$
Crystal size	$(0.26 \times 0.24 \times 0.05)$ mm^3
Crystal colour, morphology	colourless, plate

Data collection

$F(000)$	1680
D_x	1.219 Mg m^{-3}
$\theta_{min}, \theta_{max}$	4.2°, 76.4°
Completeness at θ_{max}	0.997
Radiation type	Cu $K\alpha$ ($\lambda = 1.54184$ Å)
Temperature	100 K
μ	0.640 mm^{-1}
Diffractometer	Rigaku Oxford Diffraction SuperNova
T_{min}, T_{max}	0.739, 1.000
hkl range	h: $-14 \rightarrow 14$, k: $-40 \rightarrow 40$, l: $-15 \rightarrow 15$
No. of reflections	129156 measured, 8978 independent, 8462 ($I > 2\sigma(I)$)
R_{int}	0.044
$\sin(\theta_{max})/\lambda$	0.630 Å^{-1}

Refinement

$R[F^2 > 2\sigma(F^2)]$	0.039
$wR(F^2)$	0.103
S	1.06
w	$1/(\sigma^2(F_o^2) + (0.0477P)^2 + 1.7408P)$ with $P = (F_o^2 + 2F_c^2)/3$
$(\Delta/\sigma)_{max}$	0.001
$\Delta\rho_{max}, \Delta\rho_{min}$	0.330 e Å^3, -0.238 e Å^3
No. of reflections	8462
No. of parameters / restraints	562 / 16

5.3.4 Kinetic Study of DGME into *p*-DTC Catalyzed by TTIP and DMTDN

The reaction was performed as mentioned in **Chapter 5.3.1**. The order of the reaction with respect to TTIP and DMTDN concentration was determined by plotting Ln (reaction rate) against Ln (catalyst concentration). The reaction rate was determined as the slope of the conversion curve at the beginning of the reaction (t = 0). The conversion curve was obtained by least squares fit of alcohol conversion versus time. Only the conversion in the first 20 min was used to determine the reaction rate in the early stage of the reaction (**Figure 37**).

It reveals a 0.4^{th} and a 0.5^{th} order behavior with respect to TTIP and DMTDN concentration, respectively (**Figure 38**).
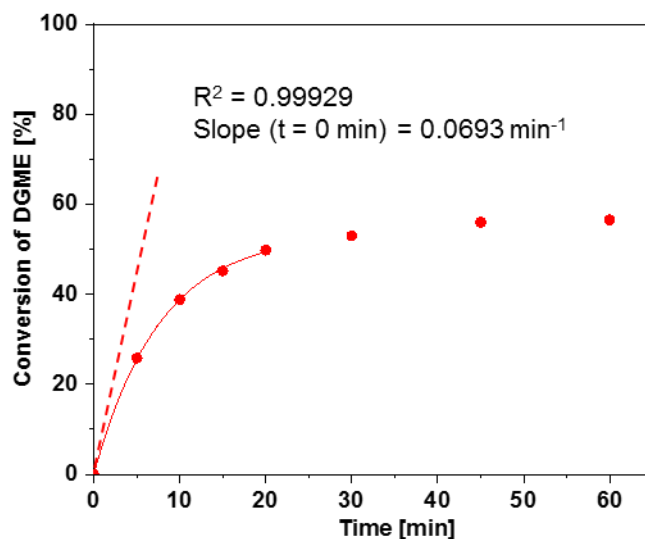
Figure 37. Schematic representation of the determination of the reaction rate by plotting the conversion of DGME as a function of the reaction time. The conversion in the first 20 min was used to determine the reaction rate.
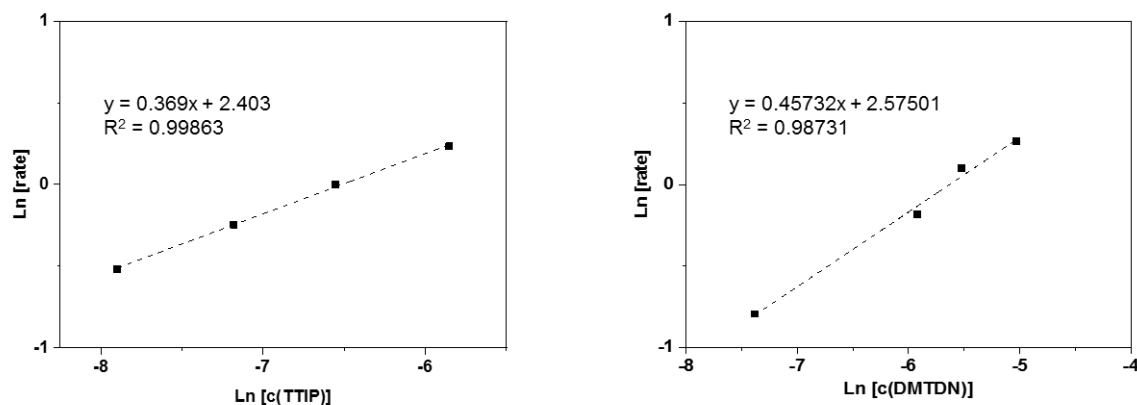
Figure 38. Plot of Ln [rate] as function of Ln [c(TTIP)] and Ln [c(DMTDN)], respectively. The slope of the straight lines are determined as the reaction order with respect to TTIP and DMTDN concentration, respectively.

5.4 Preparation of Guanidine-Crosslinked Polyiso-ureas

First, the biscarbodiimide was melted at 80 °C in an oven and poly(tetramethylene oxide) diol (polyTHF, M_n = 1000 g/mol) was dried under vacuum at 80 °C for two hours. Then both raw materials together with DMTDN (0.3% with respect to the weight of the monomers) were mixed in a mixing vessel (Utra-Turrox T-50, Ika-Werke) for 30 sec at 7000 rpm. The mixture was poured into an open mold (200 × 150 × 2 mm) at 130 °C and allowed to cure for 1 hour. The CDI index (CDI equivalents/polyol equivalents × 100) was varied from 150 to 200. The basic formulations are summarized in **Table 17**.

Table 17. Formulations of the guanidine-crosslinked polyiso-urea

index	biscarbodiimide	polyTHF	DMTDN
150	13.56 g	26.44 g	0.12 g
180	15.24 g	24.76 g	0.12 g
200	16.24 g	23.76 g	0.12 g

5.5 Study of Deblocking and Curing of Guanidine-containing Prepolymer

5.5.1 Preparation of Guanidine-containing Prepolymer

In a typical experiment, the oligomeric CDI (4.60 g, 27 mmol CDI groups) prepared from TDI was transferred under argon in a Schlenk tube. On account of the high viscosity, the oligomeric CDI was first preheated at 130 °C, then equivalent amount of DEGEE (1.85 g, 14 mmol) and DMTDN (0.3% with respect to the weight of DEGEE) were added. The reaction was first performed at 130 °C for 1 hour under an argon atmosphere, then the product was cooled at room temperature for 12 h. The synthesized guanidine-containing prepolymer was characterized by FT-IR spectroscopy (**Figure 15**).

5.5.2 Kinetic Study of Deblocking Reaction via DSC

In a typical DSC experiment for the deblocking reaction, the guanidine-containing prepolymer was sealed in the standard aluminum hermetic pans with a capacity of 100 μL. The calorimetric data were recorded under a continuous nitrogen flow. The measurement was performed using the dynamic method with the heating rate of 5, 8 and 10 K/min.

In the DSC thermogram, it was noticed that a glass transition of the guanidine-containing prepolymer was found at around 25 °C. (**Figure 39, 10 K/min as example**) However, this glass transition shifted to around 30 °C in the following dynamic run with the same heating rate, which might be attributed to the unreacted DEGEE remaining in the prepolymer. Thus, the second dynamic run was used to determine the deblocking temperature and to study the reaction kinetics.
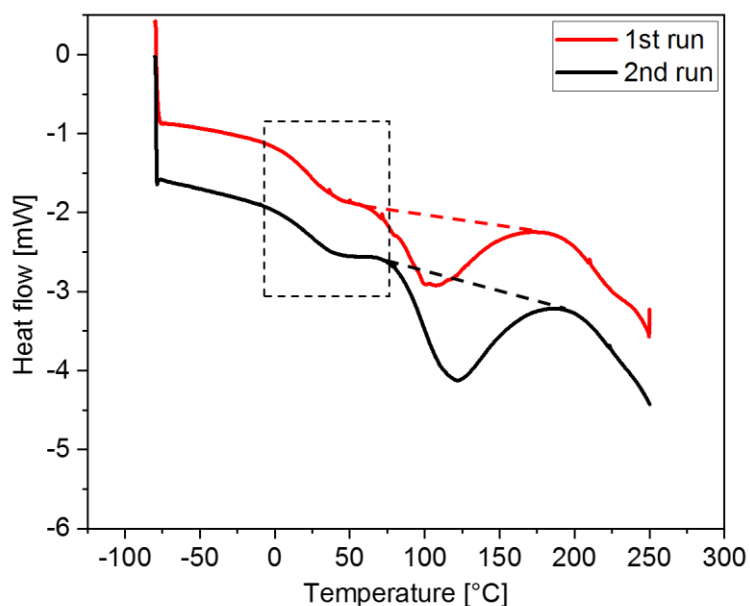
Figure 39. The DSC curve of the first and second run for the dynamic measurement of the deblocking reaction. The result with the heating rate of 10 K/min was used as an example.

5.5.3   Kinetic Study of Curing Reaction against Alcohol via DSC

In a typical DSC experiment for the curing reaction, the sample was prepared by mixing the guanidine-containing prepolymer with DEGEE in the molar ratio of 1:1. In order to achieve a homogenous sample, the mixture was slightly heated. Once the both reactants were miscible, the sample was immediately cooled in ice bath. Then, ca. 10 mg of the sample was sealed in the standard aluminum hermetic pans with a capacity of 100 μL. The calorimetric data were recorded under a continuous nitrogen flow. The isothermal measurements were performed at a certain temperature from 110 – 130 °C, followed by a dynamic scan at 5 K/min to determine the residual reaction enthalpy. The dynamic measurements were performed from -80 °C to 300 °C with the heating rate of 10, 15 and 20 K/min.
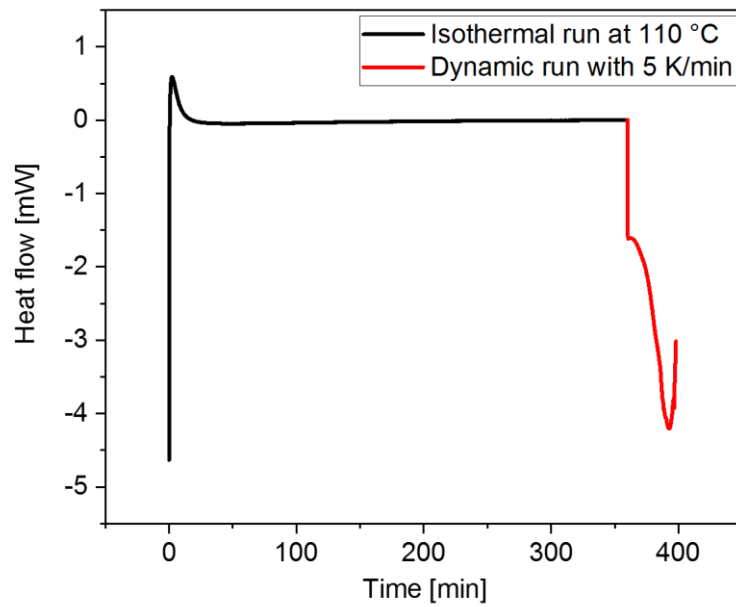
Figure 40. The DSC curve of the isothermal measurement and the following dynamic measurement of the curing reaction. The result of the measurement at 110 °C was used as an example.

6   Safety Data

The chemicals used in this work are listed with safety instructions in **Table 18**.

Table 18. Safety instruction of the chemicals used in this work

Substances	GHS Pictograms	Hazard Sentences	Precaution Sentences
Dichloromethane	GHS07, GHS08 **Warning**	H315-H319-H336-H351	P201-P261-P264-P280-P304 + P340 + P312-P308 + P313
Di(ethylene glycol) ethyl ether	–	–	–
Diethylene glycol monomethyl ether	GHS08 **Harmful**	H361d	P281-P308 + P313
Dimethyltin dineodecanoate (Fomrez UL28)	GHS07, GHS08 **Danger**	–	–
1-Methoxy-2-propanol	GHS02, GHS07 **Warning**	H226-H336	P261
3-Methyl-1-phenyl-2-phospholene 1-oxide	GHS07, GHS08 **Warning**	H302-H351-H412	P201-P264-P273-P280-P308 + P313-P501
1,4 -Phenylene diisocyanate	GHS05, GHS07, GHS08 **Danger**	H302 + H312 + H332-H315-H318-H334	P261-P280-P305 + P351 + P338-P342 + P311
Polytetrahydrofuran	–	H412	P273

Substances	GHS pictograms	Hazard Sentences	Precaution Sentences
Tetrachloromethane	GHS06, GHS08 **Danger**	H301 + H311 + H331-H317-H351-H372-H412-H420	P261-P273-P280-P301 + P310 + P330-P403 + P233-P502
Tetrahydrofurane	GHS02, GHS07, GHS08 **Danger**	H225-H302-H319-H335-H351	P210-P280-P301 + P312 + P330-P305 + P351 + P338-P370 + P378-P403 + P235
Titanium isopropoxide	GHS02, GHS07 **Warning**	H226-H319-H336	P210-P305 + P351 + P338-P370 + P378
Toluene diisocyanate	GHS06, GHS08 **Danger**	H315-H317-H319-H330-H334-H335-H351-H412	P260-P280-P284-P304 + P340 + P310-P342 + P311-P403 + P233
p-Toluidine	GHS06, GHS08, GHS09 **Danger**	H301 + H311 + H331-H317-H319-H334-H351-H410	P261-P280-P284-P301 + P310 + P330-P304 + P340 + P312-P342 + P311-P403 + P233
o-Tolyl isocyanate	GHS07, GHS08 **Danger**	H302 + H312 + H332-H315-H319-H334-H335	P261-P280-P305 + P351 + P338-P342 + P311
p-Tolyl isocyanate	GHS07, GHS08 **Danger**	H302 + H312 + H332-H315-H319-H334-H335	P261-P280-P305 + P351 + P338-P342 + P311
Triethylamine	GHS02, GHS05, GHS06 **Danger**	H225-H302-H311 + H331-H314-H335	P210-P261-P280-P303 + P361 + P353-P305 + P351 + P338-P370 + P378

Substances	GHS pictograms	Hazard Sentences	Precaution Sentences
Triphenyl phosphite	GHS07, GHS09 **Warning**	H302-H315-H317-H319-H410	P280-P301 + P312 + P330-P305 + P351 + P338
Triphenylphosphine	GHS07, GHS08 **Warning**	H302-H317-H373	P280-P301 + P312 + P330-P333 + P313

7 Bibliography

[1] H.-W. Engels, H.-G. Pirkl, R. Albers, R. W. Albach, J. Krause, A. Hoffmann, H. Casselmann, J. Dormish, *Angewandte Chemie (International ed. in English)* **2013**, *52*, 9422.

[2] E. Delebecq, J.-P. Pascault, B. Boutevin, F. Ganachaud, *Chemical reviews* **2013**, *113*, 80.

[3] J. O. Akindoyo, M. D. H. Beg, S. Ghazali, M. R. Islam, N. Jeyaratnam, A. R. Yuvaraj, *RSC Adv.* **2016**, *6*, 114453.

[4] E. Sharmin, F. Zafar, in *Polyurethane* (Ed.: F. Zafar), InTech **2012**.

[5] N. V. Gama, A. Ferreira, A. Barros-Timmons, *Materials (Basel, Switzerland)* **2018**, *11*.

[6] N. Mahajan, P. Gupta, *RSC Adv.* **2015**, *5*, 41839.

[7] D. Randall, S. Lee, *The polyurethanes book*, Huntsman Polyurethanes], [Everberg, Belgium **2002**.

[8] Infiniti Research, *Global Isocyanate Market 2018-2022* **2018**.

[9] H. A. Duong, M. J. Cross, J. Louie, *Organic letters* **2004**, *6*, 4679.

[10] M. J. Galante, R. J. J. Williams, *J. Appl. Polym. Sci.* **1995**, *55*, 89.

[11] L. Maisonneuve, O. Lamarzelle, E. Rix, E. Grau, H. Cramail, *Chem. Rev.* **2015**, *115*, 12407.

[12] L. Rand, A. B. Lateef, J. A. Reeder, *J. Org. Chem.* **1971**, *36*, 2295.

[13] A. S. Nasar, S. Subramani, G. Radhakrishnan, *J. Polym. Sci. A Polym. Chem.* **1999**, *37*, 1815.

[14] H. Kothandaraman, R. Thangavel, *J. Polym. Sci. A Polym. Chem.* **1993**, *31*, 2653.

[15] A. Mühlebach, *J. Polym. Sci. A Polym. Chem.* **1994**, *32*, 753.

[16] S. Subramani, A. Sultan Nasar, T. Philip Gnanarajan, N. Padmanabha Iyer, G. Radhakrishnan, *Polym. Int.* **2000**, *49*, 546.

[17] E. Querat, L. Tighzert, J. P. Pascault, K. Dušek, *Angew. Makromol. Chemie* **1996**, *242*, 1.

[18] Panagiotis I. Kordomenos, Andrew H. Dervan, Trifunctional blocked isocyanate containing an isocyanurate ring, U.S. Patent 4,491,663, **1985**.

[19] H. Ulrich, *Chemistry and technology of carbodiimides*, Wiley, Chichester, West Sussex **2007**.

[20] A. Williams, I. T. Ibrahim, *Chem. Rev.* **1981**, *81*, 589.

[21] J. G. Kennemur, B. M. Novak, *Polymer* **2011**, *52*, 1693.

[22] A. A. Bakibaev, V. V. Shtrykova, *Russ. Chem. Rev.* **1995**, *64*, 929.

[23] A. C. Piñol, M. M. Mañas, *Chem. Commun. (London)* **1967**, *0*, 229a-229a.

[24] A. Mukherjee, T. K. Sen, P. K. Ghorai, S. K. Mandal, *Scientific reports* **2013**, *3*, 2821.

[25] H. G. Khorana, *Chem. Rev.* **1953**, *53*, 145.

[26] M. xl, M. lajczyk, K. xl, P. lbasiński, *Tetrahedron* **1981**, *37*, 233.

[27] J. Ravn, M. Ankersen, M. Begtrup, J. F. Lau, *Tetrahedron Letters* **2003**, *44*, 6931.

[28] K.-L. Wei, C.-H. Wu, W.-H. Huang, J.-J. Lin, S. A. Dai, *Macromolecules* **2006**, *39*, 12.

[29] A. H. M. Schotman, T. J. M. Weber, W. J. Mijs, *Macromol. Chem. Phys.* **1999**, *200*, 635.

[30] I. Shibata, A. Baba, H. Iwasaki, H. Matsuda, *J. Org. Chem.* **1986**, *51*, 2177.

[31] K. Hartke, F. Roßbach, *Angew. Chem.* **1968**, *80*, 83.

[32] R. Richter, *Chem. Ber.* **1968**, *101*, 174.

[33] G. Rapi, G. Sbrana, N. Gelsomini, *J. Chem. Soc. C* **1971**, *0*, 3827.

[34] L. M. Alberino, W. J. Farrissey, A. A. R. Sayigh, *J. Appl. Polym. Sci.* **1977**, *21*, 1999.

[35] H. Eilingsfeld, M. Seefelder, H. Weidinger, *Angew. Chem.* **1960**, *72*, 836.

[36] J. B. Fell, G. M. Coppola, *Synthetic Communications* **1995**, *25*, 43.

[37] J. C. SHEEHAN, J. J. HLAVKA, *J. Org. Chem.* **1956**, *21*, 439.

[38] H. Ulrich, A. A. R. Sayigh, *Angew. Chem.* **1966**, *78*, 761.

[39] H. Stetter, C. Wulff, *Chem. Ber.* **1962**, *95*, 2302.

[40] Y. Iwakura, R. Tsuzuki, K. Noguchi, *Makromol. Chem.* **1966**, *98*, 21.

[41] C. L. Stevens, G. H. Singhal, A. B. Ash, *J. Org. Chem.* **1967**, *32*, 2895.

[42] R. Appel, R. Kleinstück, K.-d. Ziehn, *Chem. Ber.* **1971**, *104*, 1335.

[43] H. J. Bestmann, J. Lienert, L. Mott, *Justus Liebigs Ann. Chem.* **1968**, *718*, 24.

[44] J. J. Monagle, J. V. Mengenhauser, *J. Org. Chem.* **1966**, *31*, 2321.

[45] T. W. Campbell, J. J. Monagle, V. S. Foldi, *J. Am. Chem. Soc.* **1962**, *84*, 3673.

[46] W. Neumann, P. Fischer, *Angew. Chem.* **1962**, *74*, 801.

[47] J. J. Monagle, *J. Org. Chem.* **1962**, *27*, 3851.

[48] H. Ulrich, *Chemistry and technology of isocyanates*, Wiley, Chichester **1996**.

[49] F. Risse, E. T. Gedig, J. S. Gutmann, *Analytical and bioanalytical chemistry* **2018**, *410*, 4109.

[50] M. Tsakos, E. S. Schaffert, L. L. Clement, N. L. Villadsen, T. B. Poulsen, *Natural product reports* **2015**, *32*, 605.

[51] R. B. Merrifield, *Angew. Chem.* **1985**, *97*, 801.

[52] S. A. Narang, *Tetrahedron* **1983**, *39*, 3.

[53] J. C. SHEEHAN, K. R. Henery-Logan, *J. Am. Chem. Soc.* **1957**, *79*, 1262.

[54] J. C. SHEEHAN, K. R. Henery-Logan, *J. Am. Chem. Soc.* **1959**, *81*, 3089.

[55] M. Aresta, A. Dibenedetto, E. Fracchiolla, P. Giannoccaro, C. Pastore, I. Pápai, G. Schubert, *J. Org. Chem.* **2005**, *70*, 6177.

[56] Z. Grabarek, J. Gergely, *Analytical Biochemistry* **1990**, *185*, 131.

[57] N. G. Dolinnaya, N. I. Sokolova, D. T. Ashirbekova, Z. A. Shabarova, *Nucleic Acids Research* **1991**, *19*, 3067.

[58] J. E. Glass (Ed.), *Technology for Waterborne Coatings*, American Chemical Society, Washington, DC **1997**.

[59] R. M. Lum, *J. Polym. Sci. Polym. Chem. Ed.* **1979**, *17*, 3017.

[60] D. W. Brown, R. E. Lowry, L. E. Smith, *Macromolecules* **1981**, *14*, 659.

[61] S.-D. Ding, Z.-P. Liu, T. Yang, G.-C. Zheng, Y.-Z. Wang, *J Polym Res* **2010**, *17*, 63.

[62] A.-L. Chen, K.-L. Wei, R.-J. Jeng, J.-J. Lin, S. A. Dai, *Macromolecules* **2011**, *44*, 46.

[63] Frithjof Hannig, Manfred Schmidt, Hartmut Nefzger, Wolfgang Friederichs, Process for the preparation of polyisocyanate containing carbodiimide and/or uretonimine groups, German Patent DE10200505883, **2005**.

[64] H. Ulrich, H. E. Reymore, *Journal of Cellular Plastics* **1985**, *21*, 350.

[65] D. K. Hoffman, *Journal of Cellular Plastics* **1984**, *20*, 129.

[66] S. Vyazovkin, N. Sbirrazzuoli, *Macromol. Rapid Commun.* **2006**, *27*, 1515.

[67] A. Yousefi, P. G. Lafleur, R. Gauvin, *Polym. Compos.* **1997**, *18*, 157.

[68] M. R. Kamal, S. Sourour, *Polym. Eng. Sci.* **1973**, *13*, 59.

[69] M. R. Kamal, *Polym. Eng. Sci.* **1974**, *14*, 231.

[70] B. Fernandez d'Arlas, L. Rueda, P. M. Stefani, K. de La Caba, I. Mondragon, A. Eceiza, *Thermochimica Acta* **2007**, *459*, 94.

[71] H. L. Friedman, *J. polym. sci., C Polym. symp.* **1964**, *6*, 183.

[72] N. Sbirrazzuoli, *Macromol. Chem. Phys.* **2007**, *208*, 1592.

[73] J. H. Flynn, L. A. Wall, *J. Polym. Sci. B Polym. Lett.* **1966**, *4*, 323.

[74] T. Ozawa, *BCSJ* **1965**, *38*, 1881.

[75] C. D. Doyle, *J. Appl. Polym. Sci.* **1961**, *5*, 285.

[76] A. W. COATS, J. P. REDFERN, *Nature* **1964**, *201*, 68.

[77] H. E. Kissinger, *J. RES. NATL. BUR. STAN.* **1956**, *57*, 217.

[78] S. Vyazovkin, *J. Comput. Chem.* **2001**, *22*, 178.

[79] D. Dieterich, W. Keberle, H. Witt, *Angew. Chem. Int. Ed. Engl.* **1970**, *9*, 40.

[80] R. Tennebroek, I. van der Hoeven-van Casteren, R. Swaans, S. van der Slot, P. J. M. Stals, B. Tuijtelaars, C. Koning, *Polym. Int.* **2018**, *9*, 281.

[81] F. E. Golling, R. Pires, A. Hecking, J. Weikard, F. Richter, K. Danielmeier, D. Dijkstra, *Polym. Int.* **2018**, *52*, 9422.

[82] L. Maisonneuve, O. Lamarzelle, E. Rix, E. Grau, H. Cramail, *Chem. Rev.* **2015**, *115*, 12407.

[83] G. Rokicki, P. G. Parzuchowski, M. Mazurek, *Polym. Adv. Technol.* **2015**, *26*, 707.

[84] J. Guan, Y. Song, Y. Lin, X. Yin, M. Zuo, Y. Zhao, X. Tao, Q. Zheng, *Ind. Eng. Chem. Res.* **2011**, *50*, 6517.

[85] G. Liu, G. Wu, S. Huo, C. Jin, Z. Kong, *Progress in Organic Coatings* **2017**, *112*, 169.

[86] K. Hartke, M. Radau, *Arch. Pharm. Pharm. Med. Chem.* **1972**, *305*, 654.

[87] R. J. Batrice, C. E. Kefalidis, L. Maron, M. S. Eisen, *Journal of the American Chemical Society* **2016**, *138*, 2114.

[88] H. Liu, M. Khononov, N. Fridman, M. Tamm, M. S. Eisen, *Inorganic chemistry* **2017**, *56*, 3153.

[89] A. Imberdis, G. Lefèvre, P. Thuéry, T. Cantat, *Angew. Chem.* **2018**, *130*, 3138.

[90] M. I. Siling, T. N. Laricheva, *Russ. Chem. Rev.* **1996**, *65*, 279.

[91] R. Ghosh, A. G. Samuelson, *Chemical communications (Cambridge, England)* **2005**.

[92] A. J. Bloodworth, A. G. Davies, *J. Chem. Soc.* **1965**.

[93] I. G. Hinton, R. F. Web, *J. Chem. Soc.* **1961**.

[94] Y. Iwakura, K. Noguchi, *BCSJ* **1967**, *40*, 2383.

[95] M. Cristea, S. Ibanescu, C. N. Cascaval, D. Rosu, *High Performance Polymers* **2009**, *21*, 608.

[96] H. H. Winter, F. Chambon, *Journal of Rheology* **1986**, *30*, 367.

[97] H. H. Winter, in *Structure and Dynamics of Polymer and Colloidal Systems* (Eds.: R. Borsali, R. Pecora), Springer Netherlands. Dordrecht **2002**, p. 439.

[98] G. Grause, S. Hirahashi, H. Toyoda, T. Kameda, T. Yoshioka, *J Mater Cycles Waste Manag* **2017**, *19*, 612.

[99] C. M. Hansen, *Ind. Eng. Chem. Prod. Res. Dev.* **1969**, *8*, 2.

[100] B. Schneier, *J. Polym. Sci. B Polym. Lett.* **1972**, *10*, 245.

[101] J. E. Mark (Ed.), *Polymer data handbook*, Oxford University Press, New York, NY **1999**.

[102] J. Lu, R. P. Wool, *Polym. Eng. Sci.* **2007**, *47*, 1469.

[103] W. Neumann, P. Fisher, *Angew. Chem. Int. Ed. Engl.* **1962**, *1*, 621.

[104]   K. Wagner, K. Findeisen, W. Schäfer, W. Dietrich, *Angew. Chem. Int. Ed. Engl.* **1981**, *20*, 819.

[105]   A. P. Gies, W. H. Heath, R. J. Keaton, J. J. Jimenez, J. J. Zupancic, *Macromolecules* **2013**, *46*, 7616.

[106]   J. H. Flynn, L. A. Wall, *J. RES. NATL. BUR. STAN. SECT. A.* **1966**, *70A*, 487.

[107]   S. Vyazovkin, N. Sbirrazzuoli, *Macromolecules* **1996**, *29*, 1867.

[108]   A. L. Daniel-da-Silva, J. C. Moura Bordado, J. M. Martín-Martínez, *J. Appl. Polym. Sci.* **2007**, *104*, 1049.

[109]   G. M. Sheldrick, *Acta crystallographica. Section A, Foundations and advances* **2015**, *71*, 3.

[110]   G. M. Sheldrick, *Acta crystallographica. Section C, Structural chemistry* **2015**, *71*, 3.

[111]   O. V. Dolomanov, L. J. Bourhis, R. J. Gildea, J. A. K. Howard, H. Puschmann, *J Appl Crystallogr* **2009**, *42*, 339.

[112]   A. L. Spek, *Acta crystallographica. Section D, Biological crystallography* **2009**, *65*, 148.

8   Appendix

8.1   ¹H-NMR Spectra of the Kinetic Studies
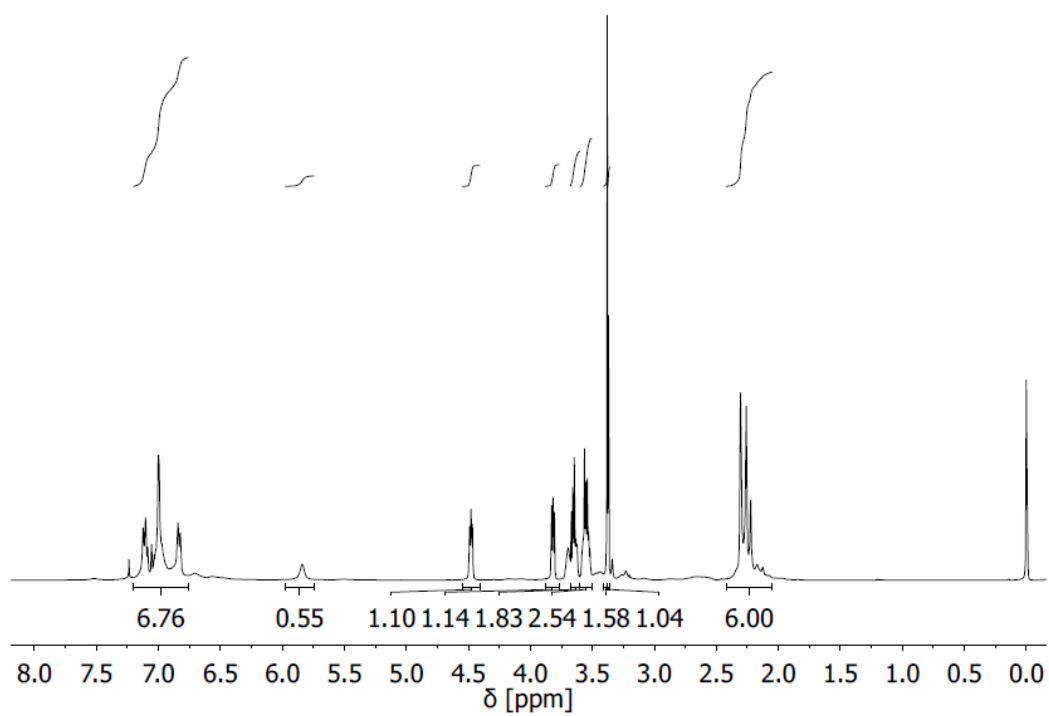
Figure 41. ¹H-NMR spectrum of the product mixture after addition of DGME and *p*-DTC catalyzed by TTIP at 60 °C.
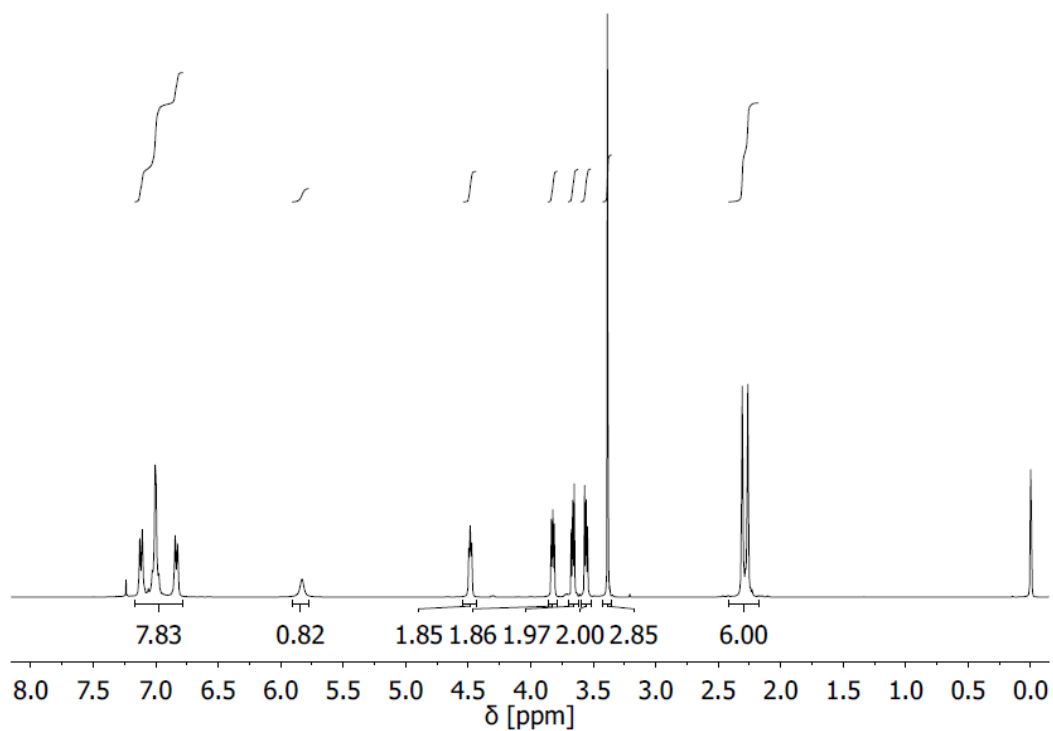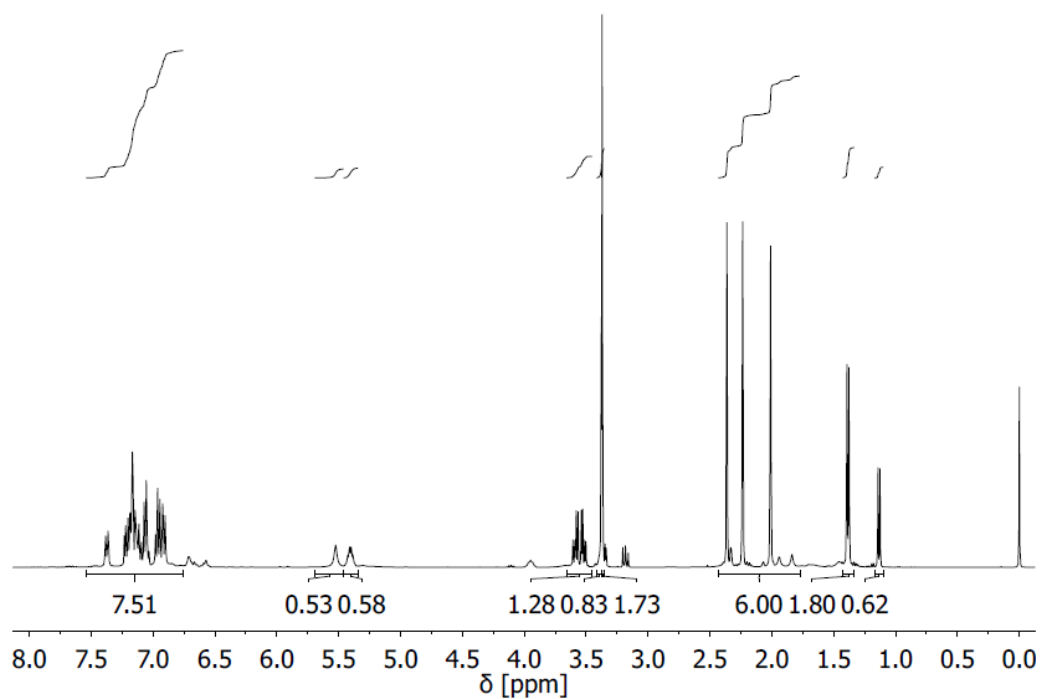
Figure 42. ^{1}H-NMR spectrum of *iso*-urea **1-1** after addition of DGME and *p*-DTC catalyzed by TTIP at 130 °C.
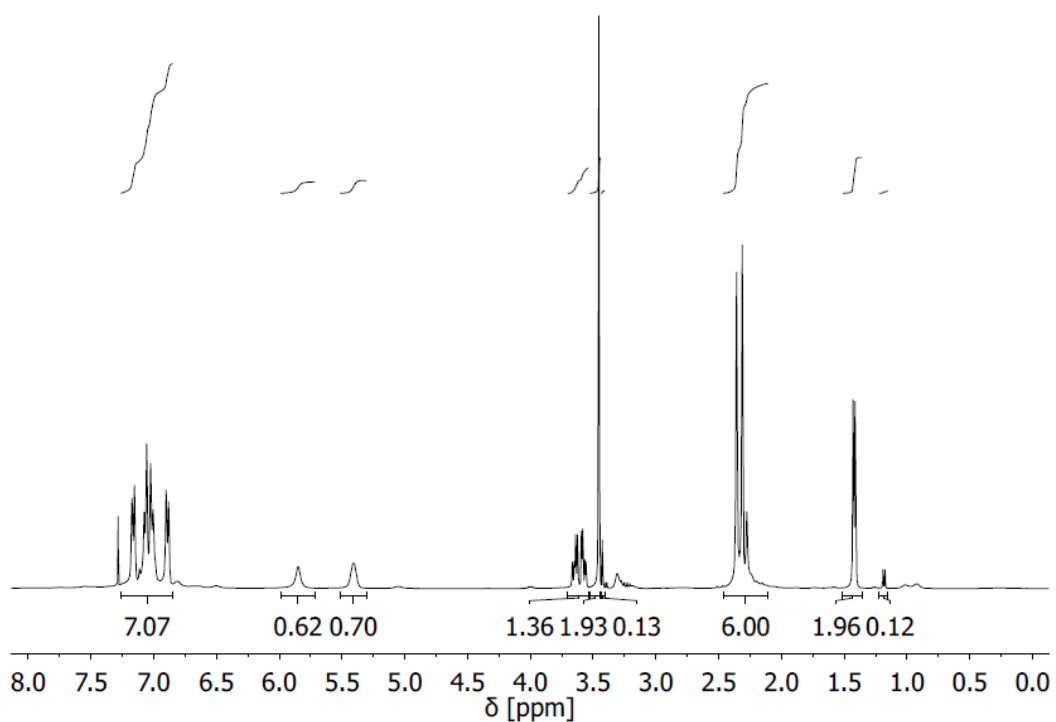
Figure 43. ^{1}H-NMR spectrum of the product mixture after addition of 1-methoxy-2-propanol and *p*-DTC catalyzed by TTIP at 60 °C.
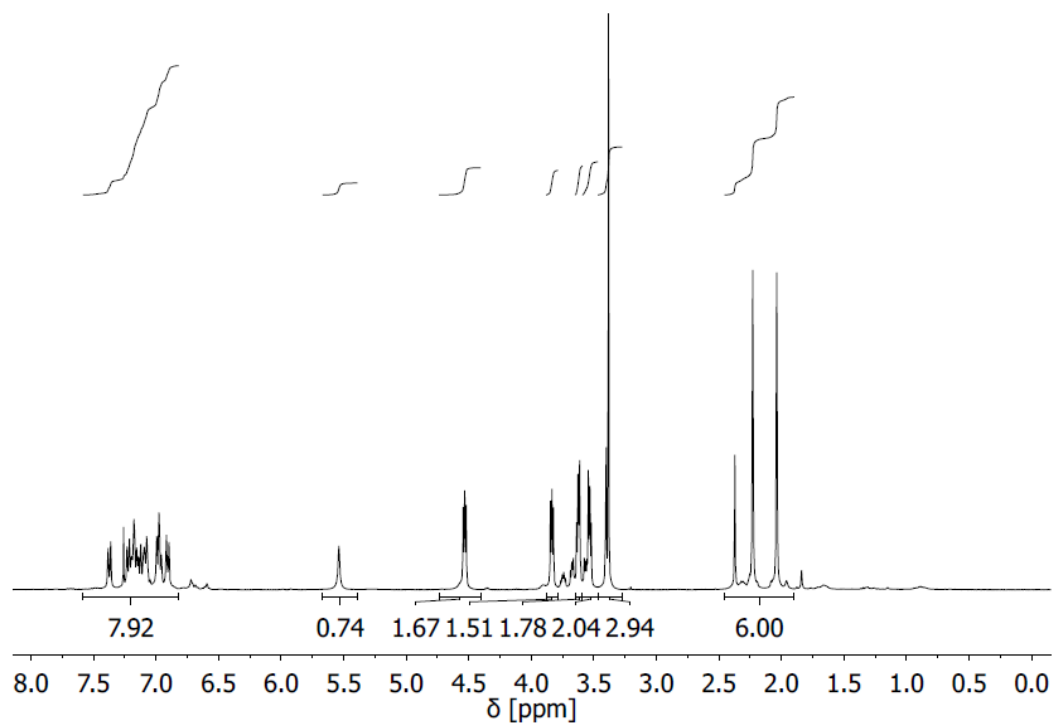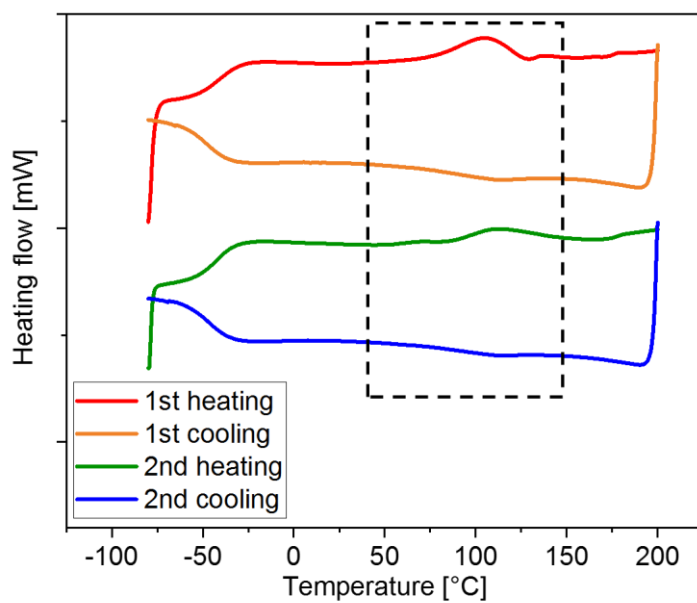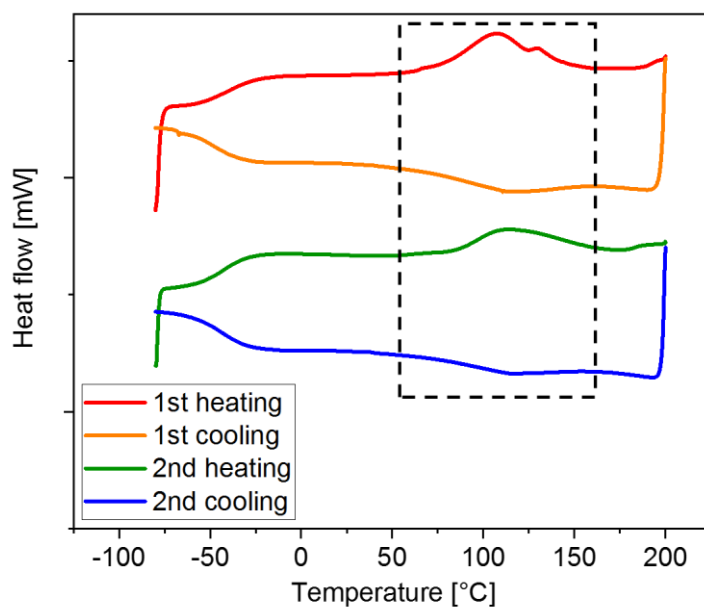
Figure 44. ^{1}H-NMR spectrum of the product mixture after addition of DGME and *o*-DTC catalyzed by TTIP at 60 °C.

Figure 45. ^{1}H-NMR spectrum of the product mixture after addition of 1-methoxy-2-propanol and *o*-DTC catalyzed by TTIP at 60 °C.

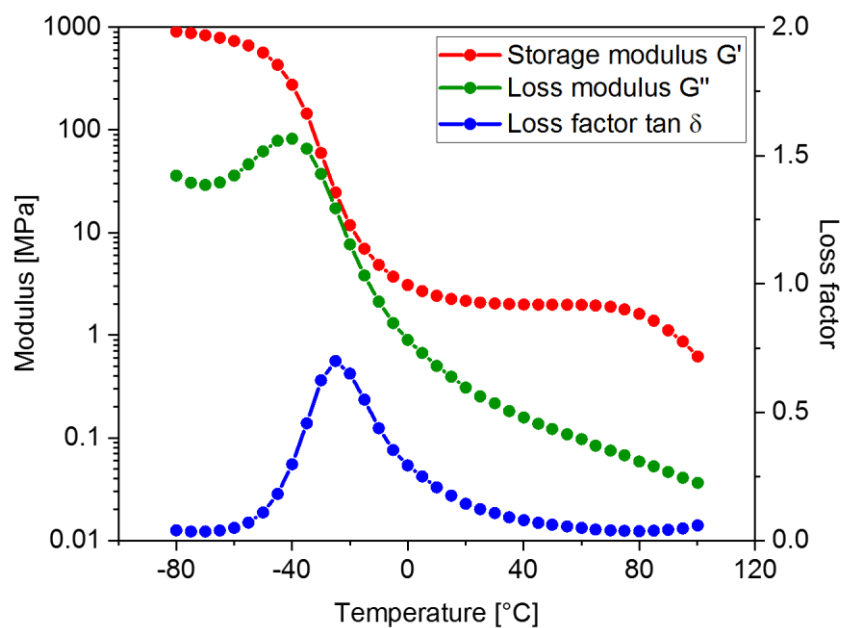## 8.2 DSC Thermograms of Guanidine Crosslinked Polyiso-urea

Figure 46. DSC thermogram of the polyiso-urea products with index 150.

Figure 47. DSC thermogram of the polyiso-urea products with index 180.

8.3 DMA Results of Guanidine Crosslinked Polyiso-urea

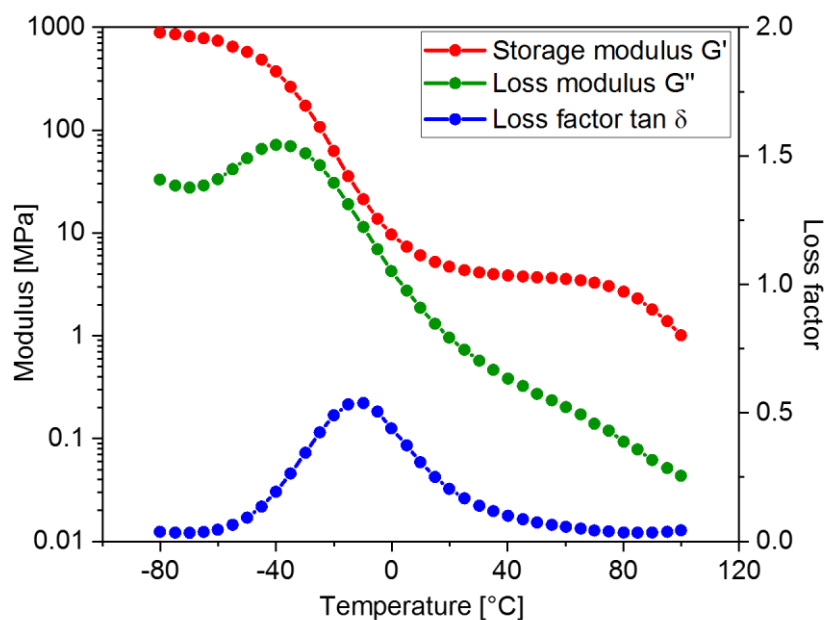**Figure 48.** DMA thermogram of the polyiso-urea product with index 150.
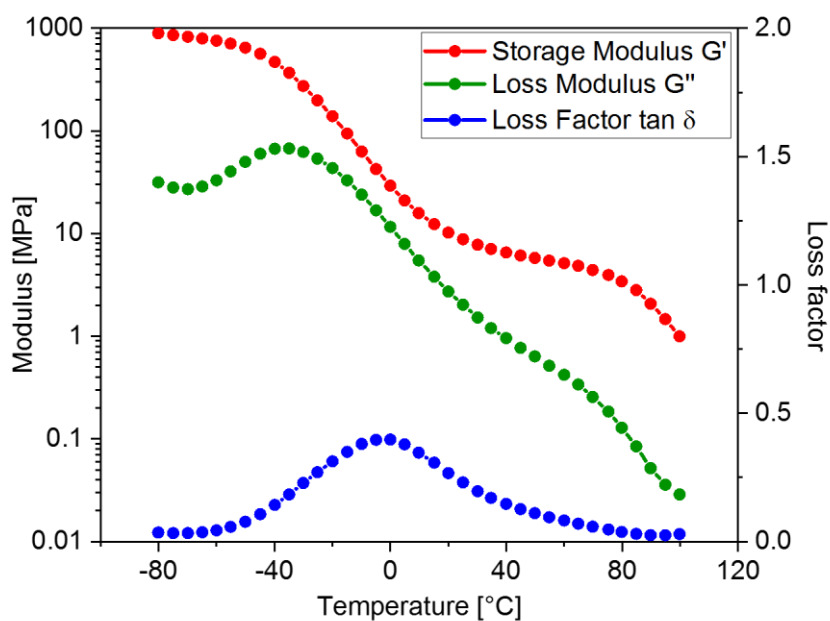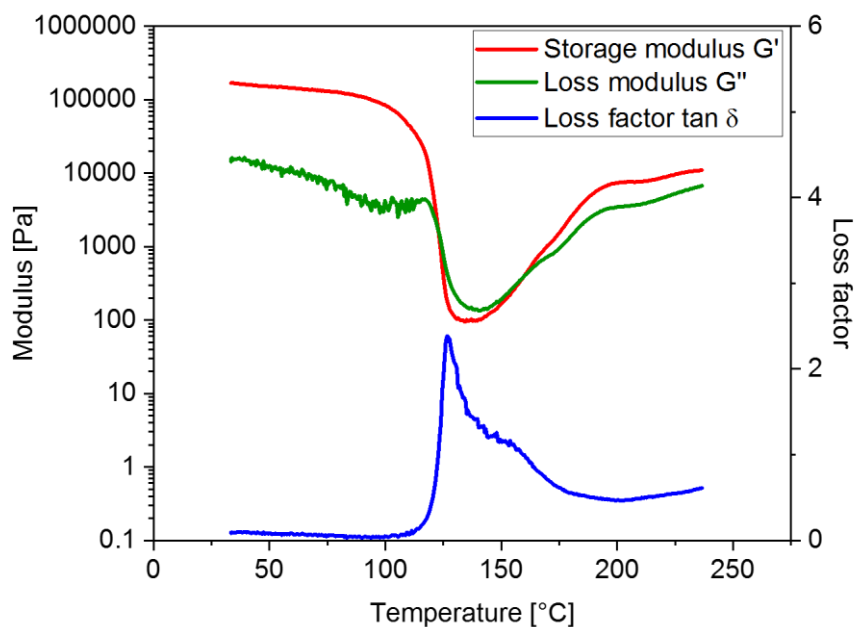

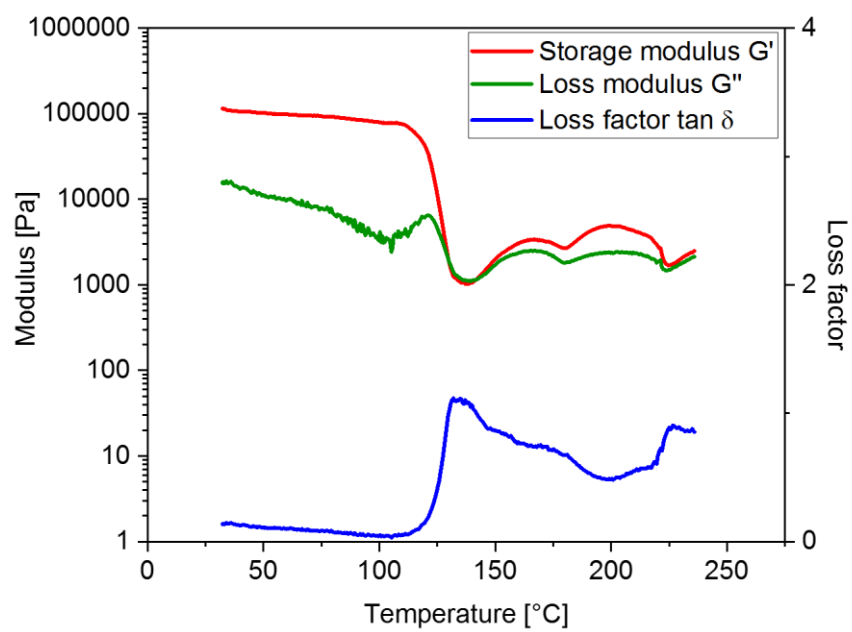**Figure 49.** DMA thermogram of the polyiso-urea product with index 180.

Figure 50. DMA thermogram of the polyiso-urea product with index 200.

8.4 Rheological Results of Guanidine Crosslinked Polyiso-urea

Figure 51. The temperature sweep of the polyiso-urea product with index 180 at 1 Hz.

Figure 52. The temperature sweep of the polyiso-urea product with index 200 at 1 Hz.

Acknowledgements

I would never have been able to finish my PhD as well as this thesis without the support, guidance, help, and encouragement from all the following people, so I would like to take this opportunity to express my gratitude to them.

First and foremost, I would like to thank Prof. Dr. Gerrit A. Luinstra for giving me the opportunity to conduct my study in his research group on this very interesting and promising topic. I am so glad that I get the room to play with this chemistry and I really enjoy it.

My special thanks are given to my advisor, Prof. Dr. Berend Eling, who let me experience the field of polyurethane research. I would thank him for his generous contribution of knowledge and experience, valuable comments and encouragement from the start to the end of my PhD. His guidance helped me in all the time of research and writing of this thesis.

The work on this thesis was financially supported by BASF Polyurethanes GmbH. I really appreciate their trust and support during my whole PhD. My sincere thanks also go to Dr. Rebecca Sure from BASF SE in Ludwigshafen for her help in DFT calculations. Thank Stefan Auffarth for his very kind help and scientific support.

A part of results in this thesis were worked out by Veronika Eilermann, Ali Said and Marvin Czarny during their master or bachelor thesis. Thank you for your excellent laboratory work and the results are very supportive and useful.

I am also very thankful to all the colleagues in the research group as well as other coworkers in TMC. I am perpetually grateful to be part of such a loving and supportive family. Thank my lab colleagues, Anna and Daniell in my early days of PhD and Mengyu in the last one and a half years. In particular, Mengyu has helped me a lot in the DSC measurements. Cheers to our best time in A310. I would like to thank Karen, not only for her generous help in rheology measurements, but also for so many interesting talks. I will always be glad to listen to your experiences and opinions, not only in chemistry but also from your own. I am also sincerely grateful to Jessica, Wolf, Niklas and Fabian. Thank you Jessica not only for helping me correct my thesis, but also inviting me to your wedding and I very appreciate. Wolf, thank you for your very kind help in tensile tests. Thank you Niklas for your suggestions both in chemistry and career for the future. Fabian, wish we can still jog together in the future, but you indeed run much faster than me. Thank my good friends Shaojian, Jiaojiao, Xia, Xiaoxiao, Guannan and Song, I will never forget our great time in Hamburg.
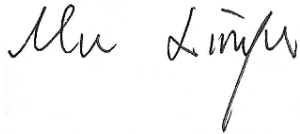
Finally, I owe a great deal of thanks to my parents, my wife and the whole family. You are always by my side and inspiring me all the time. During my PhD, I lost my grandfather forever, who raised me up and always cared about my life. This thesis is also for you.

Declaration on Oath

I hereby declare on oath that I have written the present dissertation by my own and have not used other than the acknowledged resources and aids. I hereby declare that I have not previously applied or pursued for a doctorate (Ph.D. studies).

Hamburg, 10.07.2020